UNIVERSITÀ DEGLI STUDI DI TRIESTE

Sede Amministrativa del Dottorato di Ricerca

XXIII CICLO DEL

DOTTORATO DI RICERCA IN

INGEGNERIA DELL'INFORMAZIONE

ONLINE CHARACTERIZATION OF HIGH-FREQUENCY PERCUSSIVE VENTILATOR

Settore scientifico-disciplinare ING-INF/06

DOTTORANDO

FABIO RISCICA

RESPONSABILE DOTTORATO DI RICERCA (Coordinatore Corso/Direttore Scuola)

PROF. WALTER UKOVICH

FIRMA: 

RELATORE

PROF. AGOSTINO ACCARDO – UNIVERSITÀ DI TRIESTE

FIRMA: 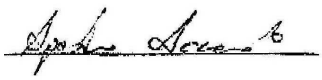

SUPERVISORE/TUTORE

PROF. AGOSTINO ACCARDO – UNIVERSITÀ DI TRIESTE

FIRMA: 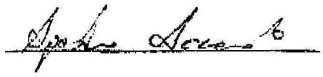

CORRELATORE

DOTT. UMBERTO LUCANGELO – UNIVERSITÀ DI TRIESTE

FIRMA: 

ANNO ACCADEMICO 2009/2010

Index

Introduction

The lungs, the essential organ of respiration, are mechanically and geometrically complex structure, whose function is intrinsically dependent on the morphology, properties and interactions of its components. The study of the mechanical behavior of this system is that chapter of respiration known as respiratory mechanics. Although the respiratory mechanics is not the only process involved in breathing (other essential elements are gas exchange in the alveolar-capillary, transport of gas to and from the cells and the regulation of ventilation), it nevertheless represents a fundamental aspect of respiratory function, widely studied in physiology. As a, gas exchange abnormalities are associated with abnormalities of the mechanical properties of the respiratory system. So the monitoring of respiratory mechanics is a fundamental aspect in management of patient who depends on the mechanical ventilator in order to:

- characterize the pathophysiology of the disease below the acute respiratory failure and help in the diagnosis;
- study the disease and assess its progression;
- provide guidelines for therapeutic measures, such as the application of positive end expiratory pressure (PEEP), the change of posture, etc.
- optimize the ventilation mode and its setting regard of changes in the patient's condition and thus improve the interaction patient-ventilator;
- prevent complications dependent on ventilation.

Given the complexity of the respiratory system, these studies get significant benefits from the use of simple models intended to describe the main functional characteristics of respiratory mechanics. The modern monitoring systems provide valuable information regarding the adequacy of the treatment choices made, especially if they are able to measure

online the viscoelastic properties of respiratory mechanics. The models used to describe the characteristics of the respiratory system are sufficiently suitable to describe the reality of things depending on the frequency content of the signal flow or pressure with which the patient is ventilated [Otis et al., 1956;Mead and Whittenberger, 1954; Mount, 1955]. For this reason the use of unconventional ventilators forces to review the models and to use more appropriate models [Dorkin et al 1998]. In recent years it has been clinically reviewed the usefulness of a particular type of ventilation as an alternative to Conventional Mechanical Ventilation (CMV): the High Frequency Ventilation (HFV). With the intent to perform a ventilation which minimizes iatrogenic damage, the HFV was often associated with CMV or, in some cases, has completely replaced it. The High Frequency Percussive Ventilation (HFPV) is a special mode of HFV which in the past has been successfully applied to acute respiratory failure by smoke inhalation. In addition, the HFPV found wider use in both the pediatric and neonatal than in adult patients. The usefulness of HFPV has been clinically assessed particularly in the treatment of closed head injury [Hurst JM et al 1987] acute respiratory diseases caused by burns and smoke inhalation [Lentz CW and Peterson HD 1997, Reper P et al 1998, Reper P et al 2002], newborns with hyaline membrane disease and/or acute respiratory distress syndrome [Velmahos GC et al 1999], bronchial repair [Lucangelo U et al 2006], and finally some studies demonstrated the efficacy of intrapulmonary percussive ventilation in removing bronchial secretions under diverse conditions [Natale JE et al 1994, Homnick DN et al 1995, Toussaint M et al 2003, Deakins K and Chatburn RL 2002, Antonaglia V et al 2006, Lucangelo et al 2009]. Despite the positive results obtained, the HFPV is not currently included in the ventilatory strategy of severe respiratory failure. Among the controversial aspects regarding the mode of high frequency ventilation, one of these is the lack of a universally accepted classification and a precise nomenclature. In particular, there are few studies to consider specific criteria for the routine use of HFPV. The problem lies in the fact that the high frequency components of HFPV stimulate phenomena (e.g. inertial), which are not considered in the easier lung models. This would require to replace the high frequency ventilator with a conventional ventilator, just to get a conventional assessment of the patient. To change the model to be identified in order to make efficient also in the HFPV is instead a much less risky and invasive process.

The objective of this study was first to identify models and determine appropriate methods to identify the respiratory parameters during ventilation with HFPV.

The study was carried out in partnership between Department. of Industrial Engineering and Information Technology of University of Trieste and Department of Perioperative Medicine, Intensive Care and Emergency of Cattinara Hospital of Trieste.

Chapter 1

Physiology of the respiratory system and mechanical models

As functioning units, the lung and heart are usually considered a single complex organ, but because these organs contain essentially two compartments (one for blood and one for air) they are usually separated in terms of the tests conducted to evaluate heart or pulmonary function. This chapter focuses on some of the physiologic concepts responsible for normal function and specific measures of the lung's ability to supply tissue cells with enough oxygen while removing excess carbon dioxide.

1.1 Respiration anatomy

The respiratory system consists of the lungs, conducting airways, pulmonary vasculature, respiratory muscles, and surrounding tissues and structures (Fig. 1.1). Each plays an important role in influencing respiratory responses.

There are two lungs in the human chest; the right lung is composed of three incomplete divisions called *lobes,* and the left lung has two, leaving room for the heart. The right lung accounts for 55% of total gas volume and the left lung for 45%. Lung tissue is spongy

because of the very small (200 to 300×10^{-6} m diameter in normal lungs at rest) gas-filled cavities called *alveoli,* which are the ultimate structures for gas exchange. There are 250 million to 350 million alveoli in the adult lung, with a total alveolar surface area of 50 to 100 m^2 depending on the degree of lung inflation [Johnson, 1991].

Air is transported from the atmosphere to the alveoli beginning with the oral and nasal cavities, through the pharynx (in the throat), past the glottal opening, and into the trachea or windpipe. Conduction of air begins at the larynx, or voice box, at the entrance to the trachea, which is a fibromuscular tube 10 to 12 cm in length and 1.4 to 2.0 cm in diameter [Kline, 1976]. At a location called the *carina,* the trachea terminates and divides into the left and right bronchi. Each bronchus has a discontinuous cartilaginous support in its wall. Muscle fibers capable of controlling airway diameter are incorporated into the walls of the bronchi, as well as in those of air passages closer to the alveoli. Smooth muscle is present throughout the respiratory bronchiolus and alveolar ducts but is absent in the last alveolar duct, which terminates in one to several alveoli. The alveolar walls are shared by other alveoli and are composed of highly pliable and collapsible squamous epithelium cells. The bronchi subdivide into subbronchi, which further subdivide into bronchioli, which further subdivide, and so on, until finally reaching the alveolar level. A model of the geometric arrangement of these air passages is presented in Fig. 1.2. It will be noted that each airway is considered to branch into two subairways. In the adult human there are considered to be 23 such branchings, or generations, beginning at the trachea and ending in the alveoli. Movement of gases in the respiratory airways occurs mainly by bulk flow (convection) throughout the region from the mouth to the nose to the fifteenth generation. Beyond the fifteenth generation, gas diffusion is relatively more important. With the low gas velocities that occur in diffusion, dimensions of the space over which diffusion occurs (alveolar space) must be small for adequate oxygen delivery into the walls; smaller alveoli are more efficient in the transfer of gas than are larger ones. Thus animals with high levels of oxygen consumption are found to have smaller-diameter alveoli compared with animals with low levels of oxygen consumption.

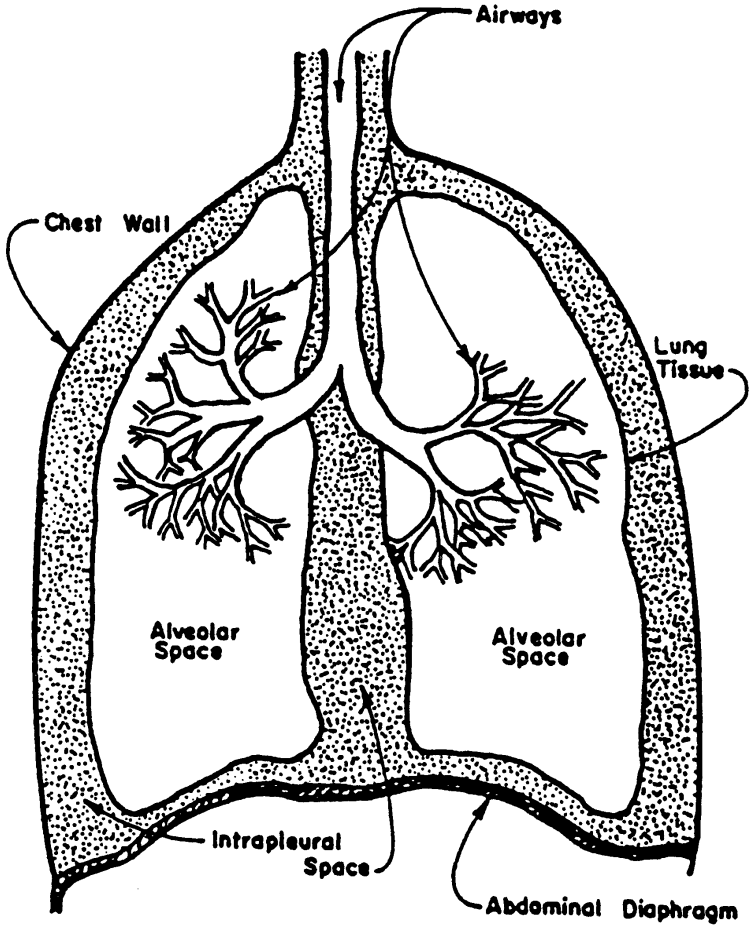

Figure 1.1 Schematic representation of the respiratory system

Alveoli are the structures through which gases diffuse to and from the body. To ensure gas exchange occurs efficiently, alveolar walls are extremely thin. For example, the total tissue thickness between the inside of the alveolus to pulmonary capillary blood plasma is only about 0.4×10^{-6} m. Consequently, the principal barrier to diffusion occurs at the plasma and red blood cell level, not at the alveolar membrane [Ruch and Patton, 1966]. Molecular diffusion within the alveolar volume is responsible for mixing of the enclosed gas. Due to small alveolar dimensions, complete mixing probably occurs in less than 10 ms, fast enough that alveolar mixing time does not limit gaseous diffusion to or from the blood [Astrand and Rodahl, 1970]. Of particular importance to proper alveolar operation is a thin surface coating of surfactant. Without this material, large alveoli would tend to enlarge and small alveoli would collapse. It is the present view that surfactant acts like a detergent, changing the stress-strain relationship of the alveolar wall and thereby stabilizing the lung [Johnson, 1991].

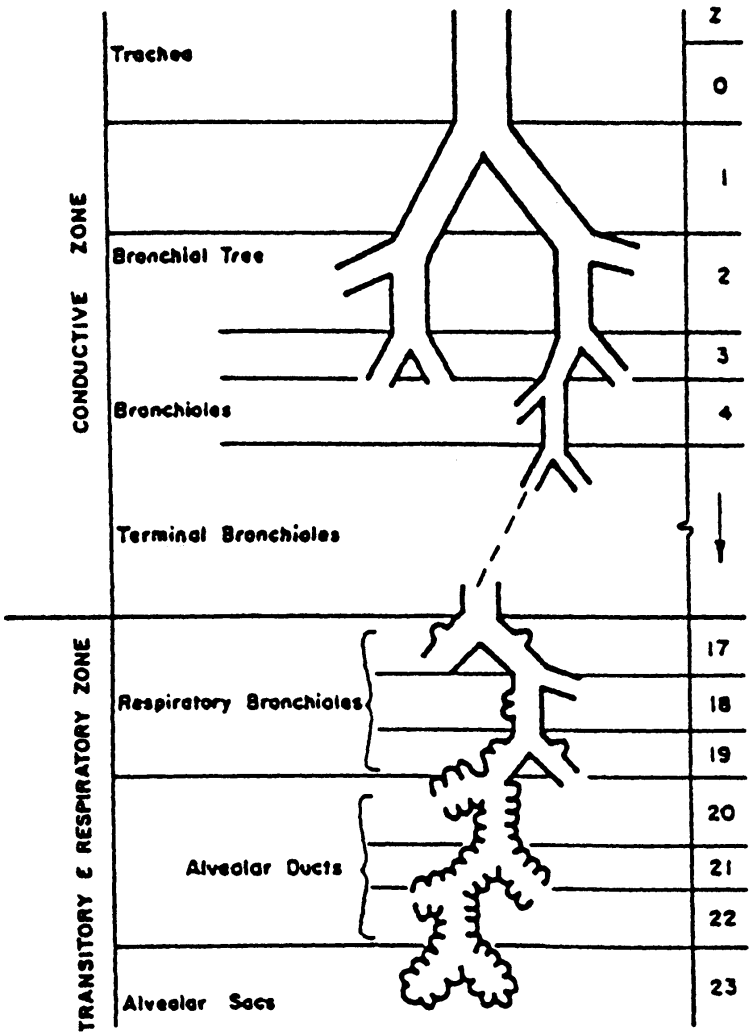

Figure 1.2 General architecture of conductive and transitory airways. [Weibel, 1963].

There is no true pulmonary analogue to the systemic arterioles, since the pulmonary circulation occurs under relatively low pressure [West, 1977]. Pulmonary blood vessels, especially capillaries and venules, are very thin walled and flexible. Unlike systemic capillaries, pulmonary capillaries increase in diameter, and pulmonary capillaries within alveolar walls separate adjacent alveoli with increases in blood pressure or decreases in alveolar pressure. Flow, therefore, is significantly influenced by elastic deformation. Although pulmonary circulation is largely unaffected by neural and chemical control, it does respond promptly to hypoxia. There is also a high-pressure systemic blood delivery system to the bronchi that is completely independent of the pulmonary low-pressure (~3330 N/m^2) circulation in healthy individuals. In diseased states, however, bronchial arteries are reported

to enlarge when pulmonary blood flow is reduced, and some arteriovenous shunts become prominent [West, 1977]. Total pulmonary blood volume is approximately 300 to 500 cm^3 in normal adults, with about 60 to 100 cm^3 in the pulmonary capillaries [Astrand and Rodahl, 1970]. This value, however, is quite variable, depending on such things as posture, position, disease, and chemical composition of the blood [Kline,1976].

The lungs fill because of a rhythmic expansion of the chest wall. The action is indirect in that no muscle acts directly on the lung. The diaphragm, the muscular mass accounting for 75% of the expansion of the chest cavity, is attached around the bottom of the thoracic cage, arches over the liver, and moves downward like a piston when it contracts. The external intercostal muscles are positioned between the ribs and aid inspiration by moving the ribs up and forward. This, then, increases the volume of the thorax. Other muscles are important in the maintenance of thoracic shape during breathing. [Ruch and Patton, 1966; Johnson, 1991]. Quiet expiration is usually considered to be passive; i.e., pressure to force air from the lungs comes from elastic expansion of the lungs and chest wall. During moderate to severe exercise, the abdominal and internal intercostal muscles are very important in forcing air from the lungs much more quickly than would otherwise occur. Inspiration requires intimate contact between lung tissues, pleural tissues (the pleura is the membrane surrounding the lungs), and chest wall and diaphragm. This is accomplished by reduced intrathoracic pressure (which tends toward negative values) during inspiration. Viewing the lungs as an entire unit, one can consider the lungs to be elastic sacs within an air-tight barrel — the thorax — which is bounded by the ribs and the diaphragm. Any movement of these two boundaries alters the volume of the lungs. The normal breathing cycle in humans is accomplished by the active contraction of the inspiratory muscles, which enlarges the thorax. This enlargement lowers intrathoracic and interpleural pressure even further, pulls on the lungs, and enlarges the alveoli, alveolar ducts, and bronchioli, expanding the alveolar gas and decreasing its pressure below atmospheric. As a result, air at atmospheric pressure flows easily into the nose, mouth, and trachea.

1.2 Lung volumes and gas exchange

Of primary importance to lung functioning is the movement and mixing of gases within the respiratory system. Depending on the anatomic level under consideration, gas movement is determined mainly by diffusion or convection. Without the thoracic musculature and rib cage, as mentioned above, the barely inflated lungs would occupy a much smaller space than they occupy in situ. However, the thoracic cage holds them open. Conversely, the lungs exert an influence on the thorax, holding it smaller than should be the case without the lungs. Because the lungs and thorax are connected by tissue, the volume occupied by both together is between the extremes represented by relaxed lungs alone and thoracic cavity alone. The resting volume V_R, then, is that volume occupied by the lungs with glottis open and muscles relaxed. Lung volumes greater than resting volume are achieved during inspiration. Maximum inspiration is represented by *inspiratory reserve volume* (IRV). IRV is the maximum additional volume that can be accommodated by the lung at the end of inspiration. Lung volumes less than resting volume do not normally occur at rest but do occur during exhalation while exercising (when exhalation is active). Maximum additional expiration, as measured from lung volume at the end of expiration, is called *expiratory reserve volume* (ERV). *Residual volume* is the amount of gas remaining in the lungs at the end of maximal expiration. *Tidal volume* V_T is normally considered to be the volume of air entering the nose and mouth with each breath. Alveolar ventilation volume, the volume of fresh air that enters the alveoli during each breath, is always less than tidal volume. The extent of this difference in volume depends primarily on the *anatomic dead space*, the 150 to 160 ml internal volume of the conducting airway passages. The term *dead* is quite appropriate, since it represents wasted respiratory effort; i.e., no significant gas exchange occurs across the thick walls of the trachea, bronchi, and bronchiolus. Since normal tidal volume at rest is usually about 500 ml of air per breath, one can easily calculate that because of the presence of this dead space, about 340 to 350 ml of fresh air actually penetrates the alveoli and becomes involved in the gas exchange process. An additional 150 to 160 ml of stale air exhaled during the previous breath is also drawn into the alveoli.

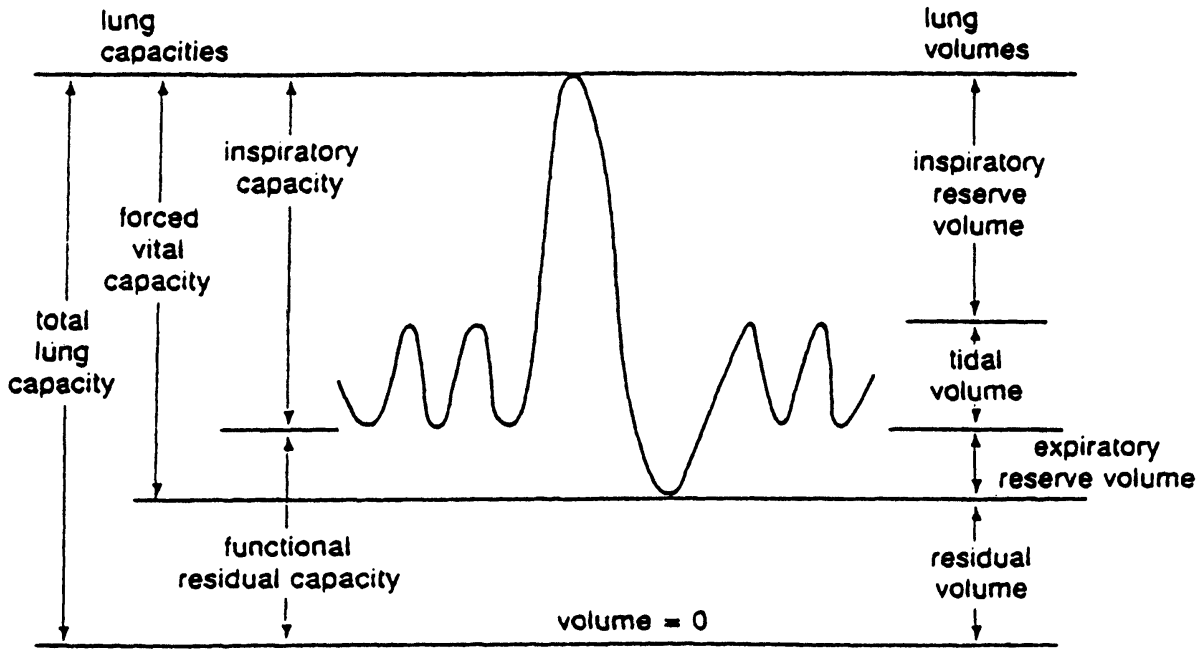

Figure 1.3 Lung capacities and lung volumes.

The term *volume* is used for elemental differences of lung volume, whereas the term *capacity* is used for combination of lung volumes. Figure 1.3 illustrates the interrelationship between each of the following lung volumes and capacities:

1. *Total lung capacity* (TLC): The amount of gas contained in the lung at the end of maximal inspiration.

2. *Forced vital capacity* (FVC): The maximal volume of gas that can be forcefully expelled after maximal inspiration.

3. *Inspiratory capacity* (IC): The maximal volume of gas that can be inspired from the resting expiratory level.

4. *Functional residual capacity* (FRC): The volume of gas remaining after normal expiration. It will be noted that functional residual capacity (FRC) is the same as the resting volume. There is a small difference, however, between resting volume and FRC because FRC is measured while the patient breathes, whereas resting volume is

measured with no breathing. FRC is properly defined only at end-expiration at rest and not during exercise.

1.3 Perfusion of the lung

For gas exchange to occur properly in the lung, air must be delivered to the alveoli via the conducting airways, gas must diffuse from the alveoli to the capillaries through extremely thin walls, and the same gas must be removed to the cardiac atrium by blood flow. This three-step process involves alveolar ventilation, the process of diffusion, and ventilatory perfusion, which involves pulmonary blood flow. Obviously, an alveolus that is ventilated but not perfused cannot exchange gas. Similarly, a perfused alveolus that is not properly ventilated cannot exchange gas. The most efficient gas exchange occurs when ventilation and perfusion are matched. There is a wide range of ventilation-to-perfusion ratios that naturally occur in various regions of the lung [Johnson, 1991]. Blood flow is somewhat affected by posture because of the effects of gravity. In the upright position, there is a general reduction in the volume of blood in the thorax, allowing for larger lung volume. Gravity also influences the distribution of blood, such that the perfusion of equal lung volumes is about five times greater at the base compared with the top of the lung [Astrand and Rodahl, 1970]. There is no corresponding distribution of ventilation; hence the ventilation-to-perfusion ratio is nearly five times smaller at the top of the lung. A more uniform ventilation-to-perfusion ratio is found in the supine position and during exercise [Jones, 1984]. Blood flow through the capillaries is not steady. Rather, blood flows in a halting manner and may even be stopped if intraalveolar pressure exceeds intracapillary blood pressure during diastole. Mean blood flow is not affected by heart rate [West, 1977], but the highly distensible pulmonary blood vessels admit more blood when blood pressure and cardiac output increase. During exercise, higher pulmonary blood pressures allow more blood to flow through the capillaries. Even mild exercise favors more uniform perfusion of the lungs [Astrand and Rodahl, 1970]. Pulmonary artery systolic pressures increases from 2670 N/m^2 (20 mm Hg) at rest to 4670 N/m^2 (35 mm Hg) during moderate exercise to 6670 N/m^2 (50 mm Hg) at maximal work [Astrand and Rodahl, 1970].

1.4 Respiratory models

The respiratory system exhibits properties of resistance, compliance, and inertance analogous to the electrical properties of resistance, capacitance, and inductance. Of these, inertance is generally considered to be of less importance than the other two properties.

Resistance is the ratio of pressure to flow:

$$R = \frac{P}{F}$$

where R = resistance, N × s/m^5

P = pressure, N/m^2

F = volume flow rate, m^3/s

Resistance can be found in the conducting airways, in the lung tissue, and in the tissues of the chest wall. Airways exhalation resistance is usually higher than airways inhalation resistance because the surrounding lung tissue pulls the smaller, more distensible airways open when the lung is being inflated. Thus airways inhalation resistance is somewhat dependent on lung volume, and airways exhalation resistance can be very lung volume–dependent [Johnson, 1991]. Respiratory tissue resistance varies with frequency, lung volume, and volume history. Tissue resistance is relatively small at high frequencies but increases greatly at low frequencies, nearly proportional to 1/f. Tissue resistance often exceeds airway resistance below 2 Hz. Lung tissue resistance also increases with decreasing volume amplitude [Stamenovic et al., 1990].

Compliance is the ratio of lung volume to lung pressure:

$$C = \frac{V}{P}$$

where C = compliance, m^5/N,

V = lung volume, m^3

P = pressure, N/m^2

As the lung is stretched, it acts as an expanded balloon that tends to push air out and return to its normal size. The static pressure-volume relationship is nonlinear, exhibiting decreased static compliance at the extremes of lung volume [Johnson, 1991]. As with tissue resistance, dynamic tissue compliance does not remain constant during breathing. Dynamic compliance tends to increase with increasing volume and decrease with increasing frequency [Stamenovic et al., 1990].

Inertance is the ratio of lung pressure to flow derivative:

$$I = \frac{P}{\dot{F}}$$

where I = inertance, N/m^5,

P = pressure, N/m^2

$\dot{F}$ = volume flow rate derivative, m^3/s^2

1.4.1 Linear model of first order

The simplest model of the respiratory system is a series combination of a resistance and a compliance (Fig. 1.4): a rough representation of the anatomy of an alveolus with its bronchial duct. This model, that will be called mechanical model, can be applied both during spontaneous ventilation and during constant flow passive ventilation.

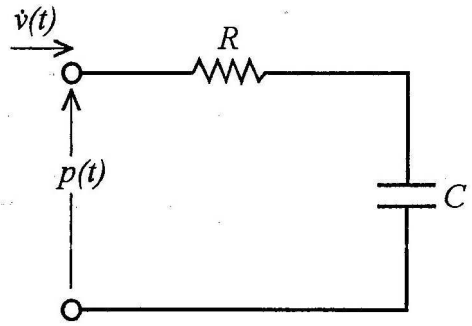

Figure 1.4 One-compartment first-order linear model.

The following mathematical equation, known as motion equation, describes its behavior:

$$p(t) = \frac{1}{C} \cdot v(t) + R \cdot \dot{v}(t)$$

where $p(t)$ is the pressure applied to the respiratory system, $v(t)$ is the pulmonary volume and $\dot{v}(t)$ is the airflow. The term $\frac{1}{C} \cdot v(t)$ corresponds to the pressure necessary to balance elastic forces; it depends on both the volume insufflated in excess of resting volume and the elastance of the respiratory system. On the other hand the term $R \cdot \dot{v}(t)$ corresponds to the pressure necessary to balance frictional forces; it is mainly due to the resistance offered to the airflow.

1.4.2 Linear models of second order

The simplest respiratory model which combines a single elastance and a single resistance does not accurately describe mechanical events such as stress relaxation. Among the more complex models which give a better description of the mechanical behavior of the respiratory system, the Otis [Otis et al., 1956], Mead [Mead and Whittenberger, 1954] and Mount [Mount, 1955] models are the most frequently used. All three models which were introduced

in the fifties, are two-compartment viscoelastic models, and obey similar equations of motion. It may therefore be useful to develop a synthetic approach combining these three models.

The Otis model (Fig. 1.5) was first proposed by Otis [Otis et al., 1956] to describe pulmonary inhomogeneities and subsequent parallel gas redistribution. It serially associates two Kelvin bodies characterized by their respective elastance (E_1 and E_2) and resistance (R_1 and R_2). The two Kelvin bodies are submitted to the same pressure, and the total deformation is the sum of each of their respective deformations.

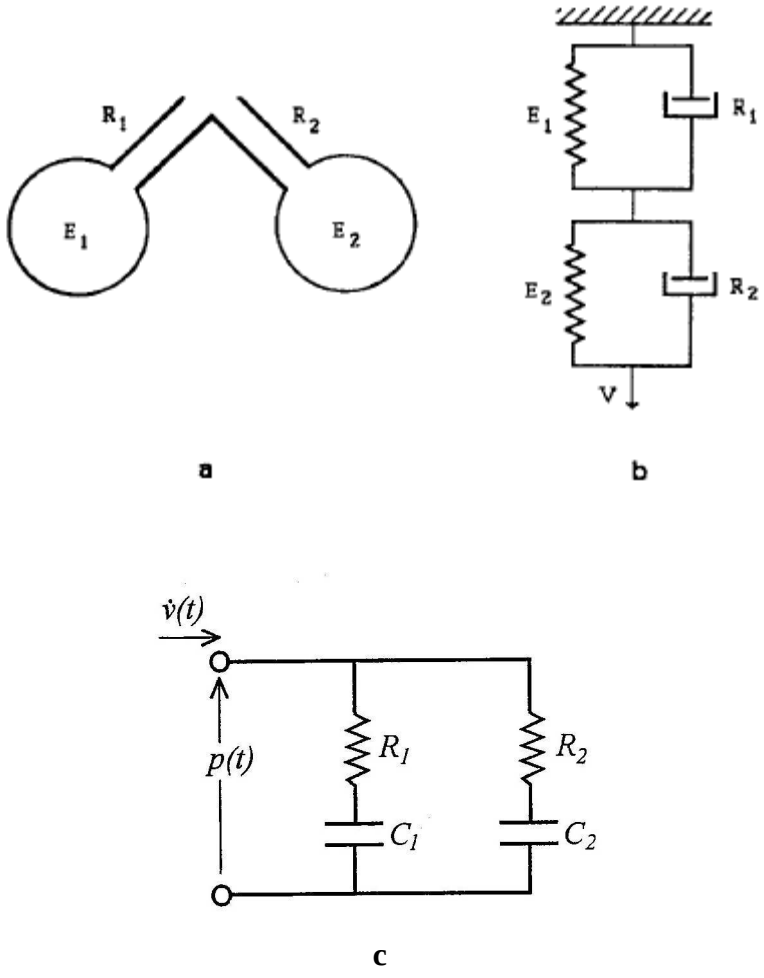

Figure 1.5 Otis' model characterizing inhomogeneous lung with parallel gas redistribution. (a) Anatomic representation. (b) Rheologic representation by two Kelvin bodies (E_1, R_1) and (E_2, R_2), serially associated. (c) Electrical analog model.

The Mead model (Fig. 1.6) was proposed by Mead [Mead and Whittenberger, 1954] to describe homogeneous lungs with central airway compliance and subsequent series gas redistribution. It consists of a central resistance (R_1) associated in parallel with an element composed of a central compliance (E_1) coupled in series with a Kelvin body characterized by its elastance (E_2) and resistance (R_2). The total pressure is the sum of the pressures induced by the central resistance, and by the central compliance plus the Kelvin body. The total deformation is the sum of the deformations of the elastic element (E_l) and of the Kelvin body (E_2, R_2).

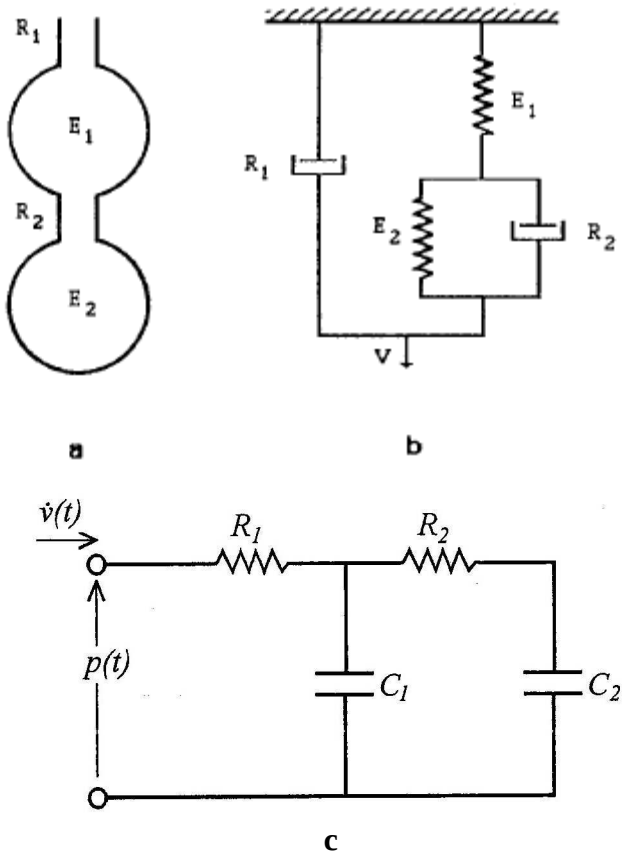

Figure 1.6 Mead's model for homogeneous lung with serial gas redistribution. (a) Anatomic representation. (b) Rheologic representation by a dashpot (R_1) associated in parallel with a spring (E_1) serially coupled with a Kelvin body (E_2, R_2). (c) Electrical analog model.

The Mount model (Fig. 1.7) originally proposed by Mount [Mount, 1955] was resumed by Bates [Bates et al, 1989]. It describes a homogeneous lung without any gas redistribution. In this model, stress relaxation originates from lung tissue and/or surfactant viscoelastic properties. The Mount model is composed of a Kelvin body (E_1, R_1) associated in parallel with a Maxwell body (E_2, R_2). The total pressure is the sum of the pressures induced by the Kelvin and the Maxwell bodies. The deformation of the Maxwell body is the sum of the deformations of its elastic and resistive elements. Each of the two elements of the Kelvin body is submitted to the same deformation as the Maxwell body.

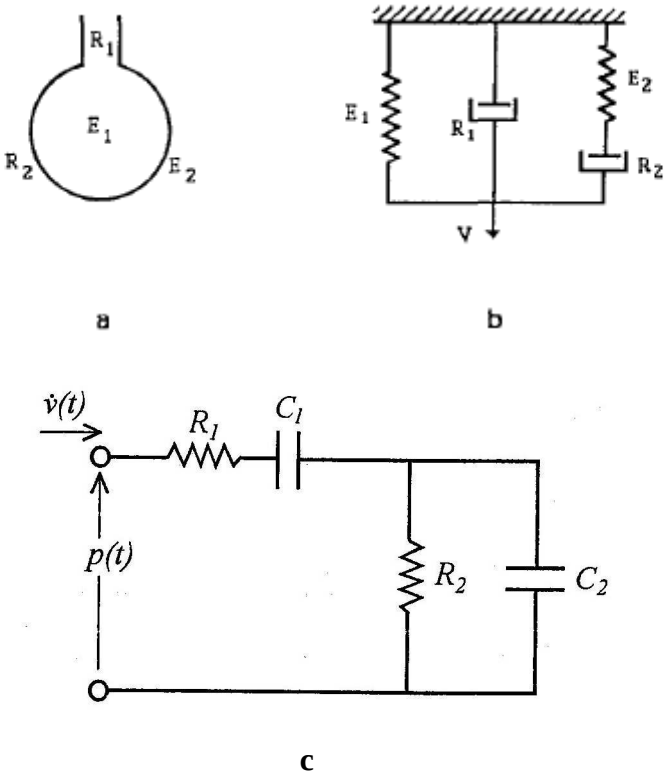

Figure 1.7 Mount's model for homogeneous lung with tissue and/or surfactant component. (a) Anatomic representation. (b) Rhelogic representation by a Kelvin body (E_1, R_1) associated in parallel with a Maxwell body (E_2, R_2). (c) Electrical analog model.

1.4.3 High frequency linear models

When the frequencies are higher than typical of traditional mechanical ventilation, the models above described lose their validity because they do not consider the peculiar feature of the system. If we limit our attention between 4 to 32 Hz, it has been proved [Dorkin et al, 1988] that a satisfactory approximation is given by simple one-compartment second-order linear model RIC (Fig. 1.8).

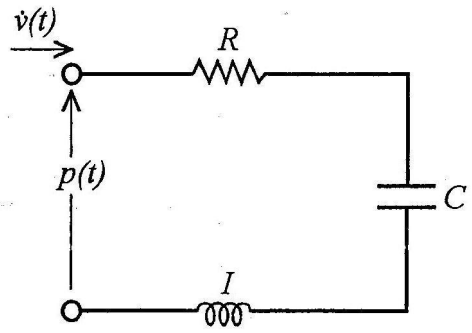

Figure 1.8 One-compartment second-order linear model.

The RIC model is a series combination of a resistance, a compliance and an inertance according to:

$$p(t) = \frac{1}{C} \cdot v(t) + R \cdot \dot{v}(t) + I \cdot \ddot{v}(t)$$

where $p(t)$ is the pressure applied to the respiratory system, $v(t)$ is the pulmonary volume, $\dot{v}(t)$ is the airflow and $\ddot{v}(t)$ its derivative that represents flow acceleration. The term $\frac{1}{C} \cdot v(t)$ corresponds to the pressure necessary to balance elastic forces; it depends on both the volume insufflated in excess of resting volume and the elastance of the respiratory system. On the other hand the term $R \cdot \dot{v}(t)$ corresponds to the pressure necessary to balance frictional forces; it is mainly due to the resistance offered to the airflow. Lastly, the product $I \cdot \ddot{v}(t)$ corresponds to the pressure necessary to overcome the system's inertia (the inertance of the respiratory system) which depends on the airflow derivative.

However, extending further on the frequencies field up to 200 Hz, it is suitable to use models more sophisticated than the simple RIC, utilizing models with more elements (Fig. 1.8).

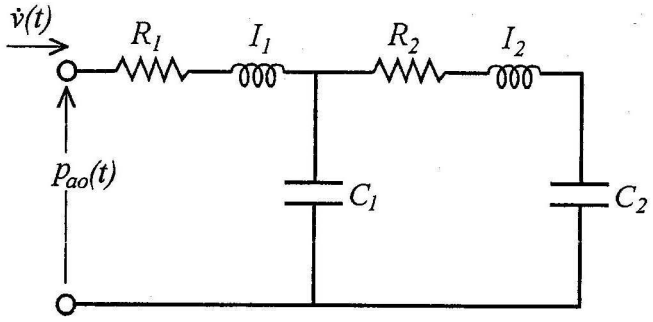

Figure 1.8 Six elements, high frequency linear model.

Chapter 2

Intensive care: mechanical ventilation and HFPV

The use of noninvasive positive pressure ventilation (NPPV) to treat both acute respiratory failure (ARF) and chronic respiratory failure (CRF) has been tremendously expanded in the last two decades in terms of spectrum of diseases to be successfully managed, settings of application/adaptation, and achievable goals [Nava et al, 2009] [Ozsancak et al, 2008] [Annane et al. 2007]. The choice of a ventilator may be crucial for the outcome of NPPV in the acute and chronic setting as poor tolerance and excessive air leaks are significantly correlated with the failure of this ventilatory technique [Scala et al, 2008]. Patient–ventilator dyssynchrony and discomfort may occur when the clinician fails to adequately set NPPV in response to the patient's ventilatory demands both during wakefulness and during sleep [Vignaux et al, 2009; Fanfulla et al, 2007]. This objective may be more easily achieved if the technical peculiarities of the applied ventilator (i.e., efficiency of trigger and cycling systems, speed of pressurization, air leak compensation, CO_2 rebreathing, reliable inspiratory fraction of O_2, monitoring accuracy) are fully understood. With the growing implementation of NPPV, a wide range of ventilators has been produced to deliver a noninvasive support both in randomized controlled trials and in "real life scenarios."

2.1 Classification of conventional ventilators

Even if any ventilator can be theoretically used to start NPPV in both ARF and CRF, success is more likely if the ventilator is able to (a) adequately compensate for leaks; (b) let the clinician continuously monitor patient–ventilator synchrony and ventilatory parameters due to a display of pressure–flow–volume waveforms and a double-limb circuit; (c) adjust the fraction of inspired oxygen (FIO_2) with a blender to ensure stable oxygenation; and (d) adjust inspiratory trigger sensitivity and expiratory cycling as an aid to manage patient–ventilator asynchronies [Scala et al, 2008]. Ventilators may be classified in four categories:

1. *Volume-controlled home ventilators* were the first machines used to deliver NPPV mostly for domiciliary care; even if well equipped with alarms, monitoring system, and inner battery, their usefulness for applying NPPV is largely limited by their inability to compensate for air leaks. Consequently, their application is today restricted to homebased noninvasive support of selected cases of neuromuscular disorders and to invasive support of ventilatory-dependent tracheostomized patients.

2. *Bilevel ventilators* are the evolution of home-based continuous positive airway pressure (CPAP) devices and derive their name from their capability to support spontaneous breathing with two different pressures: an inspiratory positive airway pressure (IPAP) and a lower expiratory positive airway pressure (EPAP) or positive end-expiratory pressure (PEEP). These machines were specifically designed to deliver NPPV thanks to their efficiency in compensating for air leaks. Due to their easy handling, transportability, lack of alarms and monitoring system, and low costs, the first generation of bilevel ventilators matched the needs for nocturnal NPPV in chronic patients with a large ventilatory autonomy. However, traditional bilevel ventilators showed important technical limitations (risk of CO_2 rebreathing due to their single-limb circuit in nonvented masks; inadequate monitoring; lack of alarms and O2 blending, limited generating pressures; poor performance to face the increase in respiratory system load; lack of battery), which have been largely overcome by more sophisticated machines. The newer generations of bilevel ventilators have gained popularity in clinical practice for application of acute NPPV especially in settings with

higher levels of care as well as to invasively support ventilatory-dependent chronic patients at home.

3. *Intensive care unit (ICU) ventilators* were initially designed to deliver invasive ventilation via a cuffed endotracheal tube or tracheal cannula either to sick patients in the ICU or to the theatre room to allow surgery procedures. Despite good monitoring of ventilatory parameters and of flow–pressure–volume waves as well as a fine setting of FIO_2 and of ventilation, performance of conventional ICU ventilators to deliver NPPV is poor as they are not able to cope with leaks. So, a new generation of ICU ventilators has been developed to efficiently assist acute patients with NPPV thanks to the option of leak compensation (i.e., "NPPV mode"), which allows partial or total correction of patient–ventilator asynchrony induced by air leaks, even if with a large intermachine variability.

4. *Intermediate ventilators* combine some features of bilevel, volume-cycled, and ICU ventilators (dual-limb circuit; sophisticated alarm and monitoring systems; inner battery; both volumetric and pressometric modes; wide setting of inspiratory and expiratory parameters). These new machines are studied to meet the patient's needs both in the home and in the hospital care context as well as to safely transport critically ill patients.

2.2 The modes of mechanical ventilation

2.2.1 Volume Assist-Control Mode (ACMV, CMV)

This is the mode used most often at the initiation of mechanically ventilated support to a patient. In the critical care unit, the initiation of mechanical ventilatory support to a patient is usually undertaken when the patient is very sick or unstable. Under such circumstances, it is desirable that the patient be spared any undue excess of work of breathing that could impose a major burden on his cardiorespiratory system. The ACMV mode ensures this. The physician

determines the tidal volume and the respiratory rate according to the needs of the patient. The preset tidal volume – or the guaranteed tidal volume (say, 500 mL) – is delivered at the set rate (say, 12 breaths/min). This guarantees the patient a minimum minute ventilation of 500 mL times 12 breaths/min = 6,000 mL/min.

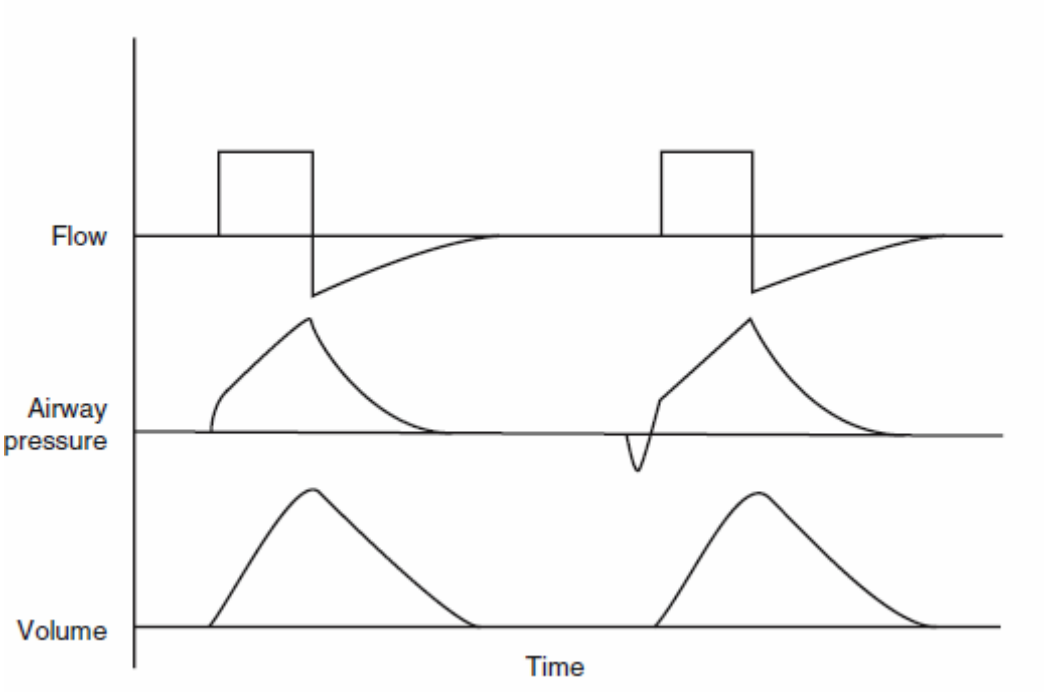

Figure 2.1 Volume-targeted ventilation: The assist-control mode.

2.2.2 Intermittent Mandatory Ventilation (IMV)

In this mode, a certain number of breaths are preset by the physician. These mandatory (compulsory) breaths are compulsorily given to the patient, irrespective of the patient's own demands. The physician sets the tidal volume and the respiratory frequency: mandatory breaths are delivered to the patient intermittently, at equal intervals of time. In between the mandatory breaths, the patient may breathe at his desired respiratory rate. The tidal volume of the *spontaneous breaths* will depend on the strength of the patient's inspiratory effort. When the patient cannot generate sufficient inspiratory force to generate satisfactory tidal volumes during his spontaneous breaths, alveolar hypoventilation can occur – unless the backup

(mandatory) rate has been set high enough to take care of most of the minute ventilation of itself.

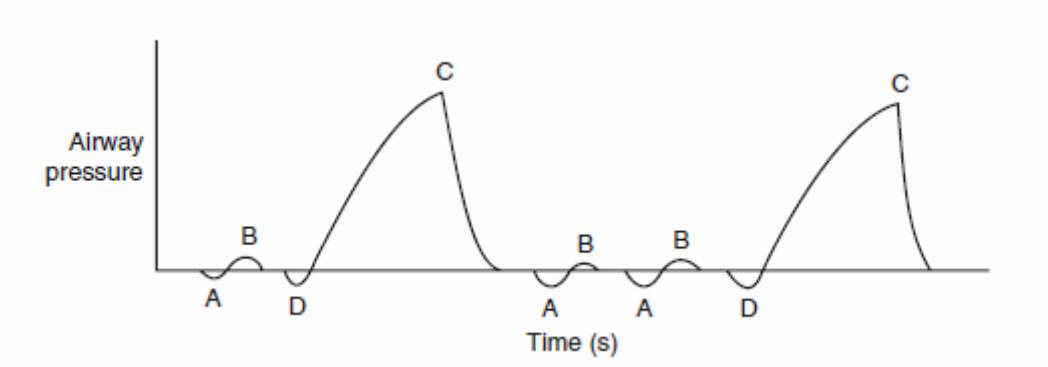

Figure 2.2 Synchronized Intermittent Mandatory Ventilation (SIMV).

Just as in the *control mode* of ventilation, if any asynchrony occurs between the patient's spontaneous inspiration and the ventilator-delivered breath, there can be "clashing" or "breath-stacking". As a result of an innovation designed to prevent patient-ventilator asynchrony, the ventilator detects the onset of the patient's spontaneous inspiratory effort and delivers the mandatory breath in synchrony with it, in a similar manner to that in the assist-control mode. Such a mode of ventilation is called synchronized intermittent mandatory ventilation (SIMV) mode (Fig. 2.2).

2.2.3 Pressure–Support Ventilation (PSV)

During pressure–supported ventilation (PSV), the ventilator augments the inspiratory effort of the patient with positive pressure support. Exhalation is passive. Since the level of the pressure support is physician-preset – given a constant strength of inspiratory effort on the part of the patient – the tidal volumes can be made to rise or fall by varying the level of the pressure support. In other words, the level of pressure support determines the tidal volumes (Fig. 23).

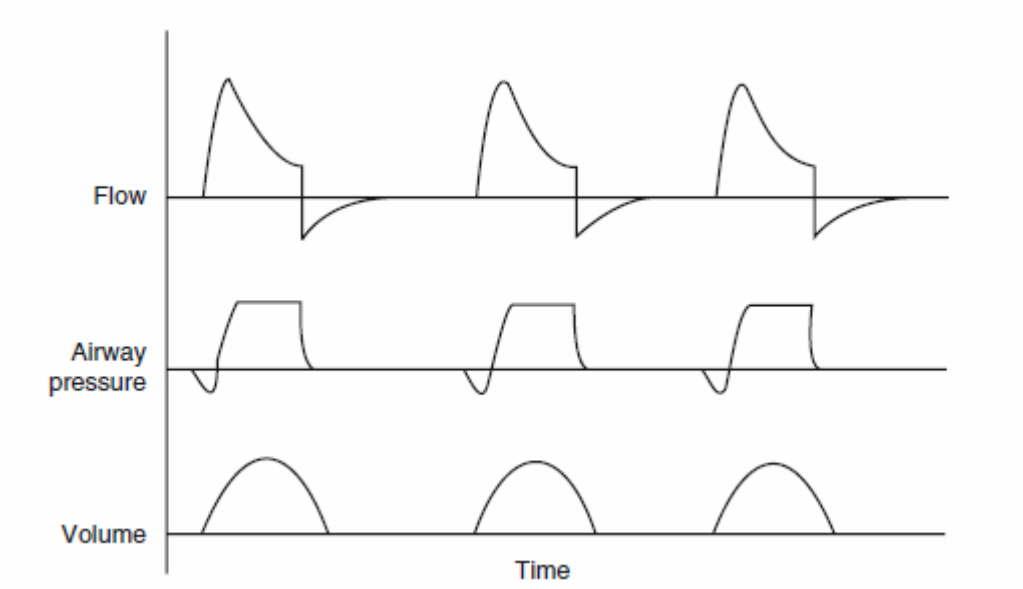

Figure 2.3 Pressure-Support Ventilation (PSV).

2.2.4 Continuous Positive Airway Pressure (CPAP)

In the spontaneously breathing individual, active inspiration is followed by passive expiration, at the end of which the airway pressure falls to the atmospheric level – the pressure at the mouth. Since the pressure at the two ends of a tube must be equal for airflow to cease, at end-expiration, alveolar pressure must necessarily equate with the atmospheric pressure. At end-expiration, alveolar pressure is low, but alveoli are prevented from collapsing completely because of the surfactant within them. When alveoli are diseased, they tend to collapse prematurely. Diseased alveoli have a tendency to collapse completely as they are deficient in surfactant, and if they are allowed to completely close, the magnitude of the force required to reopen them is likely to be considerable This means that the increase in volume is relatively small for a given increase in pressure, and this reflects a poorly compliant system (Fig. 2.4). Whenever compliance decreases for any reason the work of breathing increases. The high pressure required to open up the completely closed alveoli repetitively during each respiratory cycle can overdistend the healthier and more compliant alveoli, predisposing to volutrauma and barotrauma.

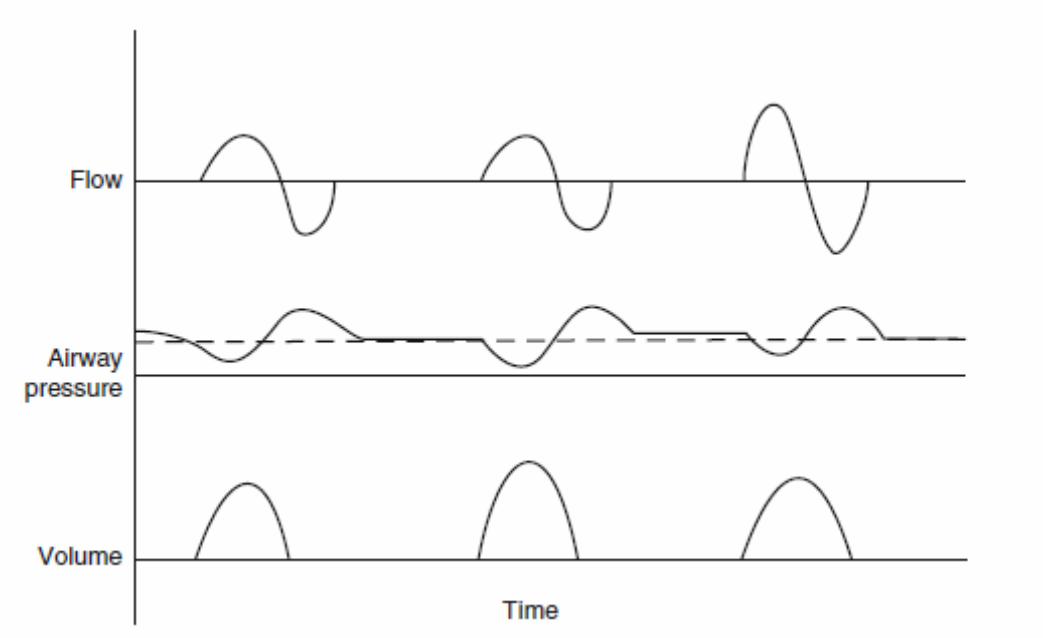

Figure 2.4 Continuous Positive Airway Pressure (CPAP).

2.2.5 Bilevel Positive Airway Pressure

The patient is ventilated at two different levels of CPAP; the switchover from one to the other level of CPAP is synchronized with the patient. Pressure–support can be added at one or both the levels of the CPAP used.

2.2.6 Airway Pressure Release Ventilation (APRV)

APRV involves the periodic release of pressure while breathing in the CPAP mode. The release in pressure may be time-cycled, or may be allowed to occur after a predesignated number of breaths; the latter mode has been termed intermittent mandatory airway pressure

release ventilation (IMPRV): like SIMV, the mandatory breaths can be synchronized to the patient's inspiratory effort.

2.2.7 Pressure-Controlled Ventilation (PCV)

In PCV, the physician only indirectly controls the tidal volume. A certain pressure limit is set. During a ventilator delivered inspiration, as air is driven into the lungs, airway pressure rises, rapidly reaching the preset pressure control level. This pressure is maintained for the duration of inspiration (Fig. 2.5). The pressure limit, the respiratory frequency, and the inspiratory time are physician-preset. Within a given inspiratory time, a higher set pressure limit will allow greater filling of the lungs: more air can enter the lungs before the airflow begins to slow, and so the tidal volumes are larger. Thus in a given patient with stable lung mechanics, the tidal volume increases if the upper pressure limit has been set high and decreases if it has been set at a low level.

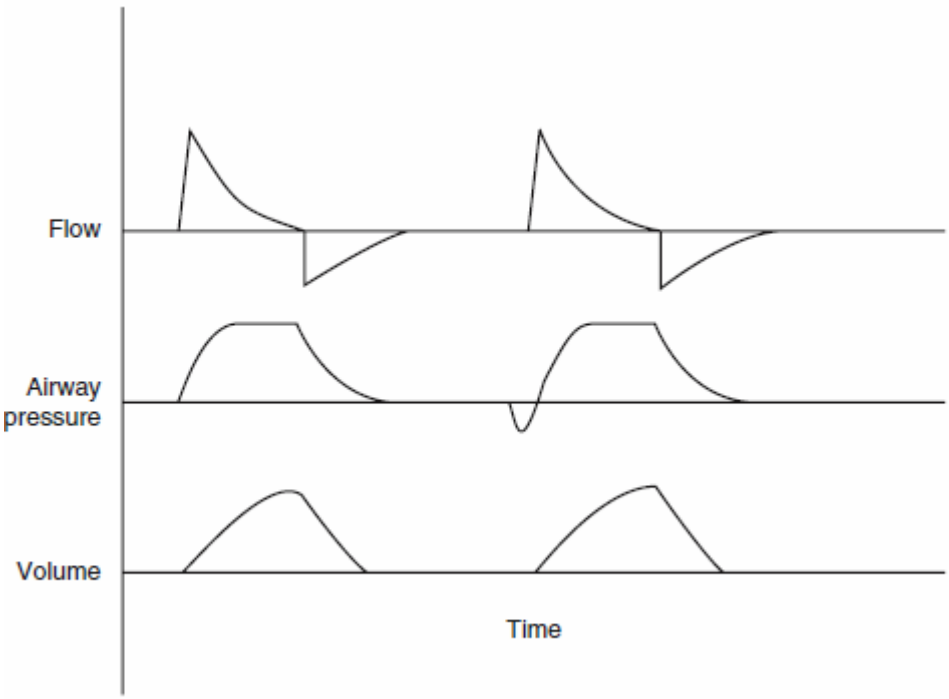

Figure 2.5 Pressure Controlled Ventilation (PCV).

2.2.8 Dual Breath Control

Modern ventilators now incorporate complex computerbased algorithms, and are capable of simultaneously controlling two variables.

Intrabreath control (dual control within a single breath, DCWB): During a part of an essentially pressure-targeted breath, flow is controlled.

Interbreath control (dual control from breath to breath, DCBB): The configuration of a pressure-targeted breath is manipulated to deliver a targeted tidal volume.

2.2.9 High Frequency Ventilation (HFV)

High frequency ventilation is a type of mechanical ventilation that employs very high respiratory rates (>60 breaths per minute) and very small tidal volumes (usually below anatomical dead space). High frequency ventilation is thought to reduce ventilator-associated lung injury (VALI), especially in the context of ARDS and acute lung injury [Krishnan, 2000]. This is commonly referred to as lung protective ventilation. There are different flavors of High frequency ventilation. Each type has its own unique advantages and disadvantages. The types of HFV are characterized by the delivery system and the type of exhalation phase. High Frequency Ventilation may be used alone, or in combination with conventional mechanical ventilation. In general, those devices that need conventional mechanical ventilation do not produce the same lung protective effects as those that can operate without tidal breathing. Specifications and capabilities will vary depending on the device manufacturer.

2.2.9.1 High Frequency Oscillatory Ventilation (HFOV)

High Frequency Oscillatory Ventilation is characterized by high respiratory rates between 3.5 to 15 hertz (210 - 900 breaths per minute). The rates used vary widely depending upon patient size, age, and disease process. In HFOV the pressure oscillates around the constant distending pressure (equivalent to Mean Airway Pressure (MAP) which in effect is the same

as Positive End Expiratory Pressure (PEEP). Thus gas is pushed into the lung during inspiration, and then pulled out during expiration. HFOV generates very low tidal volumes that are generally less than the dead space of the lung. Tidal volume is dependent on endotracheal tube size, power and frequency. Different mechanisms (Direct Bulk Flow - convective, Taylorian dispersion, Pendelluft effect, Asymmetrical velocity profiles, Cardiogenic mixing and Molecular diffusion) of gas transfer are believed to come into play in HFOV compared to normal mechanical ventilation. It is often used in patients who have refractory hypoxemia that cannot be corrected by normal mechanical ventilation such as is the case in the following disease processes: severe ARDS, ALI and other oxygenation diffusion issues. In some neonatal patients HFOV may be used as the first-line ventilator due to the high susceptibility of the premature infant to lung injury from conventional ventilation.

2.2.9.2 High Frequency Jet Ventilation (HFJV)

High Frequency Jet Ventilation employs an endotracheal tube adaptor in place for the normal 15 mm ET tube adaptor. A high pressure “jet” of gas flows out of the adaptor and into the airway. This jet of gas occurs for a very brief duration, about 0.02 seconds, and at high frequency: 4-11 hertz. Tidal volumes $\leq$ 1 ml/Kg are used during HFJV. This combination of small tidal volumes delivered for very short periods of time create the lowest possible distal airway and alveolar pressures produced by a mechanical ventilator. Exhalation is passive. Jet ventilators utilize various I:E ratios--between 1:1.1 and 1:12-- to help achieve optimal exhalation. Conventional mechanical breaths are sometimes used to aid in reinflating the lung. Optimal PEEP is used to maintain alveolar inflation and promote ventilation-to-perfusion matching. Jet ventilation has been shown to reduce ventilator induced lung injury by as much as 20%.

2.2.9.3. High Frequency Flow Interruption (HFFI)

High Frequency Flow Interruption is similar to HFJV but the gas control mechanism is different. Frequently a rotating bar or ball with a small opening is placed in the path of a high pressure gas. As the bar or ball rotates and the opening lines-up with the gas flow, a small,

brief pulse of gas is allowed to enter the airway. Frequencies for HFFI are typically limited to maximum of about 15 hertz.

2.2.9.4. High Frequency Positive Pressure Ventilation (HFPPV)

High Frequency Positive Pressure Ventilation is typically utilized by using a conventional ventilator at the upper frequency range of the device (typically 90-100 breaths per minute). A conventional breath type is used and tidal volumes are usually higher than (HFOV, HFJV and HFFI). With newer and specifically designed devices becoming popular, HFPPV is rarely used clinically any more.

2.3 High-Frequency Percussive Ventilation (HFPV)

HFPV is a non conventional ventilation mode which makes use of a phasitron, an inspiratory–expiratory valve through which gas at high pressure is driven phasically. In HFPV, HFV breaths are superimposed upon conventional pressure-controlled, time-cycled machine breaths. HFV breaths are pulsed at about 200–900 breaths/min, over “background” PCV breaths cycled at about 10–15 times a minute. In other words, HFOV breaths are given at alternating – inspiratory and expiratory – pressure levels [Salim et al, 2005]. Ventilation at relatively low airway pressures is made possible. Thus, HFPV is capable of improving both oxygenation and ventilation without exposing the patient to the effects of high intrathoracic pressure. As a consequence, it has less of a propensity to produce hypotension, barotrauma, or intracranial hypertension in blunt head injury than do other modes. HFPV appears to be superior at mobilizing secretions than are other modes of HFV [Salim et al, 2005]. Pharmacologic paralysis is not generally required.

2.3.1 Principles of HFPV

One of several controversial aspects surrounding modes of high frequency ventilation (HFV) is that there is no universally accepted classification or defined nomenclature for these various methods [Froese AB, 1984] Depending on the frequency used, the maneuvers may be divided into high frequency jet ventilation (HFJV) and its variant, high frequency flow interruption (HFFI), high frequency oscillation (HFO) and high frequency positive pressure ventilation (HFPPV). Basically, HFPPV uses lower frequencies (60-300 cycles/min), while HFO uses higher frequencies (60-2400 cycles/min). However, this classification does not take into account that HFO can also use low working frequencies. Technically, all modes of HFV share at least 3 basic elements: a high pressure flow generator, a safety valve, and a breathing circuit connected to the patient [Gioia et al, 1985] [Branson, 1995]. HFPV may be defined as flow-regulated time-cycled ventilation that creates controlled pressure and delivers a series of high frequency subtidal volumes in combination with low frequency breathing cycles. The only system that delivers HFPV is the VDR® 4 (Volumetric Diffusive Respiration). The system may be defined as a time-cycled pressure-controlled ventilator equipped with a high frequency flow generator connected to a device (the phasitron) that provides the interface between the patient and the machine

2.3.2 General characteristics of HFPV system

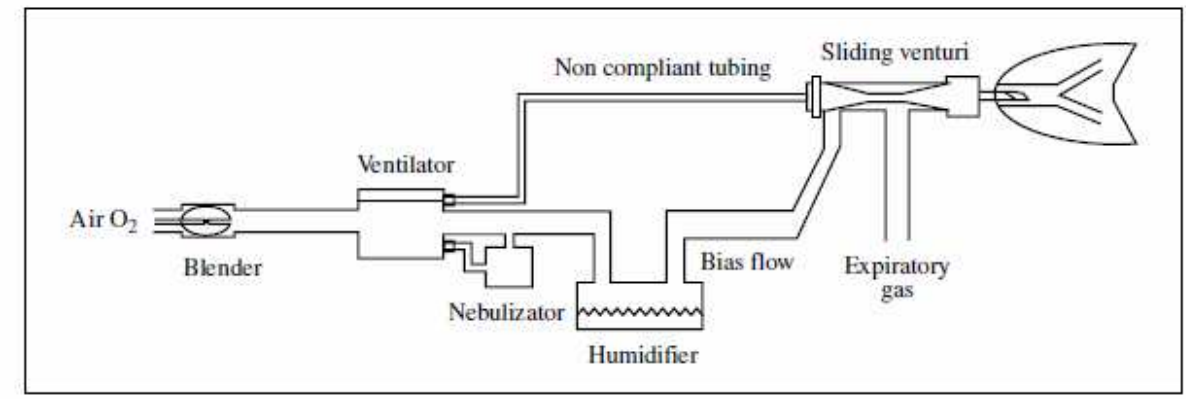

Figure 2.6 Schematic diagram of the HFPV system.

Figure 2.6 is a schematic diagram of the circuit. The ventilator is connected to a high pressure air generator, fed by 2 normal sources of oxygen and air. Two inspiratory circuits, a high pressure and a low pressure circuit, branch off the ventilator. The low pressure circuit is connected to 2 systems located downstream from one another, the humidifier and the nebulizer. The 2 circuits are connected to the phasitron from which the expiratory circuit branches. The phasitron also has a system for real time recording and visualization of pressure delivered to the patient. Measurement is made distal to the high pressure pulsatile flow source, which is located near the connection to the endotracheal tube.

The nebulization system (Figure 2.7) is connected to a volume reservoir and served by an accessory line that delivers a high pressure flow synchronized with that connected to the phasitron. This feature allows administration of aerosolized bronchodilators and mucolytic agents to reduce the viscosity of secretions so that they can be liquefied and more effectively

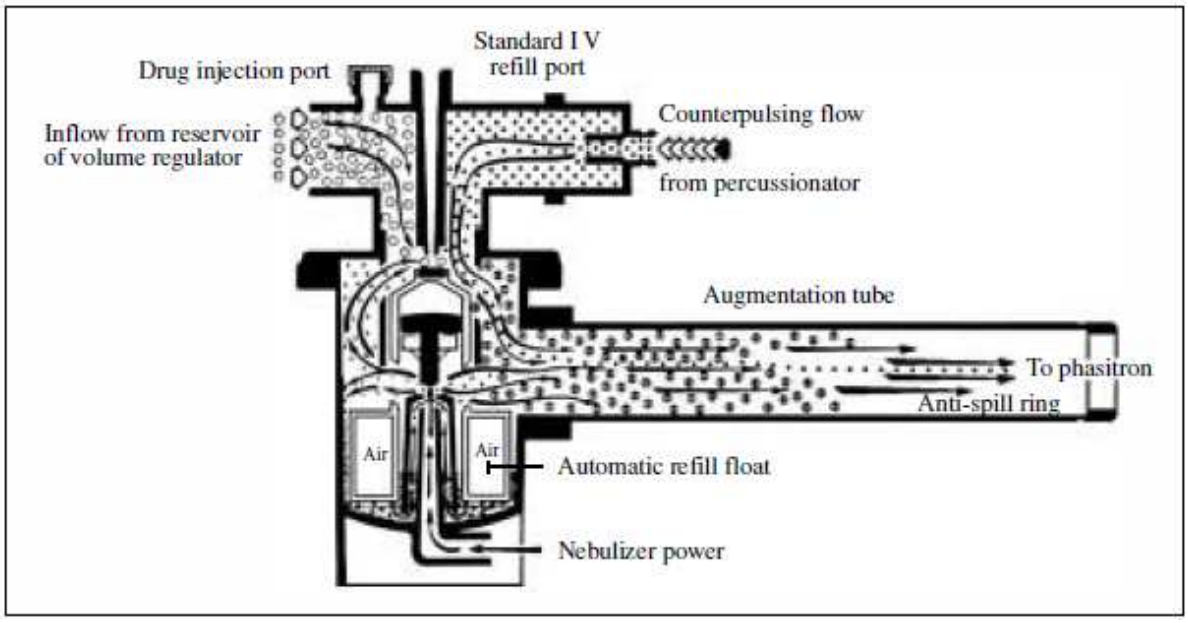

Figure 2.7 Nebulization system during HFPV.

removed. The nebulization and humidification systems provide the inspiratory circuit with a gas mixture that is appropriately heated and 100% humidified.

The phasitron constitutes the heart of this mode of ventilation. It is composed of a hollow cylinder in which the airflow from the high pressure circuit causes a spring-controlled piston to move back and forth (Figure 2.8).

Based on the Venturi principle, the low pressure inspiratory circuit, which is connected to the humidification and nebulization systems, supports a flow volume delivery that is inversely proportional to the pressure reached at the level of the airways; in other words, when the system approaches the desired pressure level, the fraction of delivered air comes almost exclusively from the high pressure circuit.

The phasitron has 2 safety vales, an inspiratory and an expiratory valve, that ensure that the set pressure is maintained at the level of the airways; a 3rd expiratory safety valve is connected to the volume reservoir. In this way, the circuit remains constantly open to room air and allows the patient to enter at any phase of the breathing cycle, without further increasing the working pressure.

Here it is important to underline that the circuit can be used in both pediatric and adult patients.

The modalities of function of the phasitron and the characteristics of the breathing circuit provide for several interesting considerations concerning the capacities of HFPV. The phasitron permits the delivery of flow volumes through a series of mini-bursts until a pressure plateau is reached whose value and duration are operator programmable. Due to the Venturi effect, the flow delivered is converted into pressure (and viceversa) by adapting to thoracopulmonary resistance. These factors permit the flow distribution to be optimized at the level of the airways, obverting preferential ventilation, and allow the mean airway pressure to be kept relatively stable against the elastic and resistant forces of the respiratory structures, unless the VDR® 4 parameters are changed. Furthermore, since the circuit is open to room air, the risk of barotrauma is limited.

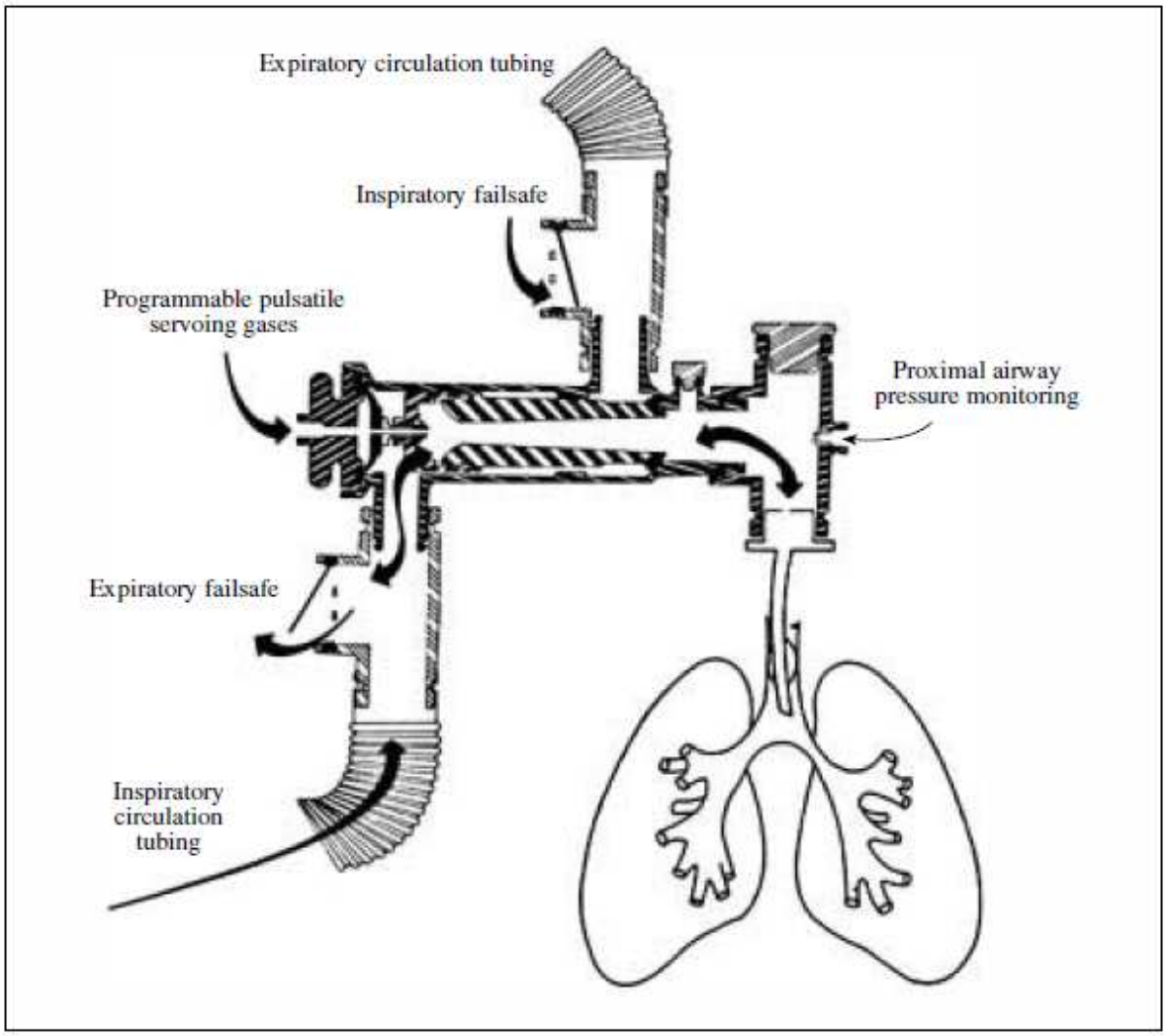

Figure 2.8 Schematic diagram of the connections to the Phasitron.

Chapter 3

The pulmonary function laboratory

The purpose of a pulmonary function laboratory is to obtain clinically useful data from patients with respiratory dysfunction. The pulmonary function tests (PFTs) within this laboratory fulfill a variety of functions. They permit quantification of a patient's breathing deficiency, diagnosis of different types of pulmonary diseases, evaluation of a patient's response to therapy, and preoperative screening to determine whether the presence of lung disease increases the risk of surgery. Although PFTs can provide important information about a patient's condition, the limitations of these tests must be considered. First, they are nonspecific in that they cannot determine which portion of the lungs is diseased, only that the disease is present. Second, PFTs must be considered along with the medical history, physical examination, x-ray examination, and other diagnostic procedures to permit a complete evaluation. Finally, the major drawback to *some PFTs* is that they require a full patient cooperation and for this reason cannot be conducted on critically ill patients. Consider some of the most widely used PFTs: spirometry, body plethysmography, and diffusing capacity.

3.1 Spirometry

The simplest PFT is the spirometry maneuver. In this test, the patient inhales to total lung capacity (TLC) and exhales forcefully to residual volume. The patient exhales into a

displacement bell chamber that sits on a water seal. As the bell rises, a pen coupled to the bell chamber inscribes a tracing on a rotating drum. The spirometer offers very little resistance to breathing; therefore, the shape of the spirometry curve (Fig. 3.1) is purely a function of the patient's lung compliance, chest compliance, and airway resistance. At high lung volumes, a rise in intrapleural pressure results in greater expiratory flows. However, at intermediate and low lung volumes, the expiratory flow is independent of effort after a certain intrapleural pressure is reached. Measurements made from the spirometry curve can determine the degree of a patient's ventilatory obstruction. Forced vital capacity (FVC), forced expiratory volumes

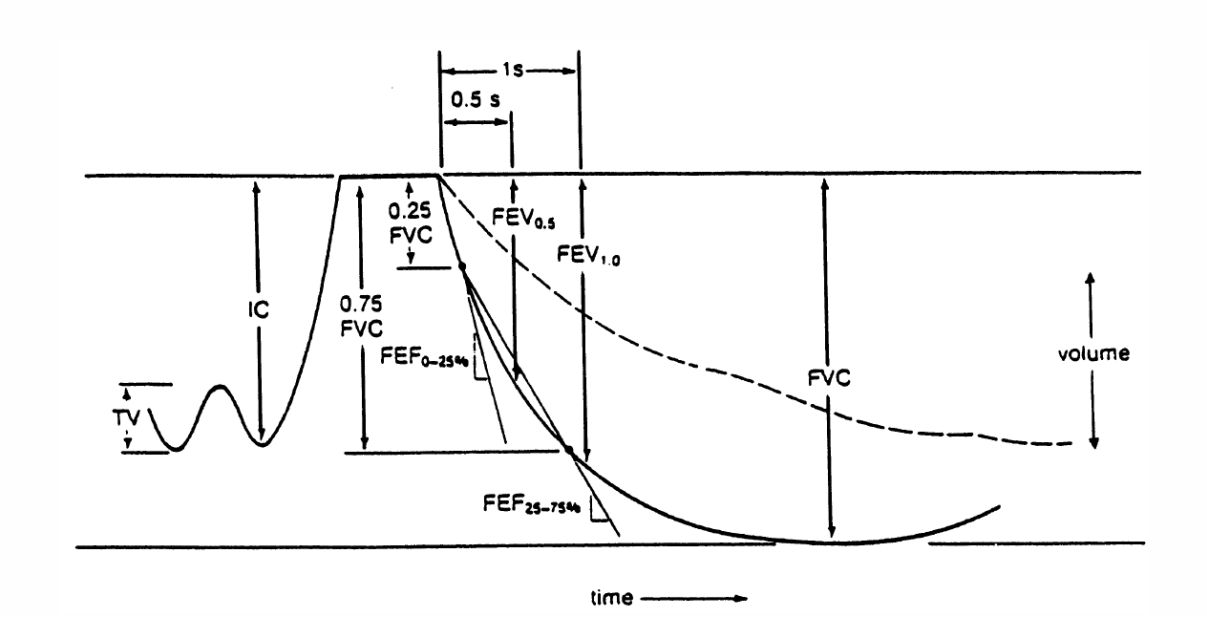

Figure 3.1 Typical spirometry tracing obtained during testing; inspiratory capacity (IC), tidal volume (TV), forced vital capacity (FVC), forced expiratory volume (FEV), and forced expiratory flows. Dashed line represents a patient with obstructive lung disease; solid line represents a normal, healthy individual.

(FEV), and forced expiratory flows (FEF) can be determined. The FEV indicates the volume that has been exhaled from TLC for a particular time interval. For example, FEV0.5 is the volume exhaled during the first half-second of expiration, and FEV1.0 is the volume exhaled during the first second of expiration; these are graphically represented in Fig. 3.1. Note that the more severe the ventilatory obstruction, the lower are the timed volumes (FEV0.5 and FEV1.0). The FEF is a measure of the average flow (volume/time) over specified portions of the spirometry curve and is represented by the slope of a straight line drawn between volume levels. The average flow over the first quarter of the forced expiration is the FEF0–25%,

whereas the average flow over the middle 50% of the FVC is the FEF25–75%. These values are obtained directly from the spirometry curves. The less steep curves of obstructed patients would result in lower values of FEF0–25% and FEF25–75% compared with normal values, which are predicted on the basis of the patient's sex, age, and height. Equations for normal values are available from statistical analysis of data obtained from a normal population. Test results are then interpreted as a percentage of normal.

Another way of presenting a spirometry curve is as a flow-volume curve. Figure 3.2 represents a typical flow-volume curve. The expiratory flow is plotted against the exhaled volume, indicating the maximum flow that may be reached at each degree of lung inflation. Since there is no time axis, a time must mark the FEV0.5 and FEV1.0 on the tracing. To obtain these flow-volume curves in the laboratory, the patient usually exhales through a pneumotach.

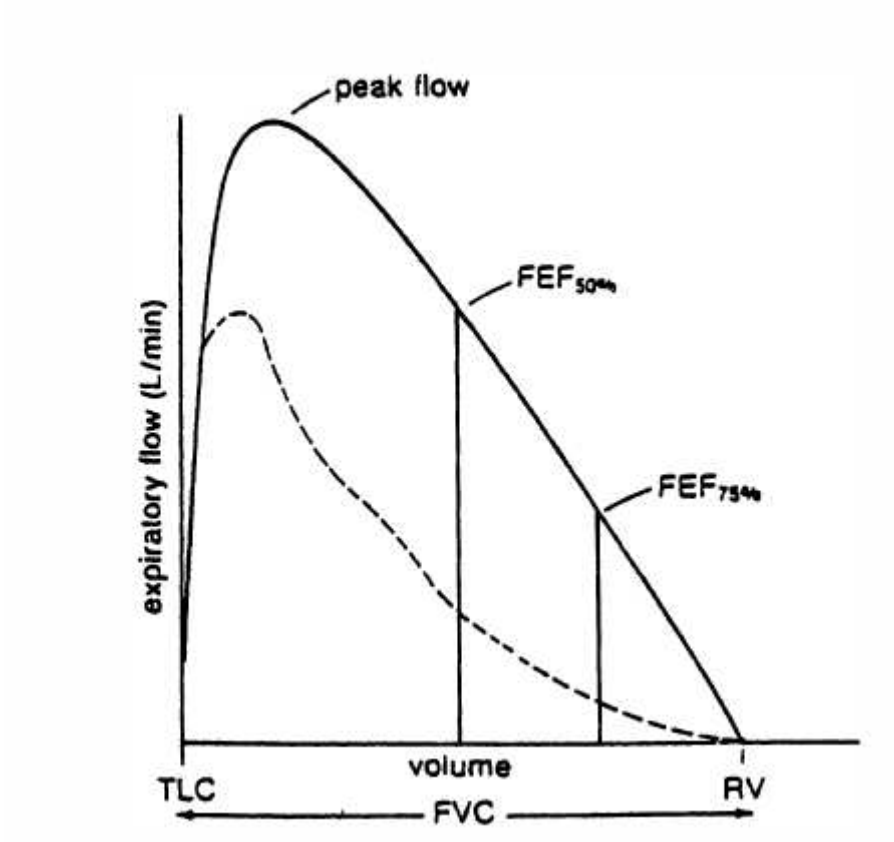

Figure 3.2 Flow-volume curve obtained from a spirometry maneuver. Solid line is a normal curve; dashed line represents a patient with obstructive lung disease.

The most widely used pneumotachograph measures a pressure drop across a flow-resistive element. The resistance to flow is constant over the measuring range of the device; therefore, the pressure drop is proportional to the flow through the tube. This signal, which is indicative of flow, is then integrated to determine the volume of gas that has passed through the tube. Another type of pneumotach is the heated-element type. In this device, a small heated mass responds to airflow by cooling. As the element cools, a greater current is necessary to maintain a constant temperature.This current is proportional to the airflow through the tube. Again, to determine the volume that has passed through the tube, the flow signal is integrated. The flow-volume loop in Fig. 3.3 is a dramatic representation displaying inspiratory and expiratory curves for both normal breathing and maximal breathing. The result is a graphic representation of the patient's reserve capacity in relation to normal breathing. For example, the normal patient's tidal breathing loop is small compared with the patient's maximum breathing loop. During these times of stress, this tidal breathing loop can be increased to the boundaries of the outer ventilatory loop. This increase in ventilation provides the greater gas exchange needed during the stressful situation. Compare this condition with that of the patient with obstructive lung disease. Not only is the tidal breathing loop larger than normal, but the maximal breathing loop is smaller than normal. The result is a decreased ventilatory reserve, limiting the individual's ability to move air in and out of the lungs. As the disease progresses, the outer loop becomes smaller, and the inner loop becomes larger.

The primary use of spirometry is in detection of obstructive lung disease that results from increased resistance to flow through the airways. This can occur in several ways:

1. Deterioration of the structure of the smaller airways that results in early airways closure.
2. Decreased airway diameters caused by bronchospasm or the presence of secretions increases the airway's resistance to airflow.
3. Partial blockage of a large airway by a tumor decreases airway diameter and causes turbulent flow.

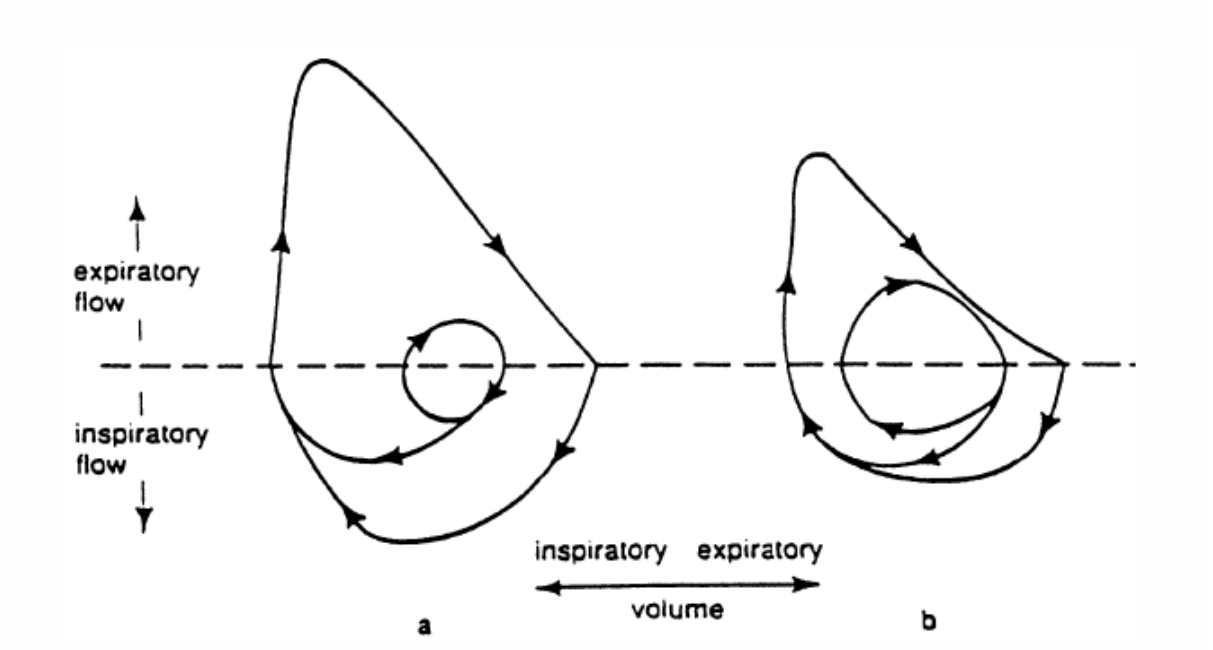

Figure 3.3 Typical flow-volume loops. (a) Normal flow-volume loop. (b) Flow-volume loop of patient with obstructive lung disease.

Spirometry has its limitations, however. It can measure only ventilated volumes. It cannot measure lung capacities that contain the residual volume. Measurements of TLC, FRC, and RV have diagnostic value in defining lung overdistension or restrictive pulmonary disease; the body plethysmograph can determine these absolute lung volumes.

3.2 Body Plethysmography

In a typical plethysmograph, the patient is put in an airtight enclosure and breathes through a pneumotach. The flow signal through the pneumotach is integrated and recorded as tidal breathing. At the end of a normal expiration (at FRC), an electronically operated shutter occludes the tube through which the patient is breathing. At this time the patient pants lightly against the occluded airway. Since there is no flow, pressure measured at the mouth must equal alveolar pressure. But movements of the chest that compress gas in the lung

simultaneously rarify the air in the plethysmograph, and vice versa. The pressare change in the plethysmograph can be used to calculate the volume change in the plethysmograph, which is the same as the volume change in the chest. This leads directly to determination of FRC. At the same time, alveolar pressure can be correlated to plethysmographic pressure. Therefore, when the shutter is again opened and flow rate is measured, airway resistance can be obtained as the ratio of alveolar pressure (obtainable from plethysmographic pressure) to flow rate [Carr and Brown, 1993]. Airway resistance is usually measured during panting, at a nominal lung volume of FRC and flow rate of ±1 liter/s.

Airway resistance during inspiration is increased in patients with asthma, bronchitis, and upper respiratory tract infections. Expiratory resistance is elevated in patients with emphysema, since the causes of increased expiratory airway resistance are decreased driving pressures and the airway collapse. Airway resistance also may be used to determine the response of obstructed patients to bronchodilator medications.

3.3 Diffusing Capacity

So far the mechanical components of airflow through the lungs have been discussed. Another important parameter is the diffusing capacity of the lung, the rate at which oxygen or carbon dioxide travel from the alveoli to the blood (or vice versa for carbon dioxide) in the pulmonary capillaries. Diffusion of gas across a barrier is directly related to the surface area of the barrier and inversely related to the thickness. Also, diffusion is directly proportional to the solubility of the gas in the barrier material and inversely related to the molecular weight of the gas. Lung diffusing capacity (DL) is usually determined for carbon monoxide but can be related to oxygen diffusion. The popular method of measuring carbon monoxide diffusion utilizes a rebreathing technique in which the patient rebreathes rapidly in and out of a bag for approximately 30 s. Figure 3.4 illustrates the test apparatus. The patient begins breathing from a bag containing a known volume of gas consisting of 0.3% to 0.5 carbon monoxide made with heavy oxygen, 0.3% to 0.5% acetylene, 5% helium, 21% oxygen, and a balance of nitrogen.

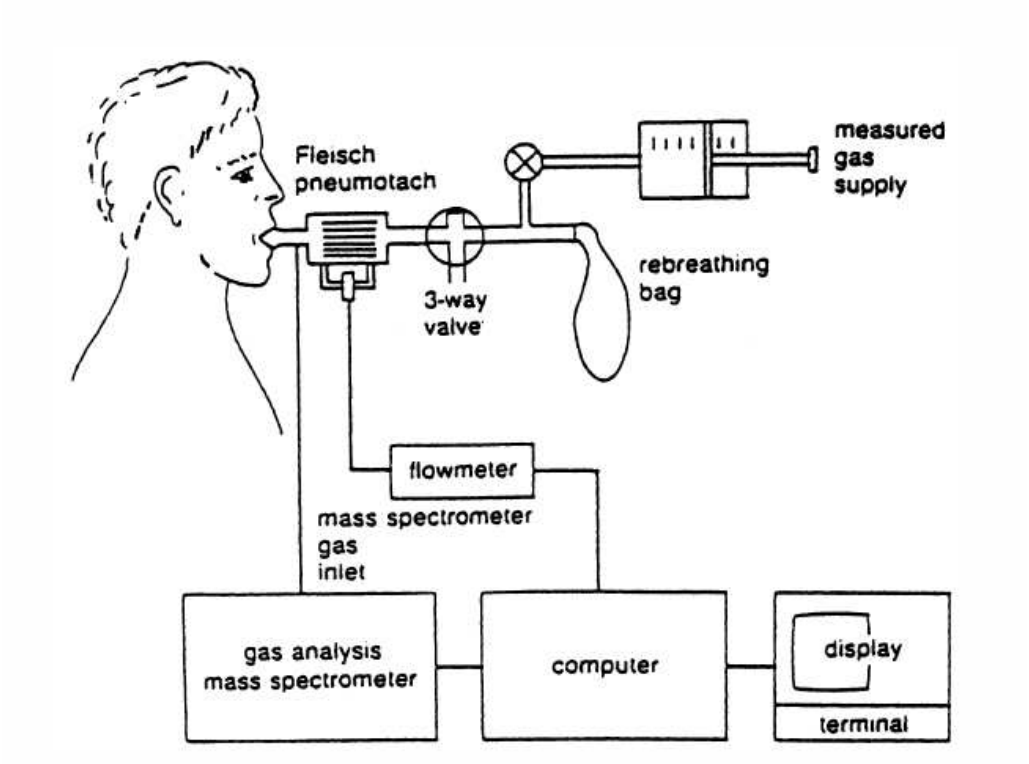

Figure 3.4 Typical system configuration for the measurement of rebreathing pulmonary diffusing capacity.

As the patient rebreathes the gas mixture in the bag, a modified mass spectrometer continuously analyzes it during both inspiration and expiration. During this rebreathing procedure, the carbon monoxide disappears from the patient-bag system; the rate at which this occurs is a function of the lung diffusing capacity. The helium is inert and insoluble in lung tissue and blood and equilibrates quickly in unobstructed patients, indicating the dilution level of the test gas. Acetylene, on the other hand, is soluble in blood and is used to determine the blood flow through the pulmonary capillaries. Carbon monoxide is bound very tightly to hemoglobin and is used to obtain diffusing capacity at a constant pressure gradient across the alveolar-capillary membrane. Decreased lung diffusing capacity can occur from the thickening of the alveolar membrane or the capillary membrane as well as the presence of interstitial fluid from edema. All these abnormalities increase the barrier thickness and cause a decrease in diffusing capacity. In addition, a characteristic of specific lung diseases is impaired lung diffusing capacity. For example, fibrotic lung tissue exhibits a decreased permeability to gas transfer, whereas pulmonary emphysema results in the loss of diffusion surface area.

Chapter 4

State of the art of methods and instruments for analysis of respiratory parameters

Post-operative analysis of respiratory mechanics in mechanically ventilated patients is useful for evaluating patient status and assessing the effect of therapy in intensive care units (ICUs). It is important to have knowledge of two main quantities which characterize breathing mechanical properties; total compliance, often measured under static conditions as an indicator of lung and chest-wall elasticity and total flow resistance, which reflects properties of both the tissue and the peripheral airways.

Several studies characterizing the main aspects of breathing mechanics have been published in recent years. These have used different lumped-parameter models, ranging from the simple two-element resistance-compliance linear model to more sophisticated physiological models which include tissue viscoelasticity, the inertial effects of the airways and branching networks, to non-linear models. However, working with non-linear models precludes the use of many powerful concepts usually adopted in the clinical investigation of respiratory mechanics (for example, the use of frequency-domain analysis: Bode diagrams and input impedance).

4.1 Linear model of first order

The simplest lumped-parameter model proposed in literature for the identification of respiratory mechanics in mechanically ventilated is the linear model with a series of two parameters: a resistance R and an elastance E. This model has had great success in clinical practice for the substance of its simplicity, the immediate interpretation of his physiological parameters and its sensitivity to changes in lung mechanics. The output of the model at each instant of time is:

$$P(t) = R \cdot Q(t) + E \cdot \Delta V(t) + P_0$$

where P(t) represents, as appropriate, the pressure at the mouth or the transpulmonary pressure; Q(t) is the total flow at the mouth; ΔV(t), obtained by numerical integration of Q(t), reflects changes in the volume of air compared with an initial reference volume; P_0 is the pressure corresponding to Q(t) and ΔV(t) both zero. In discrete time, the parameters of equation can easily be estimated from sample points by simple linear regression. Recent studies [Avanzolini G. et al, 1995; Bates J.H.T. and Lauzon A.M., 1992] have shown that this model provides a too simplified representation of the non-linearity and multi-compartmental aspects of respiratory mechanics. It is for example known as upper airway resistance is a nonlinear function of flow and as the total resistance depends on the tidal volume and is different during inspiratory and expiratory, being a continuous function of time throughout the respiratory cycle. Therefore, the parameter estimates based on first-order model depends not only on the state of the patient, but also by the experimental conditions (ventilation characteristics) as the model assumes a linearization in the neighborhood of set point.

4.2 Multivariate linear models

A first category of more complex models proposed to overcome the problem, preserves the benefits derived from the linear regression. Dependence on experimental conditions is explained by non-linear combinations of the signals of flow and volume. To consider the turbulent flow can introduce a combined signal $Q(t)\cdot|Q(t)|$, to describe the nonlinear behavior of the smaller airways, you can use $\frac{Q(t)}{\Delta V^2(t)}$; finally, to characterize the nonlinearity of the pressure-volume relation, you can use a quadratic term of volume ΔV^2. The resulting model is then:

$$P(t) = R\cdot Q(t) + k_1\cdot|Q(t)|\cdot Q(t) + k_2\cdot\frac{Q(t)}{\Delta V^2(t)} + E\cdot\Delta V(t) + k_3\cdot\Delta V^2(t)$$

It should be noted how it is possible to identify non-linear elastic and resistive properties. In practice, however, there are significant correlations between the terms of the equation that can make inaccurate estimates of the different parameters and therefore of poor clinical significance. Therefore, having chosen a number of components (functions of flow and volume), proceed with statistical techniques (stepwise regression analysis) for the selection of only significant components. This gives the added benefit of being able to identify the only really significant nonlinear characteristics.

4.3 Separate estimations in inspiration and expiration

A further refinement of the above procedure is to separate the estimates in both inspiratory and expiratory phases. Recent studies [Barbini P. et al, 2001] have shown how a simple model consisting of three constant parameters, only a total elastance over the cycle and two total resistance, one inspiratory and one expiratory, represents a significant improvement in

adjusting to the experimental data does not go to the expense of accuracy in the estimation of parameters. The corresponding equation is:

$$P(t) = R_I \cdot Q_I(t) + R_E \cdot Q_E(t) + E \cdot \Delta V(t) + P_0$$

where Q_I and Q_E are equal to the total flow Q only in the inspiratory and expiratory phase and zero elsewhere.

The above mentioned work shows that it is possible to estimate two separate resistive components, inspiratory and expiratory, and it is not necessary to decompose the elastance.

4.4 Linear models of higher order

A second approach to improve adaptation to the model of the first order is to consider higher-order linear models. However, both because of the limited frequency band signals of breathing, and because inertial effects are negligible, it is limited in practice to identify models of second order with two elastic and two viscous parameters. Systems theory can describe the linear models in the domain of the Laplace transform, via a transfer function. In the case of such models of second order, that is:

$$G(s) = \frac{P(s)}{Q(s)} = \frac{a \cdot s^2 + b \cdot s + c}{s \cdot (s + d)}$$

where a, b, c and d are the parameters to identify from flow and pressure signals. In the time domain the equation is represented by a pair of first-order linear differential equations (state equations) and an algebraic equation which expresses the output P(t) as a linear combination of the two state variables $x_1(t)$ and $x_2(t)$ and input Q(t). There are several electrical realizations of this equations, including those known as models of Mead, Otis and Mount. The resistance and elastance of each model contribute to compose the parameters of

G(s) and therefore they are obtainable algebraically. With reference to electrical analogy, G(s) is clearly interpretable as respiratory impedance and can be easily assessed by applying the theory of linear electric circuits.

4.5 Estimation of parameters by the least squares method

In the time domain, we define the following criteria function:

$$F_t(\theta) = \sum_{k=1}^{N} \left[P_s(k \cdot T) - P(k \cdot T, \theta) \right]^2$$

where θ is the vector of parameters, T is the sampling time, N is the number of sampled points, $P_s(k \cdot T)$ the k-th sampled value of the experimental pressure and $P(k \cdot T, \theta)$ the corresponding pressure predicted by the model. When the discrete-time model, $P(k \cdot T, \theta)$ is linear respect to θ, the equation reduces to a quadratic form with an only analytical minimal. It is shown that the value of the parameter vector obtained at this minimum represents an optimal estimation of the parameters. If on the contrary the model can not be represented in discrete form as a linear combination of its parameters, the minimum is found using iterative numerical optimization. The difficulties in the use of such algorithms, which require an initialization, are usually related to the presence of multiple local minimum on which the procedure can converge to different choices depending on the initial vector of parameters.

It is clear that it is extremely advantageous to have representation in linear discrete-time domain. To this purpose, especially in the case of models of higher order, it is convenient to describe the system directly in discrete time domain using finite difference equations obtained by methods of numerical integration of equations of state. The system is then represented by its transfer function G(z) in the domain of z-transformed. G(z) is alternatively obtained directly from G(s) using affine transformations from s space to z space, among which the best known are the impulse-invariance, the step-invariance and bilinear transformation. With

inverse Laplace, you can then express the output of discrete-time model $P(k \cdot T)$ as a linear combination of r (order of model) parameters α_i (i = 1, 2, ..., r) associated with output evaluated up to r previous samples and s+1 parameters β_i (i = 0, 1, 2, ..., s) related to the input evaluated at the current sample and s previous samples, that:

$$P(k \cdot T) = -\sum_{k=1}^{r} \alpha_i \cdot P[(k-i) \cdot T] + \sum_{i=0}^{s} \beta_i \cdot Q[(k-i) \cdot T]$$

This equation is called the autoregressive equation and this is a linear relationship in the parameters α_i and β_i that compose the vector θ and can therefore be estimated analytically by least squares techniques are very similar to the previous case. In particular, estimates of the viscoelastic parameters of these models of second order can be obtained by algebraic transformations of the parameter estimates of the corresponding discrete-time autoregressive equation.

The accuracy in the estimation of parameters is evaluated through a confidence region centered around $\hat{\theta}$. In terms of linearity is also defined in a closed form, otherwise is usually approximated by the algorithm of numerical optimization

The ability of the model to reproduce the experimental data (adaptation) can be assessed by the square root mean square error, commonly referred to as the RMSE (root-mean-square error), in percentage to peak pressure

Chapter 5

Development of innovative instruments for acquisition of respiratory variables

This chapter describes the instruments design and development process in the Biomedical Instrumentation Laboratory at the Trieste University [Riscica et al.2009, Riscica et al.2010].

5.1 Instrument for Pressure and Flow measurement

Existing methods for measuring respiratory parameters (pressure and flow) during the high-frequency percussive ventilation employ two different transducers [Lucangelo et al 2004]. The first is an unipolar pressure transducer that measures the absolute value of pressure in the upper respiratory tract of the patient, with a magnitude of some tens of H_2O centimetres. This measure is not critical and it is executed using suitable conditioned transducer. The other transducer quantifies the flow by using a Fleisch pneumotacograph, which converts the flow in a differential pressure, subsequently measured by using a high sensitivity pressure transducer. The typical values of flow, expressed as litres per second, are converted by the pneumotacograph in a differential pressure measured in millimetres of H_2O.

To increase the sensitivity of the system and to overcome the fast variation of the respiratory parameters in the high-frequency percussive ventilation, it is necessary to condition the output of the transducer with a sophisticated and expensive apparatus (Validyne MP-45 with carrier demodulator). This fact produces some limitations in the study of percussive ventilator carried out through offline analysis of the acquired values after analogue to digital conversion.

Manufacturer	Model	Pressure Range	Response Time
Sensym	ASDX001D44D	±70 cm H2O	2.73 – 1.11 ms
Sensirion	SDP1000-L025	±0.25 cm H2O	40 ms
Sensor Technics	HCLA02X5DB	±2.5 cm H2O	0.5 ms
All Sensors	0.25INCH-D-4V	±0.63 cm H2O	0.5 ms

Table 5.1 Pressure transducers comparison

The developed prototype is based on the use of pressure transducers of new generation with high sensitivity and reduced response time (ALL SENSORS, Amplified Very Low Pressure Sensors Series). The choice of pressure transducer was based on the features comparison of some 12-bit amplified differential low pressure sensors (Table 5.1).

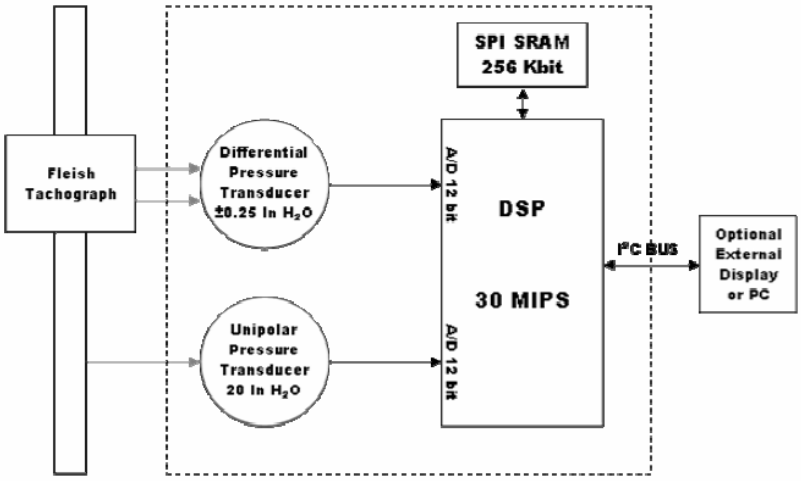

Figure 5.1 Block diagram of the DSP-based acquisition device

The block diagram (Fig.5.1) illustrates the structure of the new acquisition device. The amplified line of low pressure sensors (ALL SENSORS 0.25INCH–D-4V, 20INCH-G-4V) is based upon a proprietary technology able to reduce all output offset or common mode errors. This model provides a ratiometric 4 volt output with superior output offset characteristics. Output offset errors, due to temperature changes, as well as position sensitivity and stability to warm-up and to long time period, are all significantly improved when compared to conventional compensation methods. The sensor utilizes a silicon, micromachined, stress concentration enhanced structure which provides a very linear output to measured pressure.

The DSP (Microchip dsPIC30F2011) is based on a modified Harvard architecture; it operates up to 30 MIPS operation with analogue features (12 bit 200 Ksps A/D converter). The SPI SRAM (Microchip 23K256) is a recent serial SRAM device used for storage of acquired data. The device is well suited for applications involving bulk data transfers, DSP and other math algorithms (e.g. FFT and DFT). The acquired samples can be simply buffered and sent to an external device for visualization, memorization and elaboration, using an I^2C bus (offline mode). Moreover the data can be elaborated directly on the board and the results transmitted in real time to a visualization device (online mode).

Figures 5.2 – 5.3 show the schematics and the device prototype realized in the Biomedical Instrumentation Laboratory at the Trieste University.

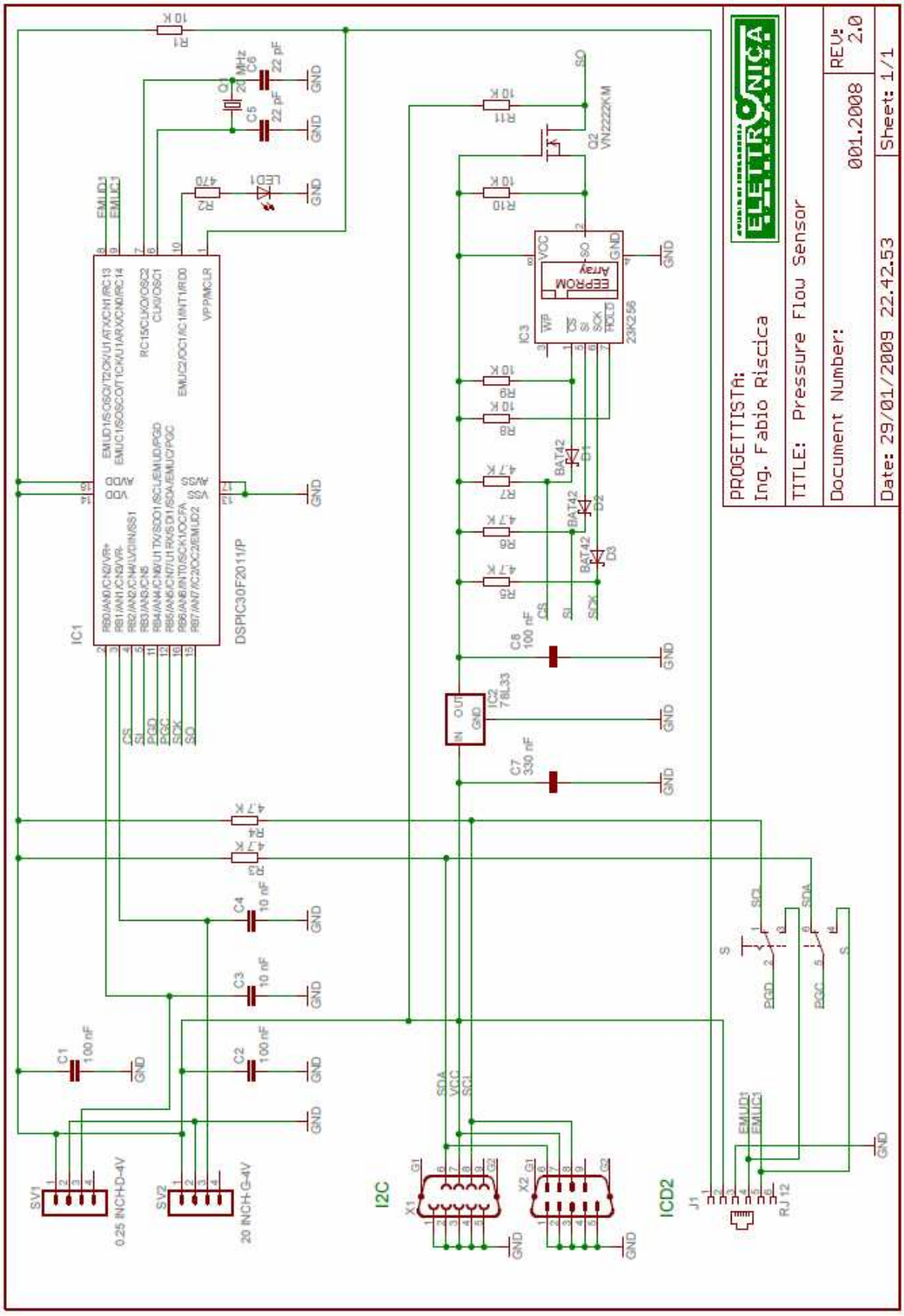

Figure 5.2 The schematic of the realized device

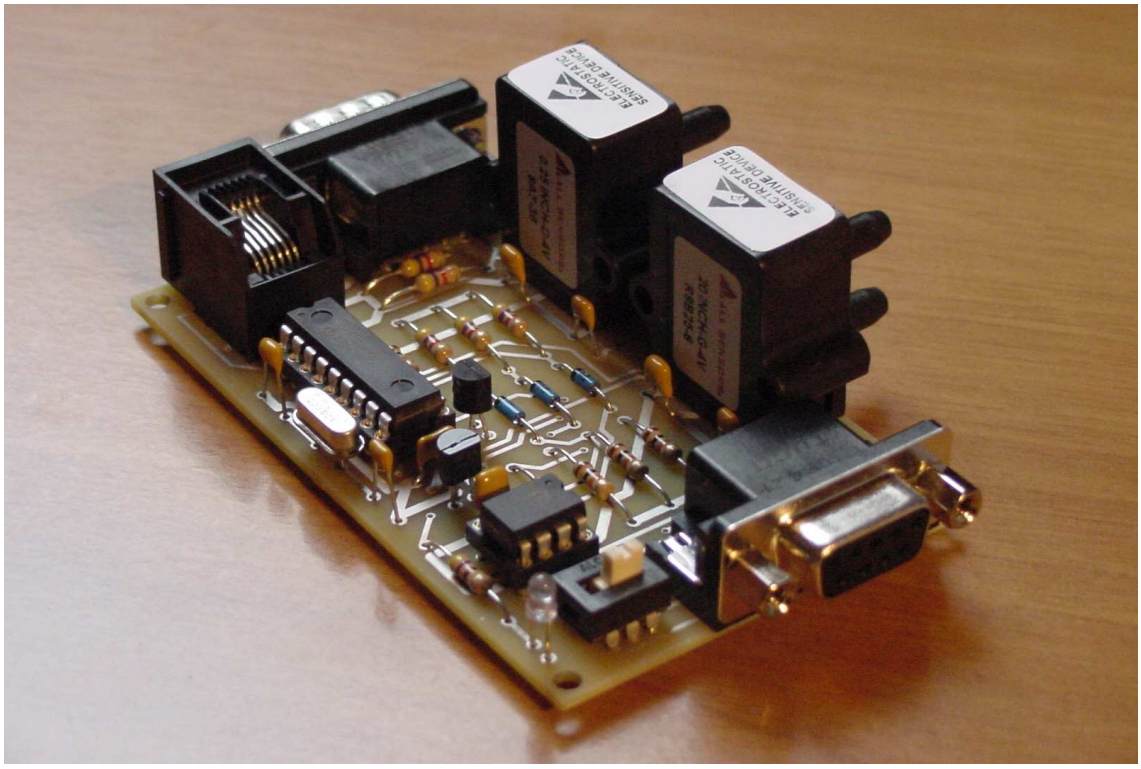

Figure 5.3 The prototype of the realized device

In order to verify the reliability of the new device a procedure was established for measuring the volume. This procedure employed a 3-litre calibrating syringe (Fukuda Sangyo, Japan) and a manually simulated respiratory cycle of approximately 12 acts per minute for 120 seconds. The volume was calculated by integrating the flow; this operation, described in [Shaw et al 1976] could introduced a maximum error of 3% that can be considered satisfactory and within the accuracy of the employed instruments.

In order to study the characteristics of percussive ventilators, after the verification of the device reliability, a test system was produced. The flow output of a Percussionaire (VDR-4, Percussionaire Corporation, USA) was connected to a lung-simulator (SMS, Medishield, UK), presenting variable R/C parameters, through a laboratory measurement system of respiratory parameters (BIO-TEK, Gas Flow Analyzer VT+ HF) and a Fleisch pneumotacograph (Type 2, 3 L/sec) to which the new device was connected.

The pressure and flow measures were carried out for 240 seconds, setting up on the VDR-4 a respiratory frequency of 15 acts per minute with I/E 1:1 and a percussive frequency of 800 cycles per minute with job pressure of 25 cm H2O and free expiratory flow. On the lung-

simulator a mechanical resistance of 0 cm H2O/(L/sec) and a compliance of 20 ml/cm H2O was fixed. The acquired data was digitally filtered with a low-pass third order Butterworth IIR filter with a cut-off frequency of 400 Hz.

The laboratory measurement system of respiratory parameters supplies directly the measured volume. The volume measured by the new instrument was calculated integrating the flow curves.

The acquired values of flow (Fig. 5.4), pressure (Fig. 5.5) and computed volume (Fig. 5.6), were evaluated considering a single respiratory act.

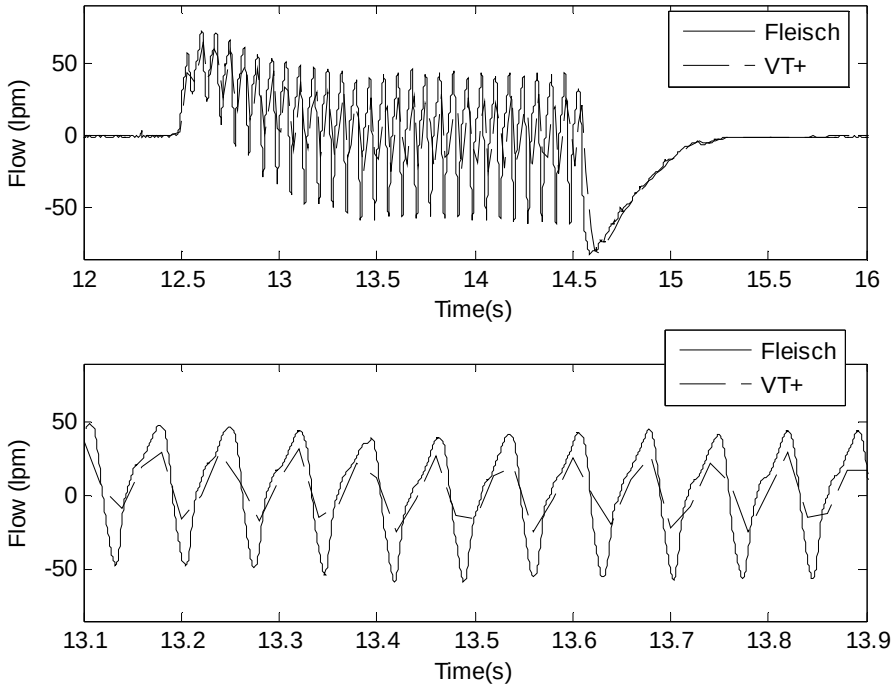

Figure 5.4 Flow behaviour along a single respiratory act (top) and a particular (bottom), acquired by means of our device (Fleisch) and the VT+ Gas Flow Analyzer.

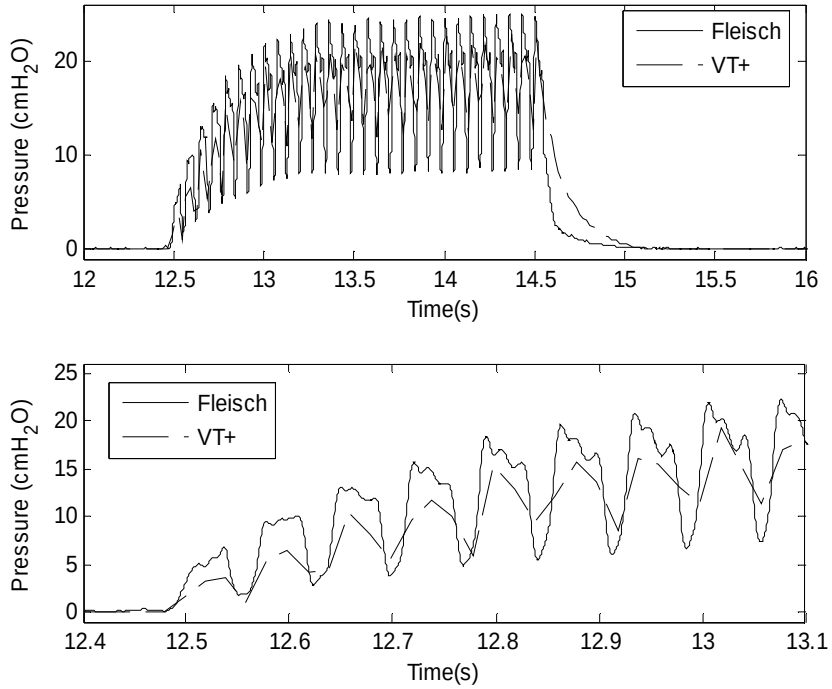

Figure 5.5 Pressure behaviour along a single respiratory act (top) and a particular (bottom), acquired by means of our device (Fleisch) and the VT+ Gas Flow Analyzer.

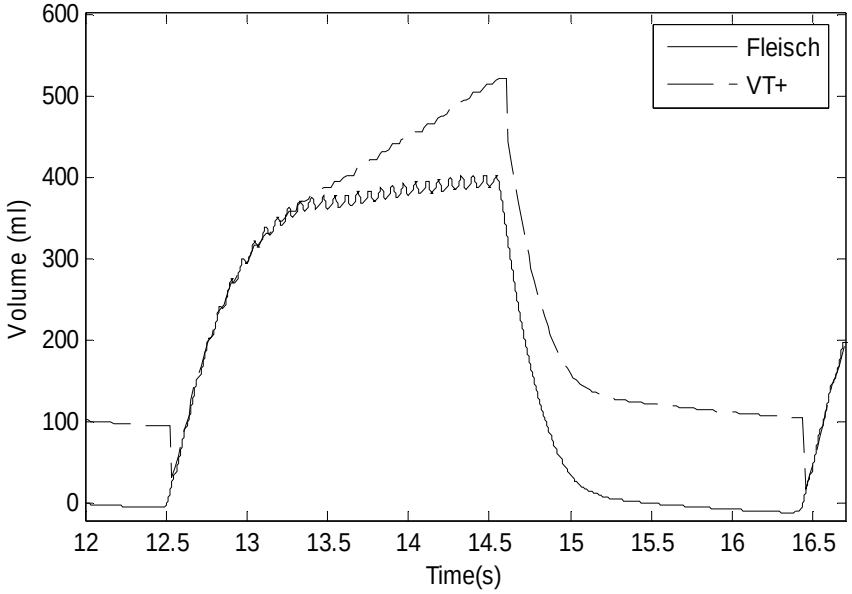

Figure 5.6 Volume behaviour obtained by integrating the flow signals of Fig.5.4.

From these figures it is evident that the sampling frequency of VT+ (50 Hz) is insufficient in the case of percussive ventilation and the volume evaluation generates an unacceptable error (Fig. 5.6). On the contrary, the sampling frequency of our device (2 KHz) produces better results. Therefore, for a correct assessment of the respiratory parameters and the volume exchanged in the high-frequency percussive ventilation, a measurement system with a wide bandwidth needs. This condition is not verified in current measurement systems of respiratory parameters which are not designed for monitoring respiratory values of such frequency range.

5.2 Portable Instrument for Volume measurement

This device is constituted (Figures 5.7 – 5.9) by a PIC microcontroller, which digitally converts the measured values of pressure and flow and computes the exchanged volume by numerical integration of the flow, sampled every 0.5 milliseconds. The RS232 transceiver is used to interface an external host which operates at RS232-C levels. That is necessary for to reduce the communication errors and to extend the host/slave distance.

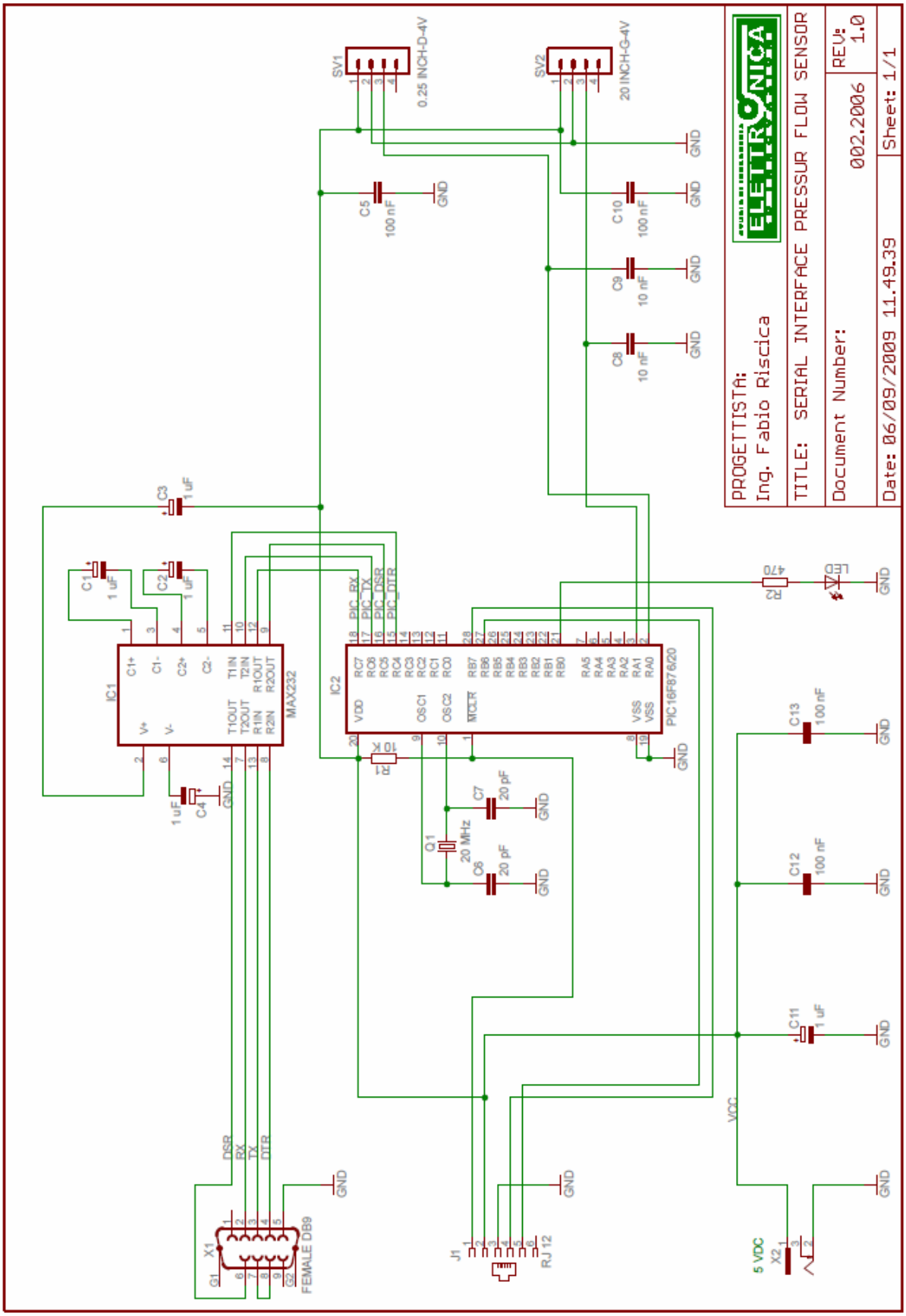

Figure 5.7 The schematic of the realized device

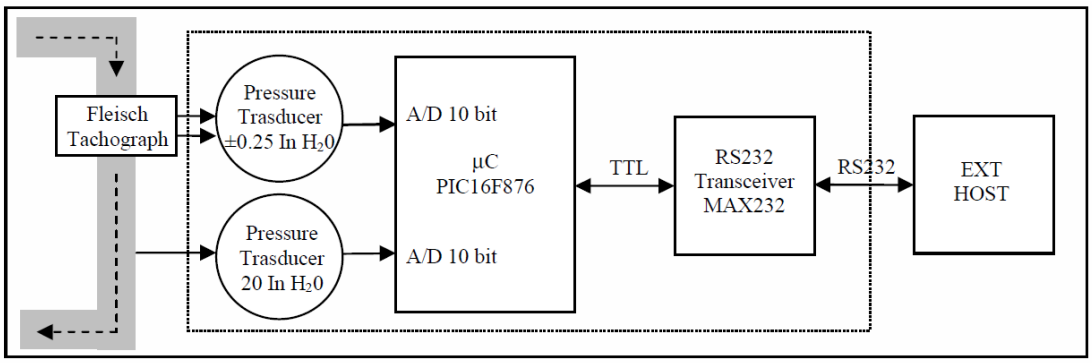

Figure 5.8 Block diagram of the device for the volume measurement

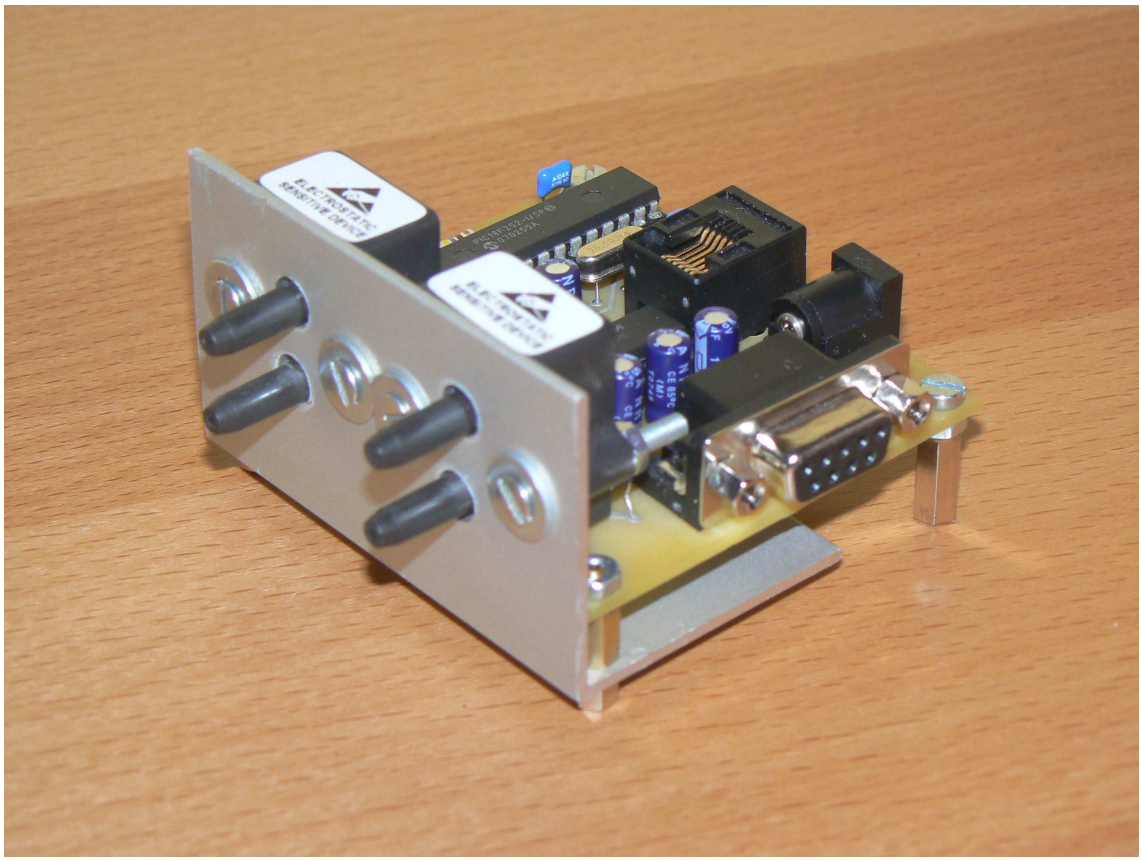

Figure 5.9 The prototype of the realized device

The microcontroller (Microchip PIC16F876) is an high performance RISC CPU based on a modified Harvard architecture; it operates up to 5 MIPS with analogue features. The

MAX232 is a RS-232 transceiver, a dual driver/receiver that includes a capacitive voltage generator to supply RS232 voltage levels from a single 5V supply.

The device works in slave mode and its acquired and computed data are available by means of an host/slave ASCII serial communication protocol (RS232-C, 115.2 kbps). An host device can periodically require the current values of pressure, flow and volume, using the commands reported in Table 5.2.

Type	Command Syntax	Slave Response
Flow request	RFxxxxcc	RFvvvvsscc
Pressure request	RPxxxxcc	RPvvvvsscc
Volume request (MSB)	MVxxxxcc	MVvvvvsscc
Volume request (LSB)	LVxxxxcc	LVvvvvsscc
Volume clear	CVxxxxcc	CVzzzzsscc

xxxx : don't care value
cc : frame checksum (xor of the previous bytes)
vvvv : requested value
zzzz : calibration value of flow stored in the device
ss : status code of the command ('00' = OK)

Table 5.2 Serial host commands

The figures 5.10 – 5.11 show the host device developed for the volume visualization in our test. The host requires the slave a volume value every 32 milliseconds and periodically update its display. The figure 5.12 shows the complete system.

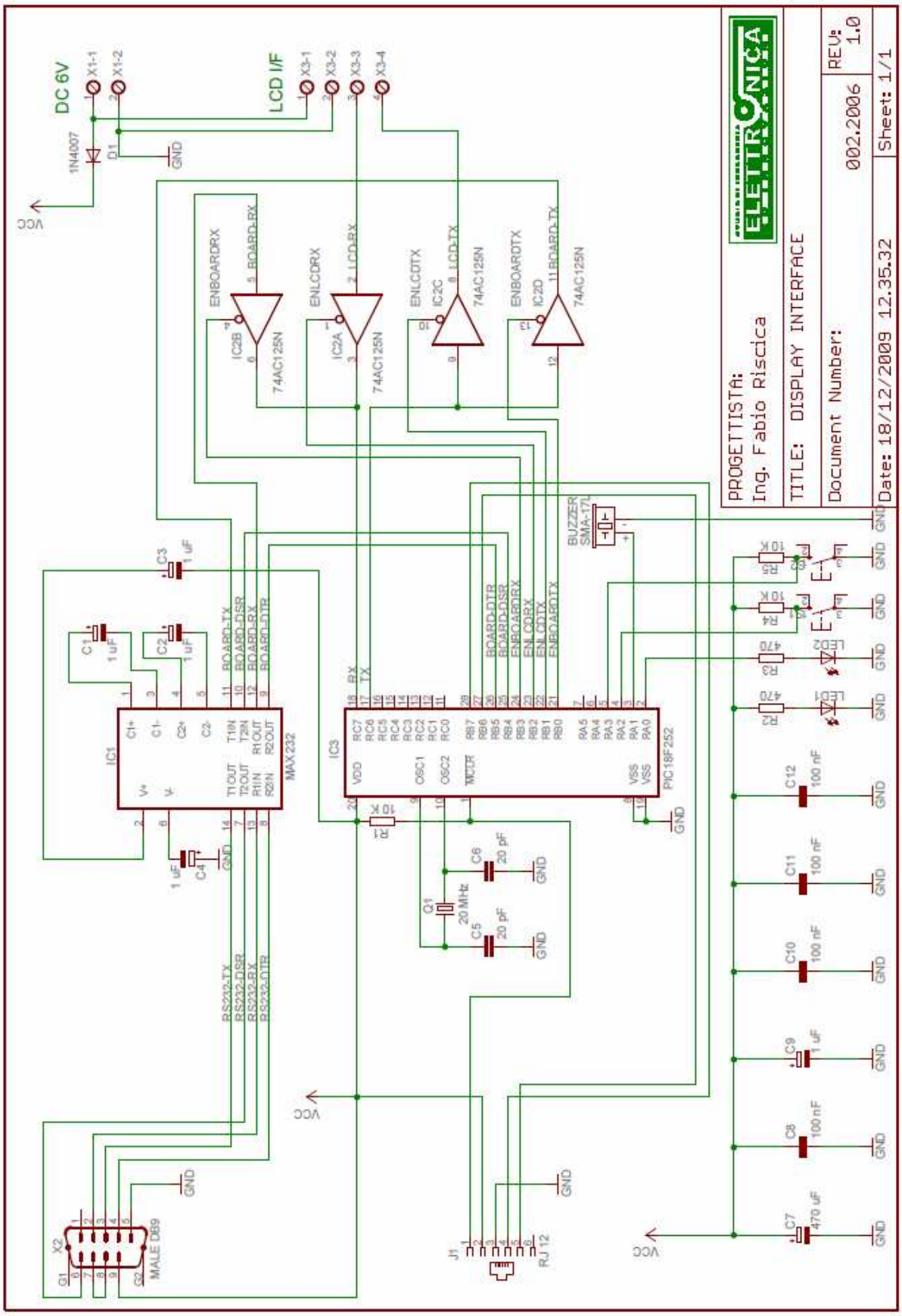

Figure 5.10 The schematic of the host device

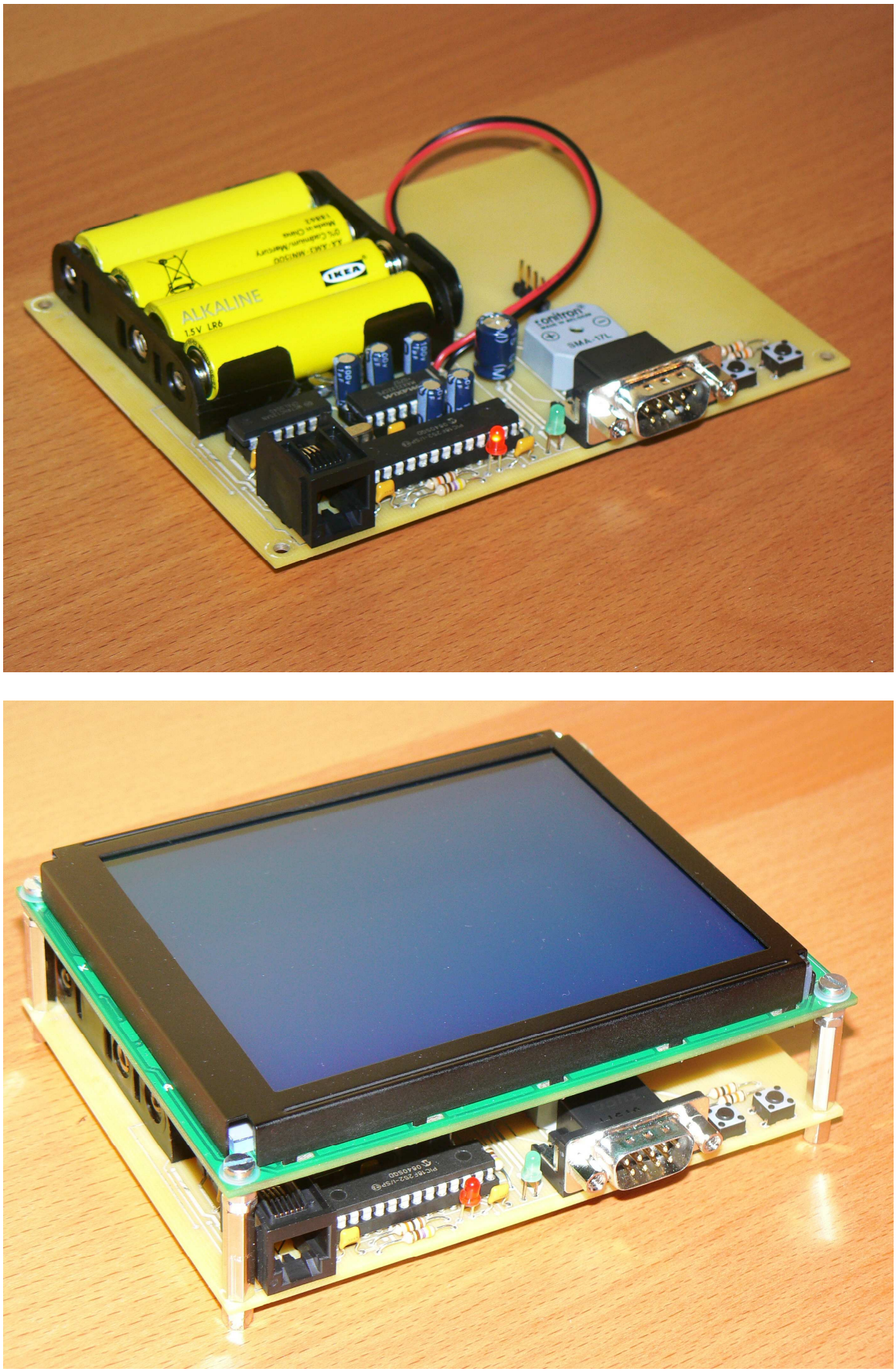

Figure 5.11 The prototype of the host device

Figure 5.12 Complete system (host and slave components)

In order to verify the reliability of the new device a procedure was established for measuring the volume. This procedure employed a 3-litre calibrating syringe (Fukuda Sangyo, Japan) and a manually simulated respiratory cycle of approximately 12 acts per minute for 120 seconds. Computation of volume by integration of the flow could introduced a maximum error of 3% that can be considered satisfactory and within the accuracy of the employed instruments [Shaw et al 1976].

In order to study the characteristics of percussive ventilators, after the verification of the device reliability, a new test system was produced. The flow output of a Percussionaire (VDR-4, Percussionaire Corporation, USA) was connected to a lung-simulator (SMS, Medishield, UK), presenting variable R/C parameters, through a laboratory measurement system of respiratory parameters (BIO-TEK, Gas Flow Analyzer VT+ HF) and a Fleisch pneumotacograph (Type 2, 3 L/sec) connected to the device. The pressure and flow measures were carried out for 240 seconds, setting up on the VDR-4 a respiratory frequency of 15 acts per minute with I/E 1:1 and a percussive frequency of 800 cycles per minute with job pressure of 25 cm H_2O and free expiratory flow. On the lung-simulator a mechanical resistance of 0 cm H_2O/(L/sec) and a compliance of 20 ml/cm H_2O were fixed.

The Table 5.3 compares the measured volume from our device (Fleisch) and the VT+ (with fixed load R=0 cm H_2O/(L/sec),C=20 ml/cm H_2O; working pressure 25 cm H_2O; respiratory frequency 15 acts to minute; free expiratory time).

Percussive frequency (cycles/min)	VT+ (ml)	Fleisch (ml)
1300	390	461
1500	736	420
1800	520	398

Table 5.3 Measured volume comparison

5.3 Modular instruments for Pressure and Flow measurement

In order to interface some pressure and flow transducer, appropriate conditioning boards were realized in the Biomedical Instrumentation Laboratory at the Trieste University.

Each board (fig. 5.13 – 5.16) mounts a pressure or a flow transducer and an 8th-order Butterworth low-pass filter (Maxim MAX291). Cut-off frequency is programmable and allows to reduce the high frequency noise that mainly affects the flow signal. This noise due

to turbulence generated in the pneumotacograph could introduce errors in the volume estimation as a result of the integration. A connector block (fig. 5.17 – 5.20) connects the conditioning boards to low cost data acquisition boards (National Instruments PCI-6023E or NI-6008). The PCI-6023E board gets up to 200 kS/s sampling and 12-bit resolution on 8 differential analog inputs. The integrated pulse generator is used to set the cut-off frequency of the on-board low-pass filter in conditioning boards.

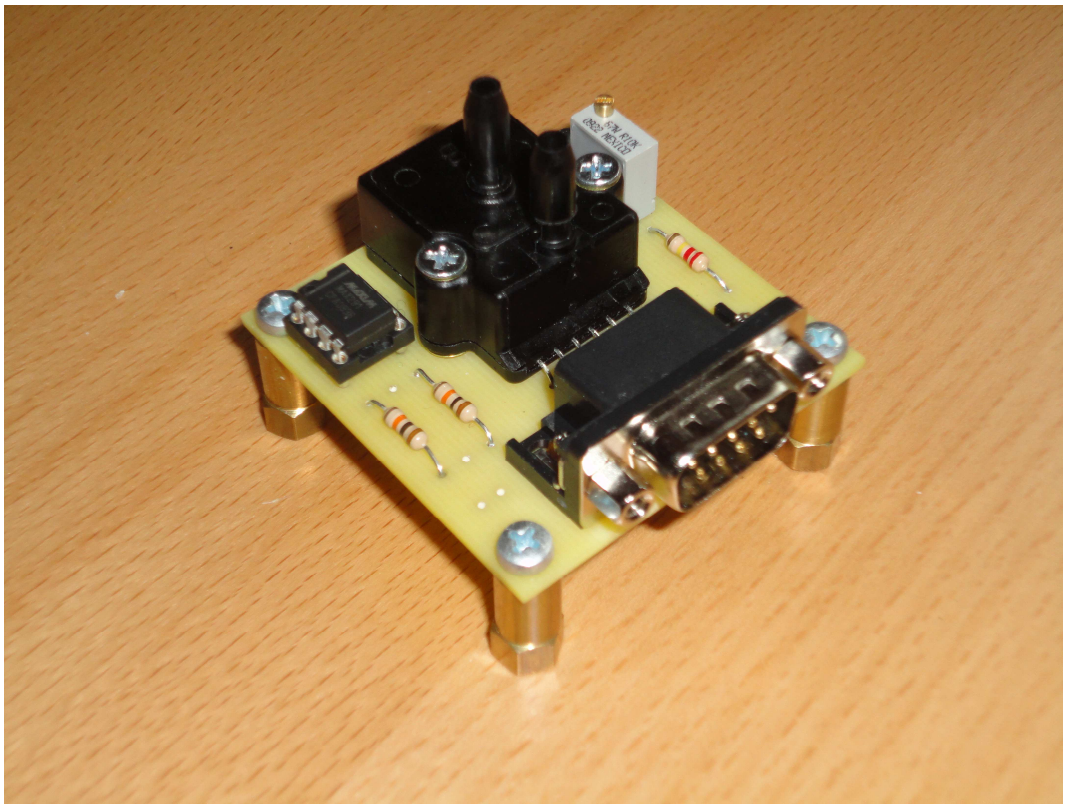

Figure 5.13 The modular pressure transducer

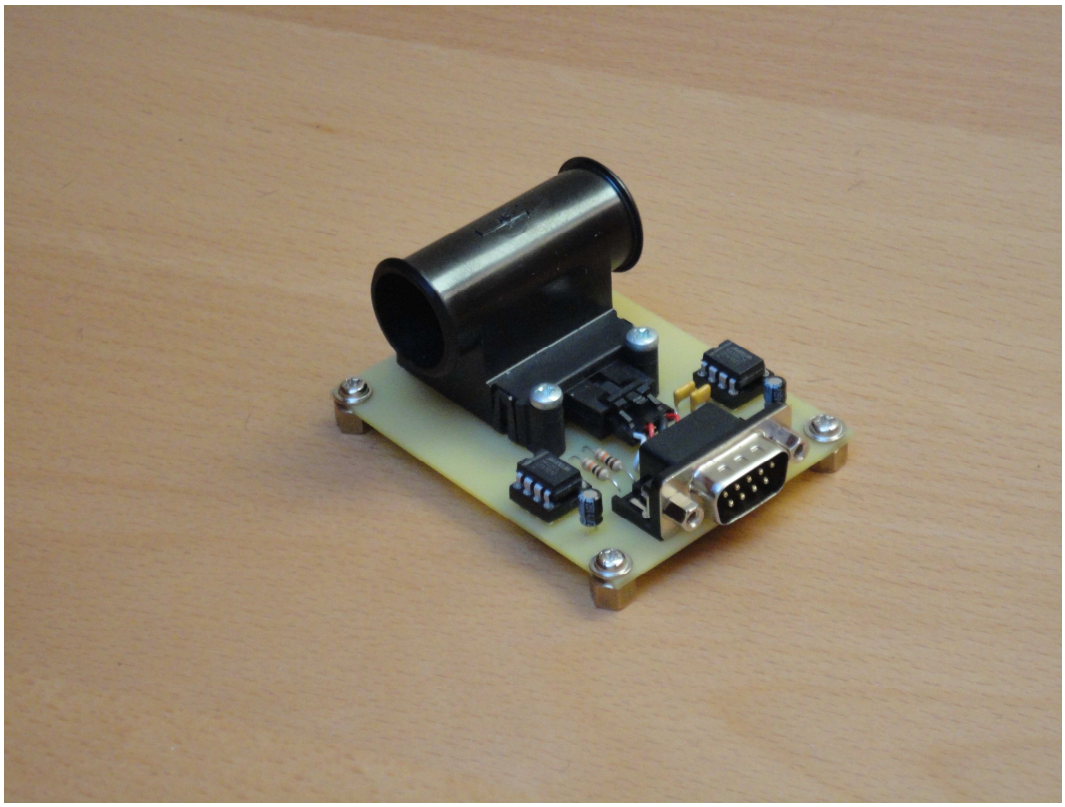

Figure 5.14 The modular flow transducer

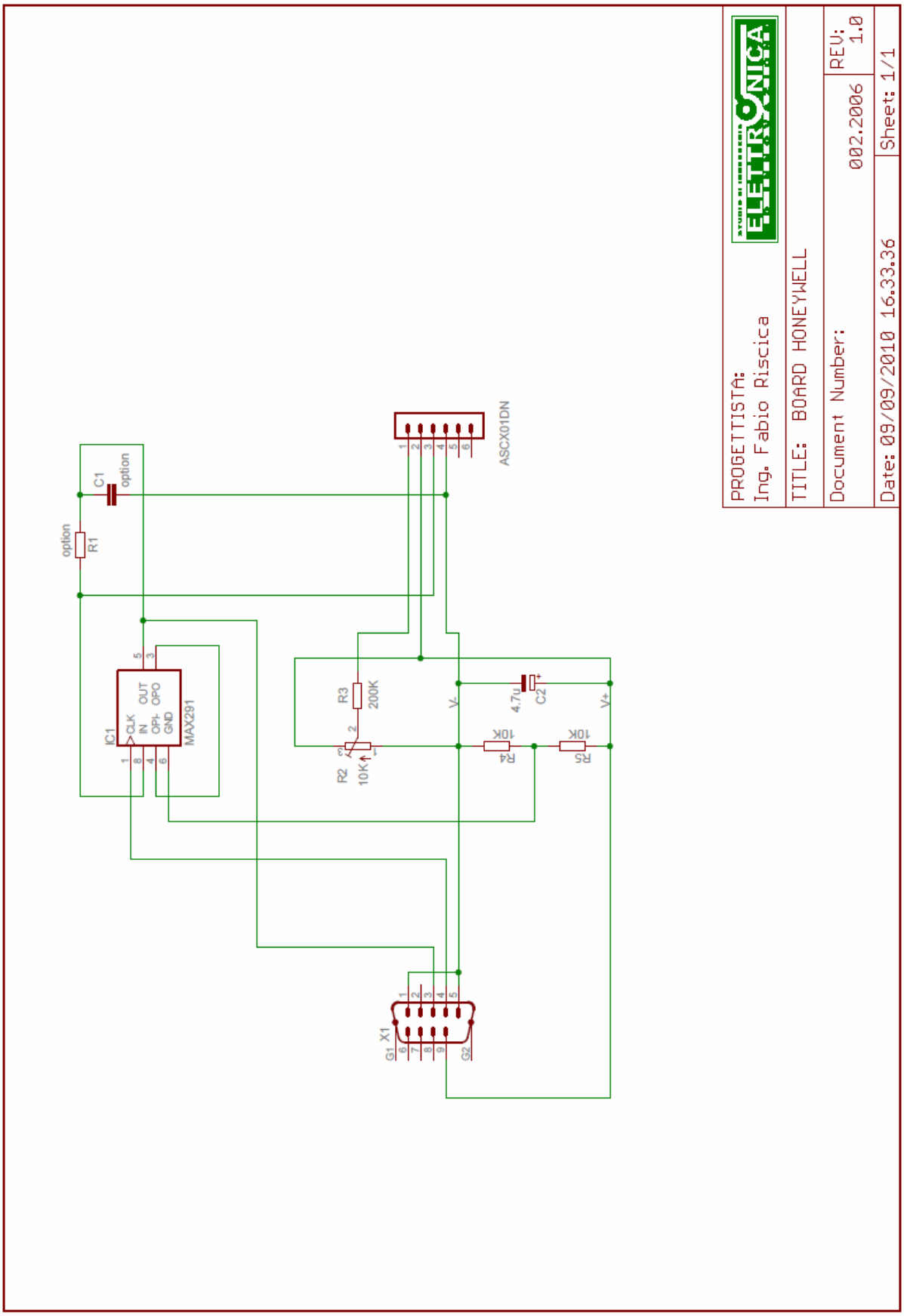

Figure 5.15 The schematic of the pressure transducer

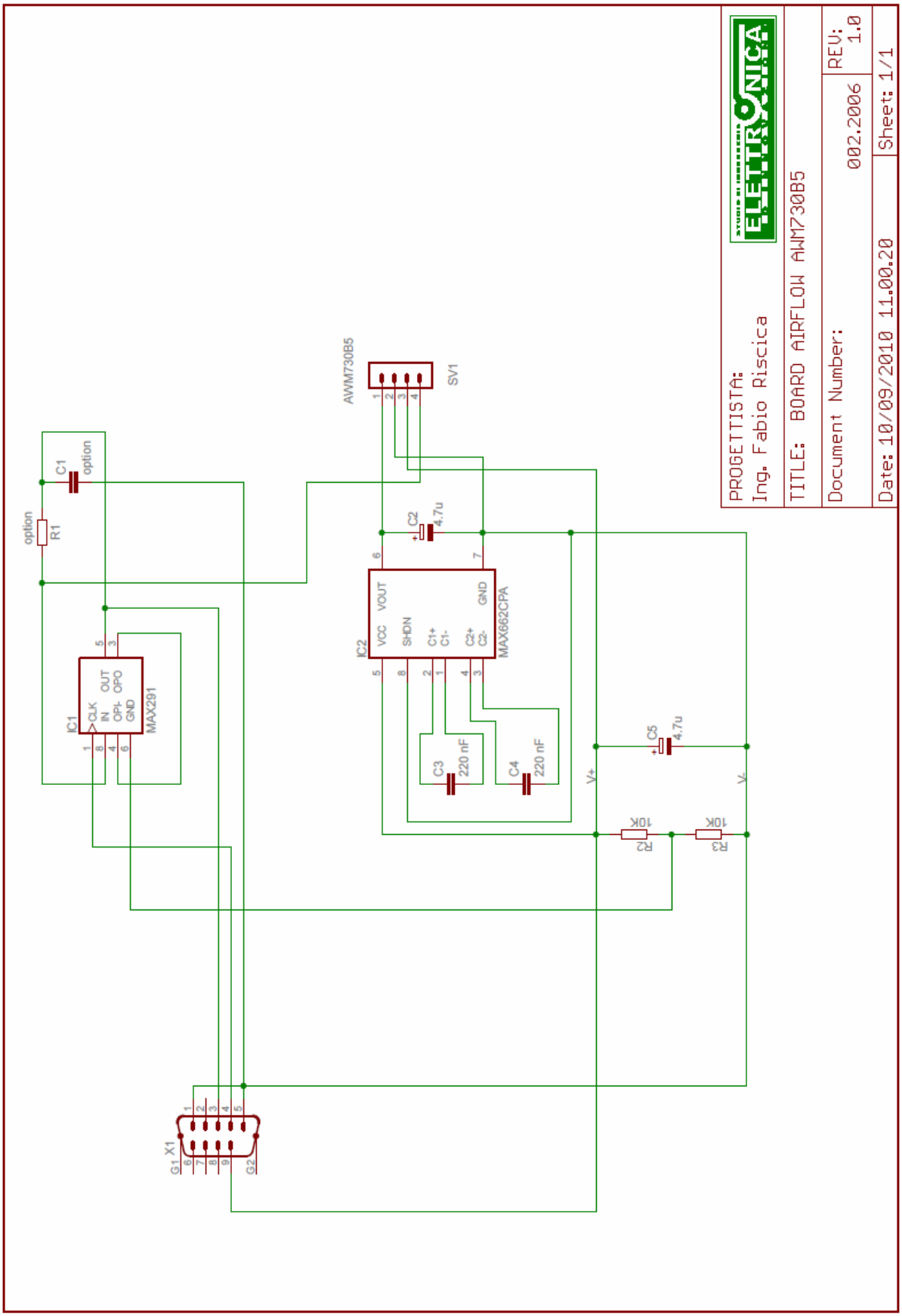

Figure 5.16 The schematic of the flow transducer

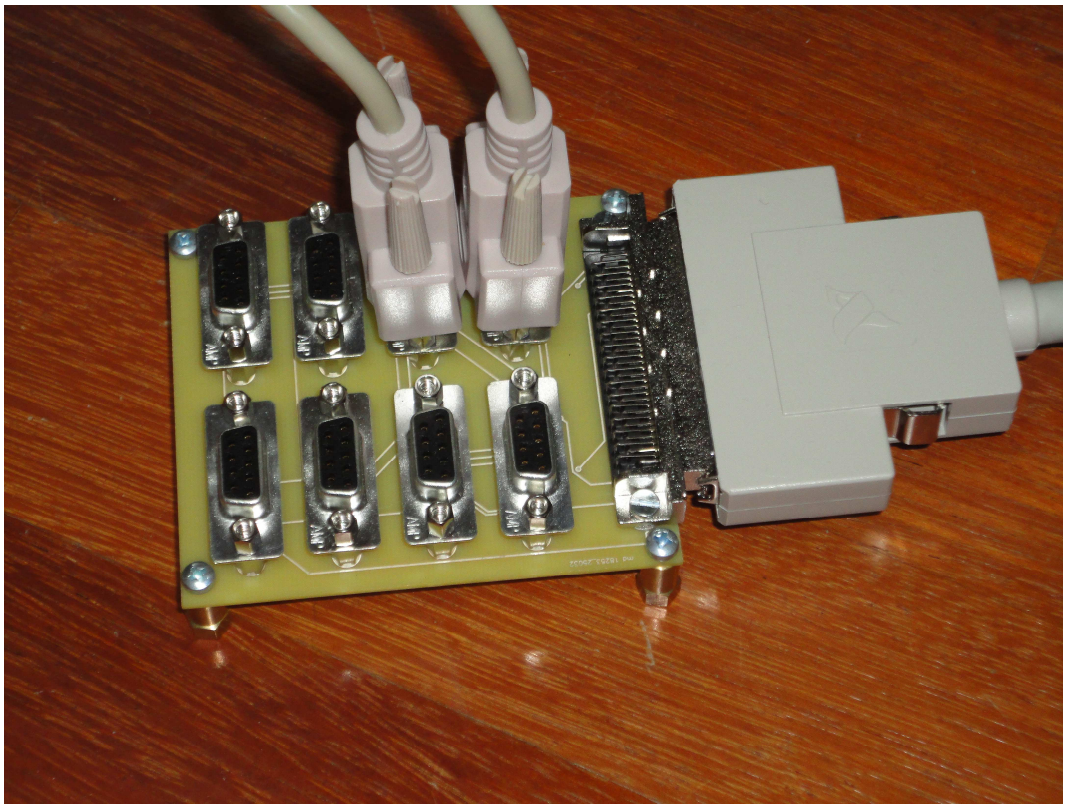

Figure 5.17 The connector block (PCI-6023 version)

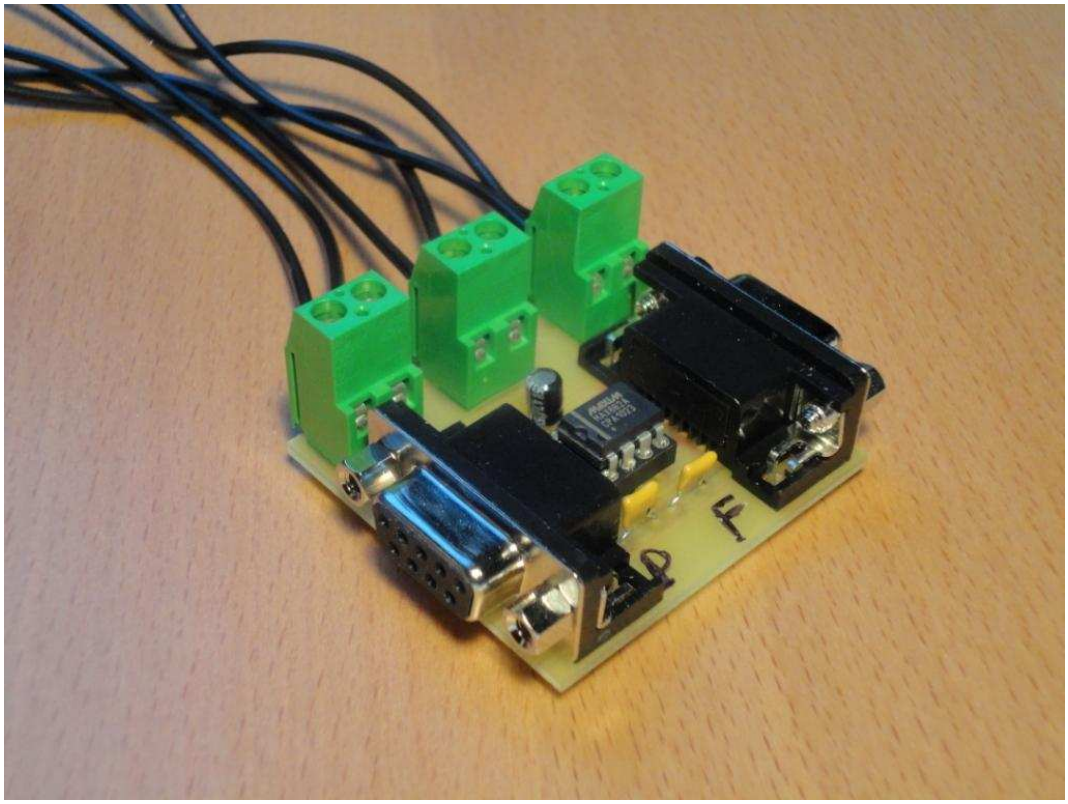

Figure 5.18 The connector block (USB-6008 version)

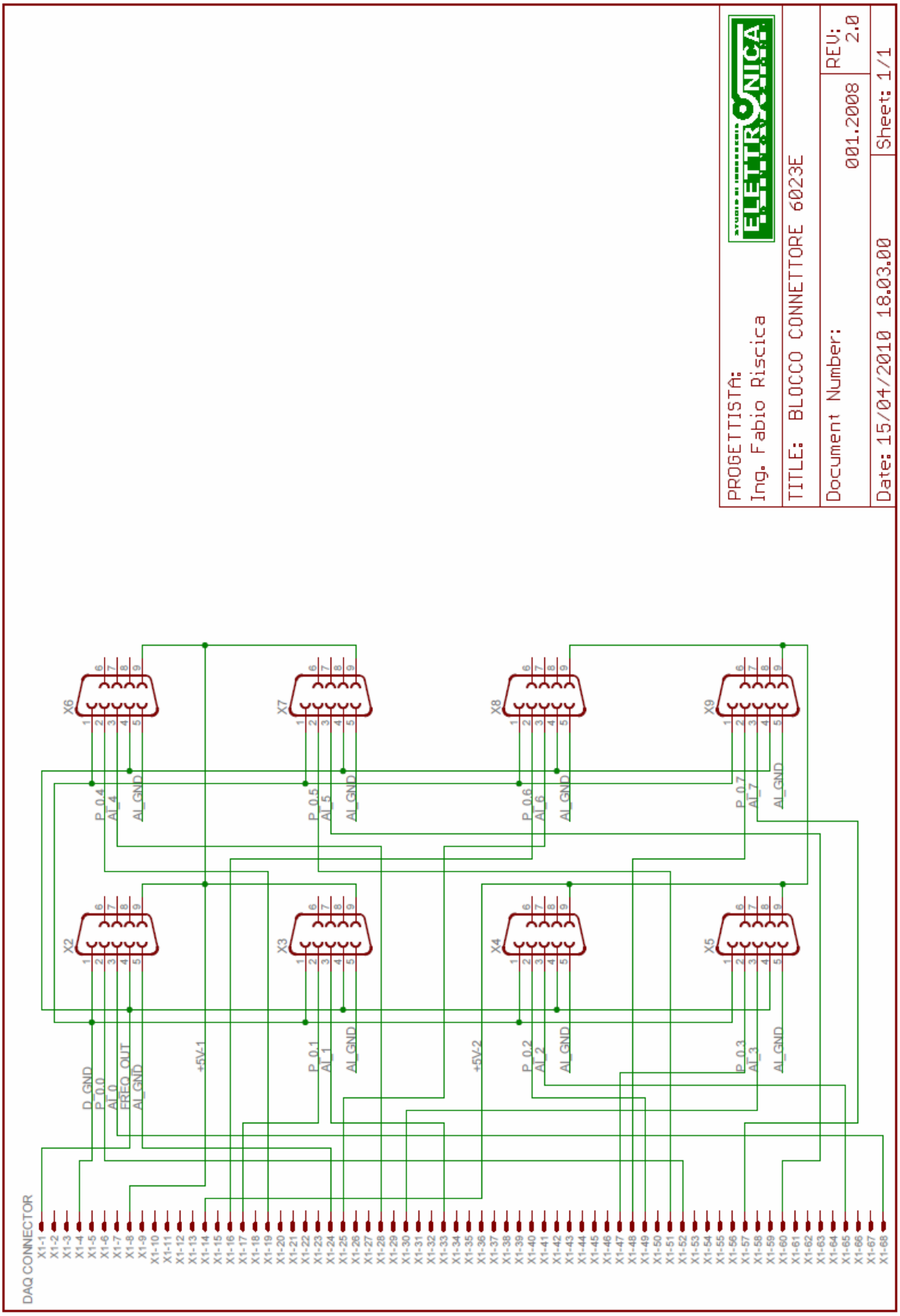

Figure 5.19 The schematic of the connector block (PCI-6023 version)

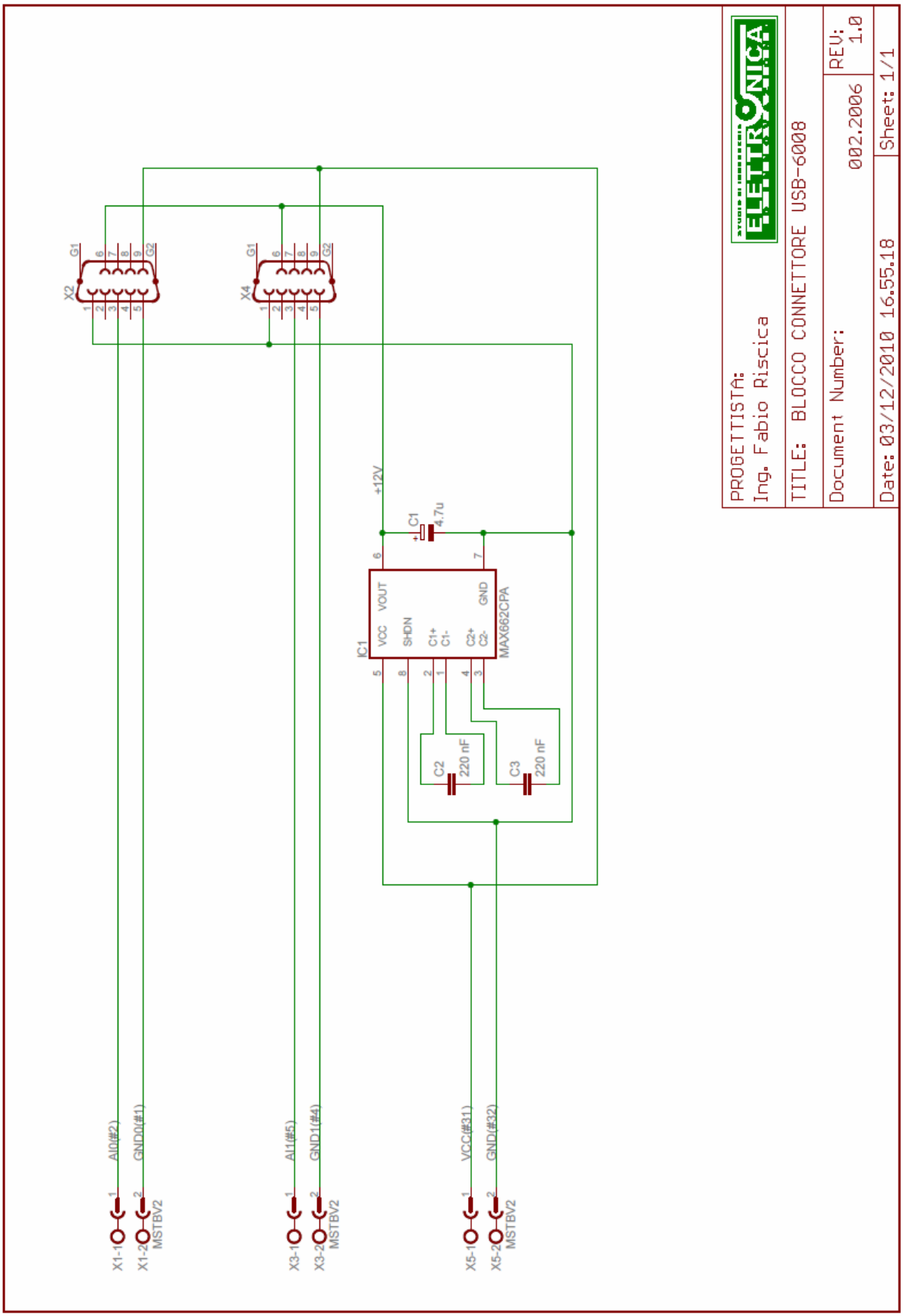

Figure 5.20 The schematic of the connector block (USB-6008 version)

Chapter 6

High Frequency Percussive Ventilator characterization

6.1 Mechanical model

Respiratory mechanics defines the behaviour of the lung and chest when subjected to changes in pressure, flow and volume induced by respiratory muscles and, in case of forced ventilation, also by mechanical ventilatory support, which cyclically act on the system. The simplest high-frequency model of the respiratory system, still currently used [Dorkin et al 1988], is an electrical analogue model constituted by a RLC circuit (fig. 6.1) which can be applied both during spontaneous and passive ventilation.

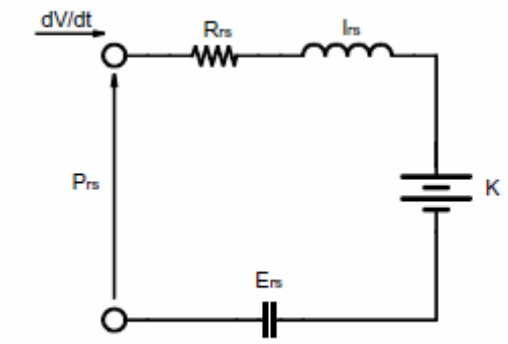

Fig. 6.1 A simple model of respiratory system.

The following mathematical equation, known as motion equation, describes its behaviour

$$P_{\mathrm{rs}} = K + E_{\mathrm{rs}} \cdot V + R_{\mathrm{rs}} \cdot \dot{V} + I_{\mathrm{rs}} \cdot \ddot{V}$$

where P_{rs} is the pressure applied to the respiratory system, V is the pulmonary volume, $\dot{V}$ is the airflow and $\ddot{V}$ its derivative that represents flow acceleration; K represents the mouth pressure when V, $\dot{V}$ and $\ddot{V}$ are zero. P_{rs} and $\dot{V}$ may be measured directly at the patient's mouth with a pressure transducer and a pneumotacograph, respectively. Volume and airflow derivative are mathematically obtained from the airflow wave as its integral and its first derivative, respectively. From the motion equation the values of the four unknown quantities K (pressure offset), E_{rs} (elastance), R_{rs} (resistance) and I_{rs} (inertance) can be estimated by fitting the equation using the sampled values of P_{rs}, V, $\dot{V}$ and $\ddot{V}$. The term $E_{\mathrm{rs}} \cdot V$ corresponds to the pressure necessary to balance elastic forces; it depends on both the volume insufflated in excess of resting volume and the elastance of the respiratory system. On the other hand the term $R_{\mathrm{rs}} \cdot \dot{V}$ corresponds to the pressure necessary to balance frictional forces; it is mainly due to the resistance offered to the airflow. Lastly, the product $I_{\mathrm{rs}} \cdot \ddot{V}$ corresponds to the pressure necessary to overcome the system's inertia (i.e. the inertance of the respiratory system) which depends on the airflow derivative. Finally, $P_{\mathrm{rs}} - K$ corresponds to the sum of the resistive, elastic and inertial pressure drops of the respiratory system.

6.2 Model parameters estimation

In order to estimate the three parameters of the respiratory system model we use the multiple linear regression approach [Kaczka et al 1995]. The n acquired flow samples $\dot{V}_i$ together with their integral V_i and derivative $\ddot{V}_i$ are used to build the first three columns of a [n x 4] matrix A, whose fourth column is composed by 1's. The corresponding n acquired samples of pressure P_i are used to create a [n x 1] vector B:

$$A = \begin{bmatrix} V_0 & \dot{V}_0 & \ddot{V}_0 & 1 \\ V_1 & \dot{V}_1 & \ddot{V}_1 & 1 \\ \dots & \dots & \dots & \dots \\ V_{n-2} & \dot{V}_{n-2} & \ddot{V}_{n-2} & 1 \\ V_{n-1} & \dot{V}_{n-1} & \ddot{V}_{n-1} & 1 \end{bmatrix}, \quad B = \begin{bmatrix} P_0 \\ P_1 \\ \dots \\ P_{n-2} \\ P_{n-1} \end{bmatrix}$$

The solution of the over-determinated system $A \cdot X = B$, where

$$X = \begin{bmatrix} E \\ R \\ I \\ K \end{bmatrix}$$

is obtained by computing the transpose A^T and by minimizing the mean square errors:

$$X = \left(A^T \times A\right)^{-1} \times A^T \times B$$

6.3 Software description

The modular system (see chapter 5.3) is connected with a National Instruments NI-6023E data acquisition board, installed in a Panel PC windows-based (Phoenix Contact PPC 5315). A Virtual Instrument, running under National Instruments LabWindows/CVI environment assuring reliability and reusability, controls data acquisition, analysis and user interface.

The implemented software realizes the following operations: at first, pressure and flow signals are acquired during a respiration cycle and the exchanged volume within the cycle is calculated by integrating the flow with a trapezoidal rule. The possible off-set present at the end of the cycle is caused by the noise due to the pressure transducer [Application Note: Noise Considerations for Integrated Pressure Sensors. Freescale semiconductors] utilized for flow measurement. The noise value can be estimated keeping in mind that the inhaled and the exhaled volumes have to be the same. In any case, the volume estimation error, due to the noise, lies within the acceptable limit of 3% and it is removed subtracting the value of the error present at the end of the cycle that is the point in which the inhaling period ends. This

point demarks a switch from an initial model in which inhaling is induced to a second model in which exhalation occurs freely. The two models are different each other about the estimate of inhaled and exhaled resistance; in this way, it is possible to obtain a significant adaptation to the experimental data, without loss of accuracy in parameters estimate [Barbini P. et al 2001]. We will not consider the second model, concerning the expiratory phase, because clinical parameters of our interest are mainly related to the inspiratory phase. A second operation concerns the estimation of resistance and elastance values by using the method previously described applied on data acquired during the inspiratory period of the analyzed respiratory cycle. Such values are updated every respiratory cycle and utilized to construct the pressure curve generated by the model using the measured flow as input. This estimated pressure curve is compared to the corresponding measured pressure curve in order to verify the validity of the model. The mean square error is used to measure the differences between measured and modelled pressures. This procedure runs during the expiratory phase, visualizing the estimated curve superimposed to the measured one in the inhalation phase. The operations are repeated for each respiration cycle.

The figure 6.2 shows the ANSI-C implementation of described algorithm.

```
#include <analysis.h>
#include <NIDAQmx.h>
#include <ansi_c.h>
#include <utility.h>
#include <acquire.h>

#define PRESSURE_TRIGGER        3
#define FLOW_TRIGGER            -0.2
#define PRETRIGGER              150
#define POSTTRIGGER             250
#define EXPIRATION_PRETRIGGER   5

#define DAQmxErrChk(functionCall) {DAQmxError = (functionCall); {if (DAQmxError < 0){goto Error;}}}

FILE *F;
int handle;
TaskHandle task1,task2;
float64 Voltage[8192];
float64 Volume[1024];
int32 samples;
int32 i;
int32 j;
float FREQUENCY;
unsigned int SAMPLING_FREQUENCY;
float64 Pressure[32768];
float64 Flow[32768];
float64 EstimatedVolume[32768];
float64 Time[32768];
double A[32768][3];
double B[32768];
double X[3];
float64 PressureEstimated[32768];
float64 Error;

int32 CreateDAQTaskInProject(TaskHandle *taskOut1)
{
    int32 DAQmxError = DAQmxSuccess;
    TaskHandle taskOut;

    DAQmxErrChk(DAQmxCreateTask("DAQTaskInProject", &taskOut));

    DAQmxErrChk(DAQmxCreateAIVoltageChan(taskOut, "Dev1/ai0", "Pressure",
        DAQmx_Val_RSE, 0, 70.307, DAQmx_Val_FromCustomScale, "PressureScale"));

    DAQmxErrChk(DAQmxCreateAIVoltageChan(taskOut, "Dev1/ai1", "Flow",
        DAQmx_Val_RSE, -2.11, 2.11, DAQmx_Val_FromCustomScale, "FlowScale"));

    DAQmxErrChk(DAQmxCfgSampClkTiming (taskOut, "", 2*SAMPLING_FREQUENCY, DAQmx_Val_Rising, DAQmx_Val_ContSamps, 1000));

    *taskOut1 = taskOut;

Error:
    return DAQmxError;
}

int32 CreateDAQTaskOutProject(TaskHandle *taskOut1)
```

Fig. 6.2 a ANSI-C implementation of estimation parameters algorithm.

```
{
    int32 DAQmxError = DAQmxSuccess;
    TaskHandle taskOut;

    DAQmxErrChk(DAQmxCreateTask("DAQTaskOutProject", &taskOut));

    DAQmxErrChk(DAQmxCreateCOPulseChanFreq (taskOut, "Dev1/freqout", "PulseOutput", DAQmx_Val_Hz, DAQmx_Val_Low, 0.0, FREQUENCY, 0.5));

    DAQmxErrChk(DAQmxCfgImplicitTiming(taskOut, DAQmx_Val_ContSamps, 100));

    *taskOut1 = taskOut;

Error:
    return DAQmxError;
}

void CVICALLBACK Calibrate(int menubar, int menuItem, void *callbackData, int panel)
{
  unsigned int CALIBRATION_SAMPLES;

  int32 counter=0;
  float64 pressure_offset = 0.0;
  float64 flow_offset = 0.0;

  //impostazione frequenza campionamento
  GetCtrlVal (PANEL, PANEL_SAMPL_FREQ, &SAMPLING_FREQUENCY);
  CALIBRATION_SAMPLES = SAMPLING_FREQUENCY*5;

  CreateDAQTaskInProject(&task1);

  //impostazione frequenza pilotaggio filtri attivi
  GetCtrlVal (PANEL, PANEL_LOW_PASS, &FREQUENCY);
  CreateDAQTaskOutProject(&task2);

  DAQmxStartTask(task1);
  DAQmxStartTask(task2);
  F = fopen("calibration.txt","w");

  while(counter <= CALIBRATION_SAMPLES*2){
     DAQmxReadAnalogF64 (task1, 128, 10.0, DAQmx_Val_GroupByScanNumber, Voltage, 1024, &samples, 0);
     if(samples){
          for (i=0;i<samples;i+=2){
               pressure_offset=pressure_offset+Voltage[i];
               flow_offset=flow_offset+Voltage[i+1];
          }
          pressure_offset = pressure_offset*2/samples;
          flow_offset = flow_offset*2/samples;
     }
     counter = counter + samples;
  }
  fprintf(F,"%f   %f",pressure_offset,flow_offset);
  fclose(F);
  DAQmxStopTask(task1);
  DAQmxStopTask(task2);
  DAQmxClearTask(task1);
```

Fig. 6.2 b ANSI-C implementation of estimation parameters algorithm.

```
DAQmxClearTask(task2);

}

void CVICALLBACK Start(int menubar, int menuItem, void *callbackData, int panel)
{
int32 counter=0;
int32 IndiceCampioni=0;
float pressure_offset;
float flow_offset;
float ACQUISITION_TIME;
float LASTVOL = 0.0;
unsigned char status = 0;
int32 Index1;
int32 Index2;
int32 Index3;
int32 IndexStart;
int32 IndexEnd;
int32 IndexExpiration;

//lettura dati calibrazione sensori
F = fopen("calibration.txt","r");
fscanf(F,"%f %f",&pressure_offset,&flow_offset);
fclose(F);

//impostazione tempo misura
GetCtrlVal (PANEL, PANEL_ACQ_TIME, &ACQUISITION_TIME);

//impostazione frequenza campionamento
GetCtrlVal (PANEL, PANEL_SAMPL_FREQ, &SAMPLING_FREQUENCY);
CreateDAQTaskInProject(&task1);

//impostazione frequenza pilotaggio filtri attivi
GetCtrlVal (PANEL, PANEL_LOW_PASS, &FREQUENCY);
CreateDAQTaskOutProject(&task2);

DAQmxStartTask(task1);
DAQmxStartTask(task2);

F = fopen("data.txt","w");

while(counter/(2*SAMPLING_FREQUENCY) <= ACQUISITION_TIME){
    DAQmxReadAnalogF64 (task1, 128, 10.0, DAQmx_Val_GroupByScanNumber, Voltage, 1024, &samples, 0);
    if(samples){
        for(i=0;i<samples;i+=2){
            Voltage[i]   -= pressure_offset;
            Voltage[i+1] -= flow_offset;
            Volume[i/2] = LASTVOL+Voltage[i+1]/SAMPLING_FREQUENCY;

            Pressure[IndiceCampioni/2+i/2] = Voltage[i];
            Flow[IndiceCampioni/2+i/2] = Voltage[i+1];
            EstimatedVolume[IndiceCampioni/2+i/2] = Volume[i/2];

            //finestra temporale
            switch(status){
                case 0 :
```

Fig. 6.2 c ANSI-C implementation of estimation parameters algorithm.

```
        if (Pressure[IndiceCampioni/2+i/2] < PRESSURE_TRIGGER){
            Index1 = IndiceCampioni/2+i/2;
            status = 1;
        }
        break;

    case 1 :
        if (Pressure[IndiceCampioni/2+i/2] > PRESSURE_TRIGGER)
        if(IndiceCampioni/2+i/2 >= Index1+PRETRIGGER){
            Index2 = IndiceCampioni/2+i/2;
            IndexStart = Index2 - PRETRIGGER;
            status = 2;
        }
        else
            status = 0;

        break;

    case 2 :
        if (Flow[IndiceCampioni/2+i/2] < FLOW_TRIGGER){
            IndexExpiration = IndiceCampioni/2+i/2 - EXPIRATION_PRETRIGGER;
            status = 3;
        }

        break;

    case 3 :
        if ((Pressure[IndiceCampioni/2+i/2] < PRESSURE_TRIGGER)&&
            (IndiceCampioni/2+i/2 >= Index2+SAMPLING_FREQUENCY/4)){
            Index3 = IndiceCampioni/2+i/2;
            status = 4;
        }

        break;

    case 4 :
        if (IndiceCampioni/2+i/2 >= Index3+POSTTRIGGER){
            IndexEnd = IndiceCampioni/2+i/2;
            status = 0;

            //azzera indice campioni
            IndiceCampioni = 0;

            //ridimensiona vettori
            for (j=0;j<IndexEnd-IndexStart;j++){
                Time[j] = (float)(j)/SAMPLING_FREQUENCY;
                Pressure[j] = Pressure[IndexStart+j];
                Flow[j] = Flow[IndexStart+j];
                EstimatedVolume[j] = EstimatedVolume[IndexStart+j];
            }

            //ridimensionamento punti notevoli
            IndexExpiration = IndexExpiration-IndexStart;

            //inizializza matrici A,B
            for (j=0;j<IndexExpiration;j++){
                A[j][0] = Flow[j];
                A[j][1] = EstimatedVolume[j];
                A[j][2] = 1;
                B[j]    = Pressure[j];
```

Fig. 6.2 d ANSI-C implementation of estimation parameters algorithm.

```
}
//calcola la soluzione del sistema sovradeterminato
GenLinEqs (A,IndexExpiration,3,B,GENERAL_MATRIX,X);

//stima la curva della pressione
for (j=0;j<IndexExpiration;j++)
    PressureEstimated[j] = Flow[j]*X[0]+EstimatedVolume[j]*X[1]+X[2];

//stima errore
Error = 0;
for (j=0;j<IndexExpiration;j++)
    Error = Error+pow(Pressure[j]-PressureEstimated[j],2);
Error = Error/IndexExpiration;

//aggiorna controlli
SetCtrlVal(PANEL,PANEL_RESISTENCE,X[0]);
SetCtrlVal(PANEL,PANEL_ELASTANCE,X[1]);
SetCtrlVal(PANEL,PANEL_ERROR,Error);

//cancellazione<vecchi grafici
DeleteGraphPlot (PANEL, PANEL_PRESSURE, -1, VAL_IMMEDIATE_DRAW);
DeleteGraphPlot (PANEL, PANEL_FLOW, -1, VAL_IMMEDIATE_DRAW);
DeleteGraphPlot (PANEL, PANEL_VOLUME, -1, VAL_IMMEDIATE_DRAW);

//plot vettori
PlotXY (PANEL, PANEL_PRESSURE, Time, Pressure, IndexEnd-IndexStart,
    VAL_DOUBLE, VAL_DOUBLE,VAL_THIN_LINE, VAL_EMPTY_SQUARE, VAL_SOLID, 1, VAL_RED);
PlotXY (PANEL, PANEL_PRESSURE, Time, PressureEstimated, IndexExpiration,
    VAL_DOUBLE, VAL_DOUBLE,VAL_THIN_LINE, VAL_EMPTY_SQUARE, VAL_SOLID, 1, VAL_BLUE);
PlotXY (PANEL, PANEL_FLOW, Time, Flow, IndexEnd-IndexStart,
    VAL_DOUBLE, VAL_DOUBLE,VAL_THIN_LINE, VAL_EMPTY_SQUARE, VAL_SOLID, 1, VAL_RED);
PlotXY (PANEL, PANEL_VOLUME, Time, EstimatedVolume, IndexEnd-IndexStart,
    VAL_DOUBLE, VAL_DOUBLE,VAL_THIN_LINE, VAL_EMPTY_SQUARE, VAL_SOLID, 1, VAL_RED);

//plot punti notevoli
PlotPoint (PANEL, PANEL_PRESSURE, (float)(IndexExpiration)/SAMPLING_FREQUENCY,
        Pressure[IndexExpiration], VAL_EMPTY_SQUARE, VAL_YELLOW);

    }
    break;
}
if(Volume[i/2]>=0){
    LASTVOL = Volume[i/2];
}
else {
    LASTVOL = 0.0;
    }
if (status == 0)
    LASTVOL = 0.0;

fprintf(F,"%f %f %f\n",Voltage[i],Voltage[i+1],Volume[i/2]);

}
```

Fig. 6.2 e ANSI-C implementation of estimation parameters algorithm.

```
    }
    counter = counter+samples;
    IndiceCampioni = IndiceCampioni+samples;
  }

  fclose(F);

  DAQmxStopTask(task1);
  DAQmxStopTask(task2);
  DAQmxClearTask(task1);
  DAQmxClearTask(task2);

}

void CVICALLBACK Exit(int menubar, int menuItem, void *callbackData, int panel)
{
  QuitUserInterface (0);
}

void main()
{
  double prescaled[7] =  {0.5, 0.85, 1.4, 2.5, 3.6, 4.15, 4.5};
  double scaled[7] =     {-5, -3.333, -1.667, 0, 1.667, 3.333, 5};

  DAQmxCreateLinScale ("PressureScale", 15.624, -3.906, DAQmx_Val_Volts, "cm H2O");
  DAQmxCreateLinScale ("FlowScale", 1.0557, -2.3754, DAQmx_Val_Volts, "l/sec");
  DAQmxCreateTableScale ("VolumeScale",prescaled , 7,scaled , 7, DAQmx_Val_Volts, "LPS");

  handle = LoadPanel (0, "acquire.uir", PANEL);
  DisplayPanel(handle);
  RunUserInterface();
}
```

Fig. 6.2 f ANSI-C implementation of estimation parameters algorithm.

6.4 Test system

In order to verify the reliability of the device, a calibration procedure employing a 3-litre calibrating syringe (Fukuda Sangyo, Japan) and a manually simulated respiratory cycle of approximately 12 breaths per minute, for 120 seconds, was established. Computation of volume by integration of the flow could introduced a maximum error of 3%.

After verification of the device reliability, a test system (*Servo-I test*) was arranged to verify the validity of the model hypothesized in the case of conventional ventilation.
The flow output of a conventional ventilator (Maquet Servo-I, MAQUET GmbH & Co, Germany) was connected to a lung-simulator (FLUKE ACCU LUNG), presenting variable R/C parameters, through a Fleisch pneumotacograph (Type 2, 3 l/sec) to which the measurement device was connected. Pressure and flow measures were carried out for 60 seconds, setting up on the ventilator a respiratory frequency of 12 breaths per minute with I/E 1:1 and a work pressure of 30 cm H_2O. On the lung simulator a mechanical resistance of 5, 20 and 50 cm H_2O/(l/sec) and a compliance of 10, 20 and 50 ml/cm H_2O (corresponding to an elastance of 100, 50 and 20 cm H_2O/l, respectively) were fixed. The lung simulator presents an inertance which can be considered close to zero.

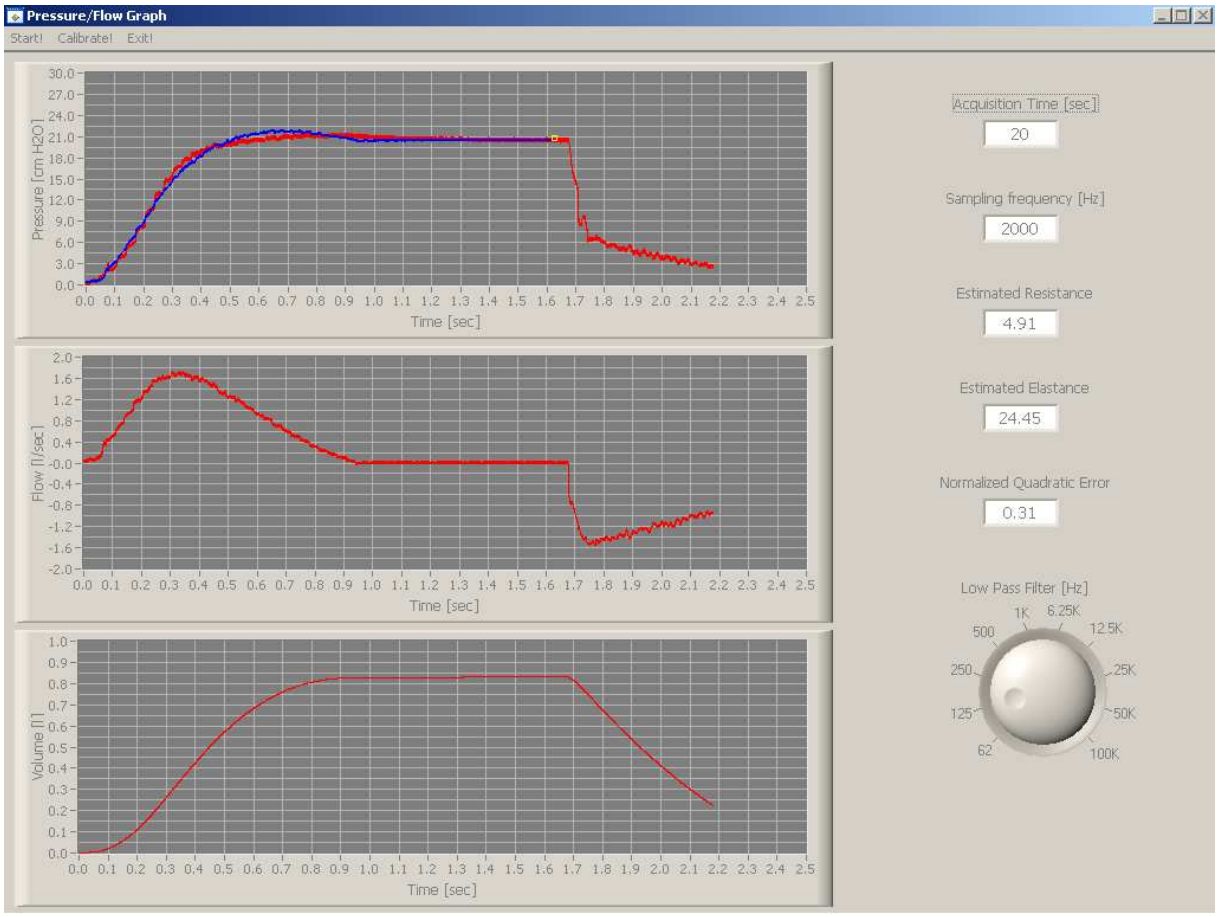

Fig. 6.3 Servo-I : Measured Pressure (top), Flow (middle) and computed (bottom) Volume during a conventional respiration cycle.

The accuracy of fixed resistance was 20% up to 2 l/sec and the accuracy of fixed elastance was 10% up to 500 ml of tidal volume [Datasheet: Portable Precision Test Lung Fluke Biomedical]. The selected cut-off frequency of on-board low-pass Butterworth filter was 125 Hz. The data acquisition system acquires 2000 samples per second for every transducer. Fig. 6.3 shows the acquired pressure and flow curves, in a respiration cycle, together with the corresponding estimated volume, automatically computed by numerical integration of the flow.

Finally, in order to compare the results determined in the case of conventional ventilation with those of the percussive ventilation, a second test (*VDR-4 test*) was realized. In the *VDR-4 test*, the output of a Percussionaire (VDR-4, Percussionaire Corporation, USA) was connected to a lung-simulator (FLUKE ACCU LUNG) and pressure and flow were acquired for 60 seconds, setting up on the VDR-4 a respiratory frequency of 15 breaths per minute with I/E

1:1 and a percussive frequency from 300 to 900 cycles per minute with work pressure of 20 cm H_2O and free expiratory flow. The selected cut-off frequency of the on-board low-pass Butterworth filter was of 500 Hz. Fig. 6.4 shows the acquired pressure and flow curves together with the estimated volume during a respiration cycle.

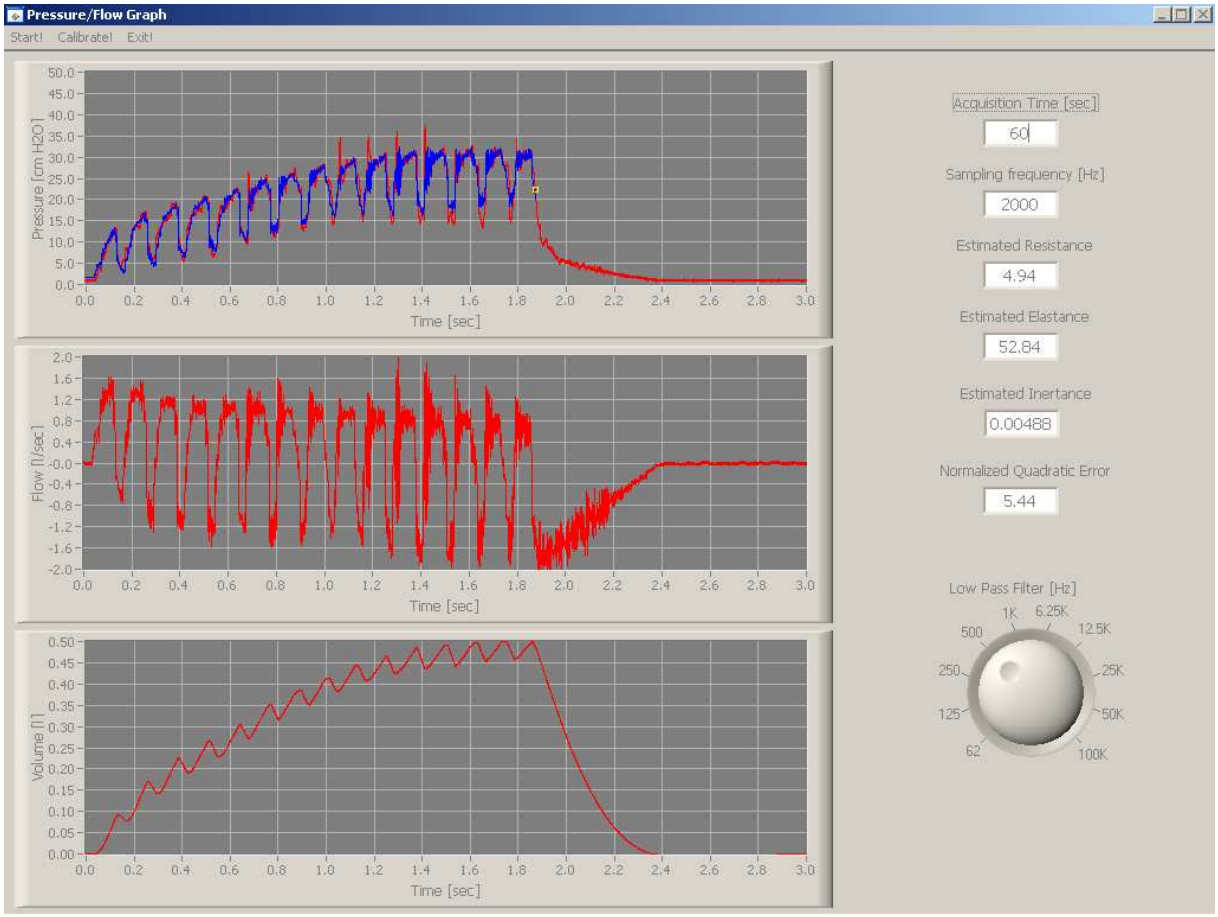

Fig. 6.4 VDR-4-Measured Pressure (top), Flow (middle) and computed (bottom) Volume during a high percussive respiration cycle.

6.5 Results and discussion

Table 6.1 shows the reference set values of resistance (R FLUKE) and elastance (E FLUKE) used in the Servo-I test, with the corresponding resistance (R mean ± 1SD) and elastance (E mean ± 1SD) estimated values together with their respective % relative estimation errors (ΔR% and ΔE%) and the normalized mean square error between measured and estimated pressure (NMSE). The mean and SD values are computed on 12 successive respiration cycles by the procedure implemented in the device.

Table 6.1 Resistance and compliance estimated during inflation by the Servo-I ventilator. Pressure and flow measures were carried out for 60 seconds, setting up on the ventilator a respiratory frequency of 12 breaths per minute with I/E 1:1 and a work pressure of 30 cm H_2O.

R FLUKE cm H_2O/(l/sec)	E FLUKE cm H_2O/l	R mean±1SD cm H_2O/(l/sec)	ΔR%	E mean±1SD cm H_2O/l	ΔE%	NMSE
5	20	5.9±0.02	18.9%	24.4±0.07	22.0%	0.03
20	20	22.2±0.25	11.1%	19.9±0.06	-0.2%	0.12
50	20	67.1±0.83	34.2%	18.6±0.14	-7.1%	0.94
5	50	5.1±0.04	2.3%	60.1±0.12	20.2%	0.09
20	50	17.4±0.04	-13.2%	58.5±0.12	17.0%	0.18
50	50	60.5±0.75	21.0%	51.2±0.28	2.3%	1.02
5	100	3.4±0.09	-33.0%	125.7±0.31	25.7%	0.22
20	100	14.6±0.11	-26.8%	118.7±0.64	18.7%	0.23
50	100	46.4±0.10	-7.2%	111.2±0.35	11.2%	0.38

In conventional ventilation case, the estimated values of the parameters are very similar to those set on the lung simulator, with a good repeatability and a low NMSE. In this case, the hypothesized model adequately estimates the behaviour of the lung simulator. The accuracy of resistance and elastance measurements by a monitoring system has also been described in some studies. A similar level of accuracy (i.e. 20% of set values) was reached in measurement of respiratory mechanic compared to known values of a neonatal lung simulators [Jackson EA et al 1995]. Lower accuracy in a monitoring system (Bicore, SensorMedics 2600, Babylog) for the resistance and compliance estimation of a lung model by means of the occlusion technique has been also reported [Hauschild M et al 1994].

The graphs of Figure 6.5 show the relations between the lung simulator set parameters and the corresponding estimated parameters.

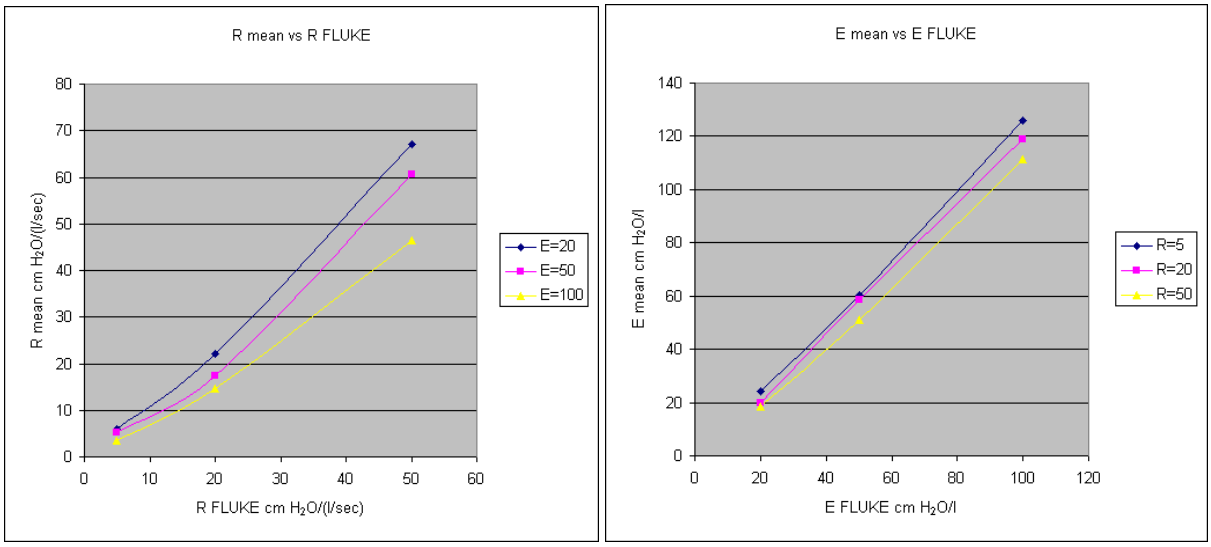

Fig. 6.5 Servo-I : R mean, E mean

Table 6.2 presents the reference values of resistance (R FLUKE) and elastance (E FLUKE) for the VDR-4 test, with the corresponding resistance (R mean ± 1SD) and elastance (E mean ± 1SD) estimated values together with their % relative estimation errors (ΔR% and ΔE%) and the normalized mean square error between measured and estimated pressure (NMSE). The percussive frequency was fixed to 450 cycles/minute.

Table 6.2 Resistance and compliance estimated during inflation by the VDR-4 percussive ventilator. Measures were carried out for 60 seconds, setting up on the VDR-4 a respiratory frequency of 15 breaths per minute with I/E 1:1 and a percussive frequency of 450 cycles per minute with work pressure of 20 cm H_2O and free expiratory flow.

R FLUKE cm H_2O/(l/sec)	E FLUKE cm H_2O/l	R mean±1SD cm H_2O/(l/sec)	ΔR%	E mean±1SD cm H_2O/l	ΔE%	NMSE
5	20	4.9±0.16	-1.3%	21.9±0.19	9.4%	2.8
20	20	13.7±0.16	-31.7%	23.6±0.51	18.0%	4.7
50	20	37.2±0.56	-25.7%	31.7±1.42	58.6%	22.9
5	50	5.0±0.07	-0.70%	54.8±1.66	9.6%	5.9
20	50	14.7±0.26	-26.4%	52.1±0.78	4.2%	10.0
50	50	42.2±0.70	-15.6%	62.1±1.45	24.1%	37.8
5	100	4.9±0.06	-1.4%	116.4±5.37	16.4%	5.3
20	100	13.2±0.15	-33.7%	116.9±4.27	16.9%	9.9
50	100	41.2±0.63	-17.6%	109.8±1.84	9.8%	36.5

Similarly to Table 6.2, Table 6.3 shows the estimated values of resistance and elastance at different percussive frequency (300, 500, 700 and 900 cycles/minute).

Table 6.3 Resistance and compliance estimated during inflation by the VDR-4 percussive ventilator. Measures were carried out for 60 seconds, setting up on the VDR-4 a respiratory frequency of 15 breaths per minute with I/E 1:1 and a percussive frequency from 300 to 900 cycles per minute with work pressure of 20 cm H_2O and free expiratory flow.

R FLUKE cm H_2O/(l/sec)	E FLUKE cm H_2O/l	PERCUSS. FREQ. c/min	R mean cm H_2O/(l/sec)	E mean cm H_2O/l	NMSE
5	20	300	4.99	21.5	3.2
5	20	500	4.7	20.9	4.7
5	20	700	5.5	23.6	3.9
5	20	900	5.4	23.6	4.5
20	20	300	13.6	27.0	4.6
20	20	500	13.0	27.5	5.1
20	20	700	12.7	27.7	4.7
20	20	900	11.8	26.2	4.4
50	20	300	30.5	67.1	33.2
50	20	500	20.3	80.9	35.0
50	20	700	11.7	56.8	20.0
50	20	900	11.4	43.5	11.9
5	50	300	5.1	51.3	3.5
5	50	500	4.9	53.4	4.9
5	50	700	4.9	54.6	5.4
5	50	900	5.4	56.7	5.9
20	50	300	12.9	57.9	4.1
20	50	500	11.9	57.9	4.8
20	50	700	11.2	60.1	4.8
20	50	900	10.5	59.6	5.3
50	50	300	31.0	79.7	32.1
50	50	500	24.1	78.4	32.6
50	50	700	12.4	65.7	18.7
50	50	900	11.7	63.6	11.6
5	100	300	5.2	111.8	3.0
5	100	500	4.9	109.7	4.0
5	100	700	4.8	111.4	5.1
5	100	900	4.8	110.6	6.2
20	100	300	13.1	113.1	4.4
20	100	500	11.5	114.1	4.5
20	100	700	10.6	115.7	5.0
20	100	900	9.4	117.5	8.0
50	100	300	33.2	157.5	41.1
50	100	500	24.6	186.5	39.1
50	100	700	12.2	171.6	11.9
50	100	900	11.8	164.8	7.5

The graphs of Figure 6.6 show the relations between the lung simulator set parameters and the corresponding estimated parameters at the four diffferent percussive frequencies.

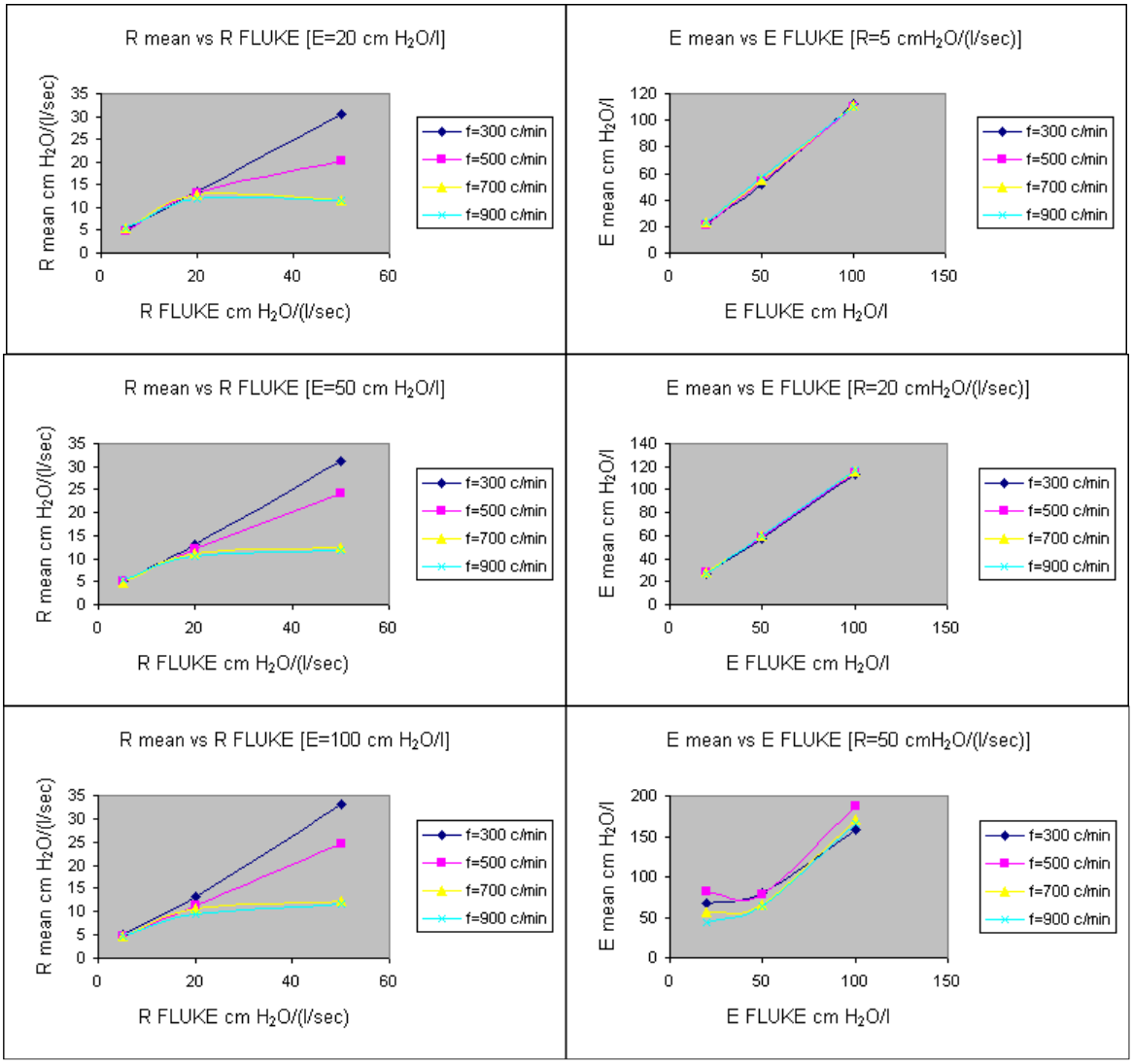

Fig.6.6 VDR-4 : R mean and E mean values at different percussive frequencies

From the results it appears necessary to distinguish the case where the resistance is less than 50 cm H_2O/(l/sec) from that in which the resistance is equal to 50 cm H_2O/(l/sec). In the first case, the mean square errors are kept low (Table 6.3) and the graphs of figure 6.6 show dependence on the frequency of lung simulator parameters. Again, until the resistance remains at reasonable values from a clinical point of view, the hypothesized simple respiratory model can adequately simulate the situation even if the mean square errors are

higher than in the case of conventional ventilation. The introduction of more sophisticated models for high frequency [Dorkin et al 1988] seems to be necessary in order to explain the found differences.

On the other hand, in case of resistance equal to 50 cm H_2O/(l/sec), the model does not seem valid anymore (Table 6.3, Figure 6.6). Moreover, Figure 6.7 shows that the mean square error (NMSE) reaches unacceptable values for R=50 cm H_2O/(l/sec).

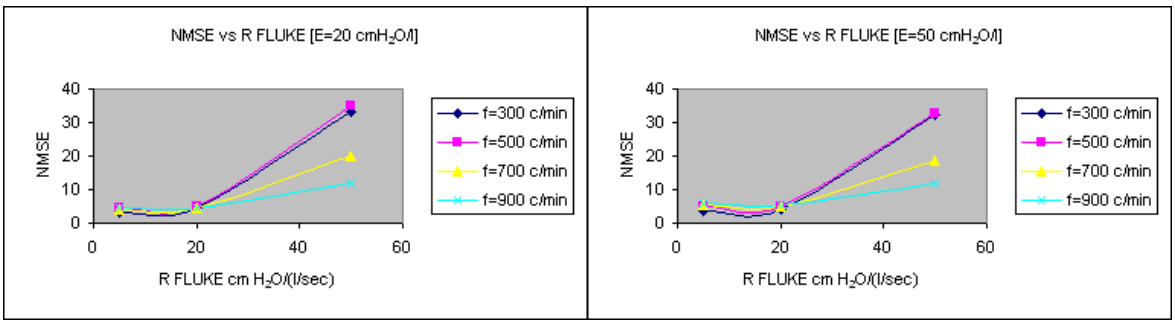

Fig.6.7 VDR-4 : NMSE versus R at different percussive frequency

Figure 6.8 shows the flow curves at different resistance values. A high frequency disturbance, which dramatically increases as the resistance rises, is well evident and this negatively influences the volume calculation. It seems reasonable to assume that this phenomenon could be due to a turbulent motion present in the pneumotachograph, caused by frequency dependent effects [Patrick F and Allan MD 2010]. This turbulence is less negligible as load resistance increases.

Moreover, Figure 6.8 compares the acquired pressure curve against the estimated one when resistance changes, highlighting the effect of the error during the estimation of volume parameters.

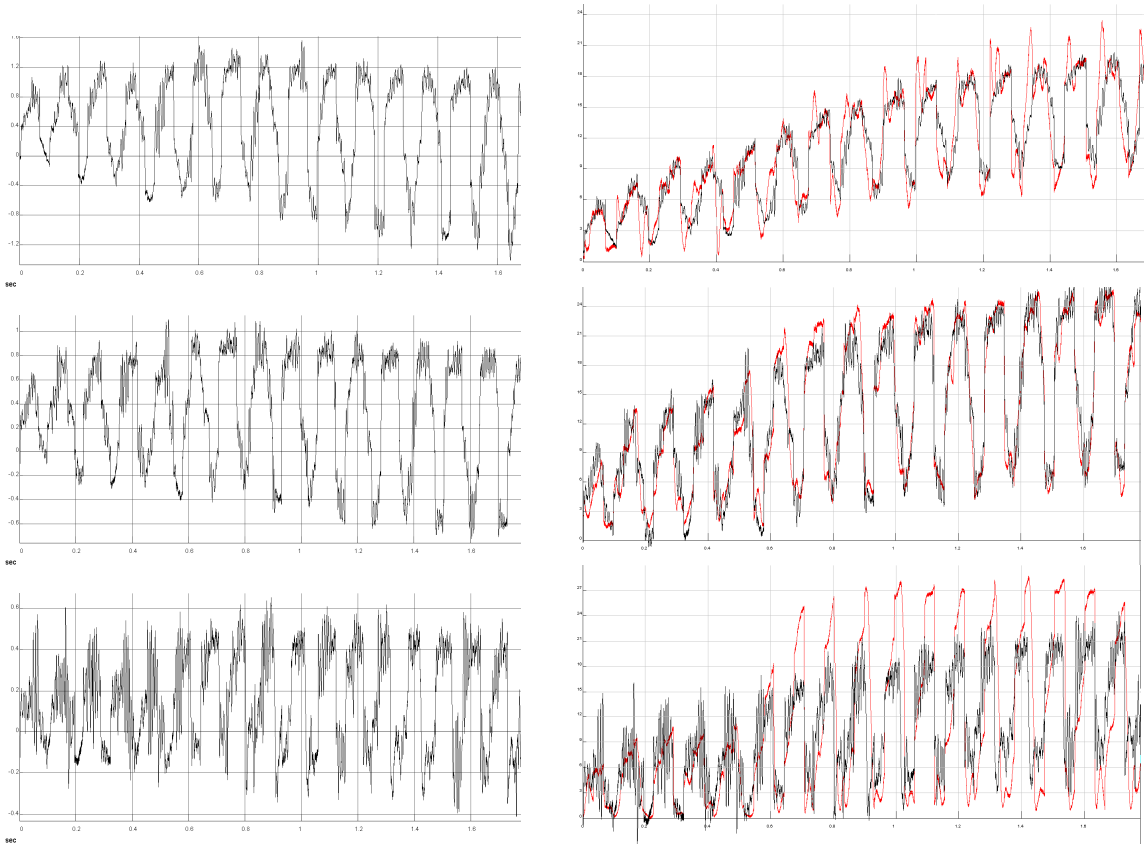

Fig.6.8 VDR-4 : Measured flow (left panel) and pressure (right panel, black line) together with the estimated pressure (right panel, red line). The latter presents a more irregular profile than the measured pressure, especially in the bottom graph. E=20 cm H_2O/l in all graphs; R=5,20,50 cm H_2O/(l/sec) from top to bottom; frequency = 450 c/min.

Even if our results are probably affected by the intrinsic limit of the lung model, as frequency dependence and a non-linear behaviour at the highest resistance, the possibility to have a real time respiratory parameters monitoring is useful for the clinical point of view. Is very important to emphasize that lung elastance is the main factor to avoid volutrauma during a pressure-controlled ventilation logic as pointed out in our recent study in which the elastance represents the most important cause of volume distribution in a two compartment model ventilated in HFPV [Lucangelo U et al 2010], while resistance does not play a particular role. For this reason the accurate estimation of elastance obtained by the computerized system is very important to set correctly the ventilator. In the present investigation our mathematical model constantly overestimates the elastance, avoiding the hazard of hyperinflation during HFPV. On the other hand, the compensative mathematical model resistance underestimation do not interfere with the delivered volume.

Our instrument allows to satisfactorily estimate respiratory parameters in the range of values of clinical interest, both in the case of conventional ventilation and in the case of percussive ventilation. Current investigation is propaedeutic to further human studies. In this case it will be mandatory to assess the effect of inertance and implement more sophisticated algorithms.

Chapter 7

Gas distribution in a two-compartment model ventilated in high-frequency percussive and pressure-controlled modes

Recently a one-compartment linear model of the respiratory system has been successfully used to demonstrate the effects of mechanical resistive and elastic loading on flow, tidal volume, and pressure curves generated by HFPV as well as on the resulting washout of gas from the lungs [Lucangelo et al, 2004; Lucangelo et al, 2006]. However, the consequences of HFPV on a mechanically heterogeneous lung have yet to be explored. It should be stressed that the effects of HFPV in a heterogeneous system are complex, since not only the mechanical interactions play an important role in the determination of gas distribution, but also the system delivering HFPV modulates tidal volume delivery in accordance with the imposed mechanical loads.

In a following study we aim to investigate in a two-compartment heterogeneous mechanical model of the lung whether different mechanical resistive and elastic loads applied to one compartment, while the other is kept constant, would modify gas distribution between the two pathways and air trapping under HFPV. Additionally, these results were compared with those generated in the same model by pressure-controlled ventilation (PCV).

We based our study on the two-compartment parallel model introduced by Otis [Otis et al, 1956], extending our previous studies [Lucangelo et al, 2004; Lucangelo et al, 2006]. In such a model the distribution of the overall flow in the separate branches depends on the impedances of each independent compartment. Under spontaneous or conventional mechanical ventilation, if the elastance (E) and resistance (R) of each pathway are identical in both branches, there will be no difference in the volume flowing into each one. However, if the separate compartments present different time constants, they will fill up according to their time constants, i.e., a shorter time constant will allow a larger volume into the corresponding compartment. The parameters of the fixed compartment were kept constant throughout the experiment and were generated by a Siemens lung simulator (Siemens Test Lung 190; Siemens AG, Munich, Germany), while the variable one was provided by a single-compartment lung simulator (Medishield, Harlow Essex, UK) characterized by three elastic loads and three resistive loads. As a result, nine different combinations were randomly tested. Ventilation of the mechanical model was provided by two different equipments: (1) HFPV was generated by a volumetric diffusive respirator (VDR-4; Percussionaire Corporation, Sandpoint, ID, USA) that delivers minibursts of respiratory gas mixtures in the proximal airways throughout the breath. (2) PCV was delivered by a Siemens Servo 900c ventilator (Siemens, Solna, Sweden). Both ventilators produced the same peak pressure, respiratory rate, and I/E ratio. No positive end-expiratory pressure (PEEP) was used in the experiments.

Pressure–time curves obtained with HFPV and PCV during one breathing cycle are shown in Fig. 7.1. Comparing both ventilatory modes, it follows that, for the same loading, PCV generates higher total tidal volume (VT) than HFPV. This was due to the larger volume directed to the fixed compartment during PCV, since there was no difference between the fractional volume injected into the variable compartment by the two ventilatory modes. In this regard, no difference was found in the time constant of the variable compartment when the two methods were compared.

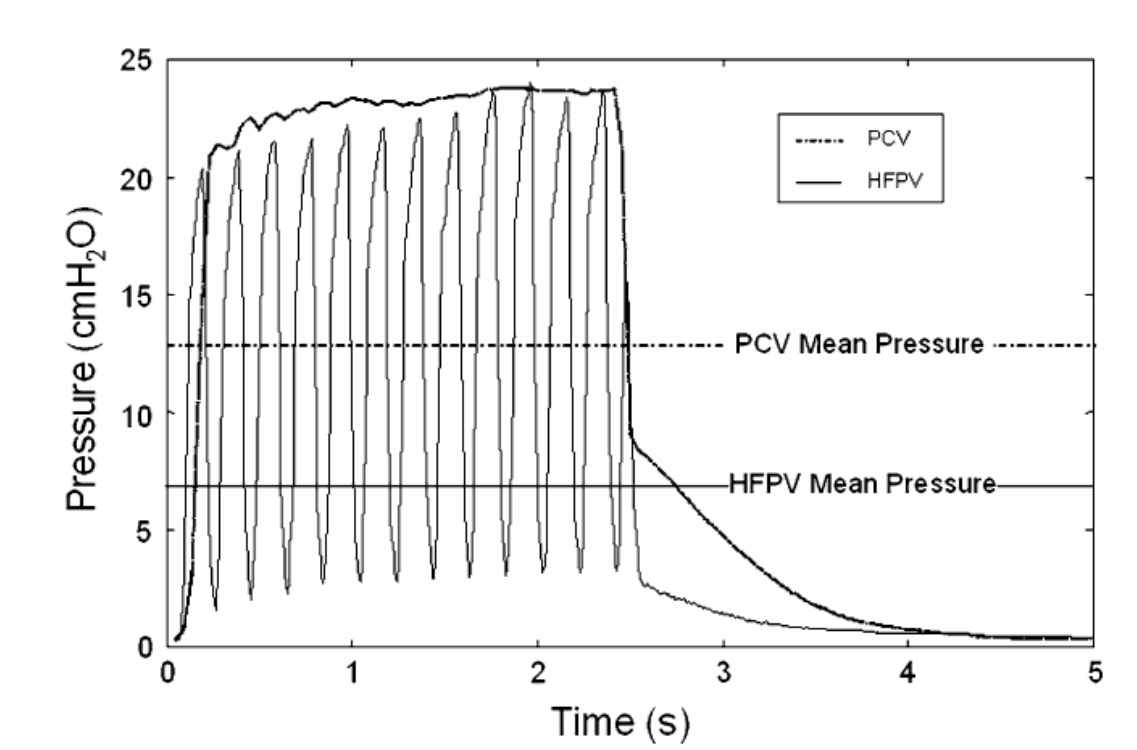

Fig.7.1 Pressure–time curves obtained with high-frequency percussive ventilation (HFPV) and pressure-controlled ventilation (PCV) during one breathing cycle.

We have contributed information on the distribution of inspired volume according to resistive and elastic loads in a two-compartment nonuniform model of the lung. HFPV accommodated volume distribution without overinflating compartments with low time constants, thus presenting a potential beneficial behavior in mechanically heterogeneous lungs. The main advantage of HFPV seems to be ventilation at a lower mean airway pressure and lower inspiratory volumes, thus providing a protective effect against volutrauma and barotrauma. At the same time, oxygenation could be maintained by the association of convective and diffusive ventilation. Finally, the findings of this bench study suggest that comparison between HFPV and conventional ventilation in terms of supposed volume delivery should be carefully considered.

Conclusions and future developments

The measurement of respiratory mechanics is essential in intensive care respiratory medicine. Nevertheless, the respiratory mechanism is rarely measured in the ventilator-dependent patients to the belief that these measures are even more difficult to obtain and to interpret and unreliable, especially in the case of high-frequency percussive ventilation, on which there are few studies .

In this work the basis of the characterization of high-frequency percussive ventilator were laid, identifying the characteristics of elastic and resistive load.

The ventilation conditions currently used in medicine mostly include the adjustment of the frequency of percussion and pressure peak, and then the work has been addressed towards the analysis of these variables, proving to be adequate to justify the positive results obtained in intensive care, in the treatment of patients with certain respiratory problems.

An important result is the possibility of obtaining estimates of respiratory parameters which, within acceptable limits of error, provide the evolutionary trend of respiratory-mechanical characteristics of a patient independently of the frequency of percussion. Therefore, it is not necessary to replace the percussive ventilator with a conventional for the measure of those parameters. This allow to follow the temporal evolution of the resistive and viscoelastic conditions, the latter particularly dependent upon removal of bronchial secretions.

The high-frequency percussive ventilation combines together two complementary mechanisms: the high oscillation frequency (diffusive behavior) and pressure controlled ventilation (convective behavior). The prevalence of either depends on the mechanical impedance characteristics, but their combined action leads to a sufficient exchange of pulmonary gases in patient and in all situations.

From the obtained results we can deduce that the VDR-4 is a versatile ventilator which provides adequate ventilation at all load conditions, as a result of the use of a Venturi type device, which allows the patient to enter at any stage of ventilation with his spontaneous

breathing, as the circuit remains constantly open to the air, reducing the danger of barovolutrauma.

In vivo studies are required to verify the assumptions made by the results of simulations. In the future, it may be useful a further comparison with the performance of the flow control ventilation, a technique widely used in intensive care.

The numerous parameters that can be set on the Percussionaire increase the possible studies. The validity of a given model should also be studied according to:

- the ratio between rise time and fall time;
- the presence of percussion on expiration;
- the increase of the end-expiratory pressure.

References

Annane D, Orlikowski D, Chevret S et al. 2007. Nocturnal mechanical ventilation for chronic hypoventilation in patients with neuromuscular and chest wall disorders. Cochrane Database Syst Rev (4):CD001941.

Antonaglia V, Lucangelo U, Zin WA et al. 2006. Intrapulmonary percussive ventilation improbe the outcome of patients with acute exacerbation of chronic obstructive pulmonary disease using an helmet. Crit Care Med 34:2940–2945.

Astrand PO, Rodahl K. 1970. Textbook of Work Physiology. New York, McGraw-Hill.

Avanzolini G. et al. 1995. Influence of flow pattern on the parameter estimates of a simple breathing mechanics model. IEEE Trans. Biomed. Eng. 42:394-402.

Barbini P. et al, 2001. Comparison of estimates of inspiratory and expiratory resistance and elastance in mechanically ventilated patients. Computer Methods in Biomechanics and Biomedical Engineering 3.pp 237-242.

Bates, J. H. T., Brown K. and Kochi T. 1989. Respiratory mechanics in the normal dog determined by expiratory flow interruption. J. Appl. Physiol. 67:2276-2285.

Bates J.H.T. and Lauzon A.M. 1992. A non statistical approach to estimate confidence intervals about model parameters: application to respiratory mechanics. IEEE Trans.Biomed.Eng. 39:94-100.

Branson RD. 1995. High-frequency ventilators. Respiratory care equipment. 458-446.

Carr JJ, Brown JM, 1993. Introduction to Biomedical Equipment Technology. Englewood Cliffs, NJ, Prentice-Hall.

Deakins K and Chatburn RL. 2002. A comparison of intrapulmonary percussive ventilation and conventional chest physiotherapy for the treatment of at electasis in the pediatric patients. Respir Care 47:1162–1167.

Dorkin H.L., Lutchen K.R., Jackson A.C. 1988. Human respiratory input impedance from 4 to 200 Hz: physiological and modelling considerations. J. Appl. Physiol. 64:823-831.

Fanfulla F, Taurino AE, Lupo ND et al. 2007. Effect of sleep on patient/ventilator asynchrony in patients undergoing chronic non-invasive mechanical ventilation. Respir Med 101(8):1702–1707.

Froese AB. High-frequency ventilation: a critical assessment. 1984. Critical care: state of the art. 5:A3-51.

Gioia FR, Rogers MC. 1985. High-frequency ventilation of the lungs. Recent advances in anaesthesia and analgesia. 63-78.

Hauschild M, Schmalisch G and Wauer RR.1994. Accuracy and reliability of commercial lung function diagnostic systems and respiratory monitors in newborn infants. Klin Padiatr 206:167-174.

Homnick DN, White F and De Castro C. 1995. Comparison of effects of an intrapulmonary percussive ventilator to standard aerosol and chest physiotherapy in treatment of cystic fibrosis. Pediatr Pulmonol 20:50–55.

Hurst JM, Branson RD and De Haven CB 1987. The role of high-frequency ventilation in posttraumatic respiratory insufficiency. J Trauma 27:236 –242.

Jackson EA, Coates AL, Gappa M and Stocks J. 1995. In vitro assessment of infant pulmonary function equipment. Pediatr Pulmonol 19:205-213.

Johnson AT. 1991. Biomechanics and Exercise Physiology. New York, Wiley.

Jones NL. 1984. Normal values for pulmonary gas exchange during exercise. Am Rev Respir Dis 129:544–546.

Lentz CW and Peterson HD 1997. Smoke inhalation is a multilevel insult to the pulmonary system. Curr Opin Pulm Med 3:221–226.

Kaczka et al. 1995. Assessment of time-domain analyses for estimation of low-frequency respiratory mechanical properties and impedance spectra Ann Biomed Eng 23:135-151.

Kline J. (ed). 1976. Biologic Foundations of Biomedical Engineering. Boston, Little, Brown.

Krishnan JA, Brower RG. 2000. High-frequency ventilation for acute lung injury and ARDS. Chest 118(3): 795–807.

Lucangelo et al. 2003. High frequency percussive ventilation. Principles and technique. Minerva anestesiol 69:841-851.

Lucangelo et al. 2004. Effects of mechanical load on flow, volume and pressure delivered by high-frequency percussive ventilation. Respiratory Physiology & Neurobiology 142:81-91.

Lucangelo U, Antonaglia V, Zin WA, Fontanesi L, Peratoner A, Bird FM, Gullo A. 2004. Effects of mechanical load on flow, volume and pressure delivered by high-frequency percussive ventilation. Respir Physiol Neurobiol 142:81–91.

Lucangelo U, Antonaglia V, Zin WA, Berlot G, Fontanesi L, Peratoner A, Bernabe` F, Gullo A. 2006. Mechanical loads modulate tidal volume and lung washout during high-frequency percussive ventilation. Respir Physiol Neurobiol 150:44–51.

Lucangelo et al. 2009. High-frequency percussive ventilation improves perioperatively clinical evolution in pulmonary resection. Critical Care Medicine (37) 5:1663-1669.

Lucangelo U, Accardo A, Bernardi A, Ferluga M, Borelli M, Antonaglia V, Riscica F and Zin WA. 2010. Gas distribution in a two-compartment model ventilated in high-frequency percussive and pressure-controlled modes. Intensive Care Med 36:2125-2131.

Mead, J., Whittenberger J.L. 1954. Evaluation of airway interruption technique as a method for measuring pulmonary air-flow resistance. J. Appl. Physiol. 6: 408-416.

Mount, L. E. 1955. The ventilation flow resistance and compliance of rat lungs. J. Physiol. (London) 127:157-167.

Natale JE, Pfeifle J and Homnick DN. 1994. Comparison of intrapulmonary percussive ventilation and chest physiotherapy. Chest 105:1789-1793.

Nava S, Hill N. 2009. Non-invasive ventilation in acute respiratory failure. Lancet 374(9685):250–259

Otis, A. B., C. B. McKerrow, R. A. Bartlett, J. Mead, M. B. Mcllroy, N. J. Selverstone and E. P. Radford. 1956. Mechanical factors in distribution of pulmonary ventilation. J. Appl. Physiol. 8: 427-443.

Ozsancak A, D'Ambrosio C, Hill NS. 2008. Nocturnal noninvasive ventilation. Chest 133(5):1275–1286.

Patrick F and Allan MD. 2010. High-Frequency Percussive Ventilation Pneumotachograph Validation and Tidal Volume Analysis. Respiratory Care 55:734-740.

Reper P, Dankaert R, van Hille F et al. 1998. The usefulness of combined high-frequency percussive ventilation during acute respiratory failure after smoke inhalation. Burns 24:34–38

Reper P, Wibaux O, van Laeke P et al 2002. High frequency percussive ventilation and conventional ventilation after smoke inhalation: A randomised study. Burns 28:503-508.

Riscica F, Lucangelo U, Accardo A. 2009. Development of an innovative instrument for the online characterization of high-frequency percussive ventilators. Proceed. of World Congress 2009 of Medical Physics and Biomedical Engineers, Munich, pp.480-483.

Riscica F, Lucangelo U, Accardo A. 2010. A portable instrument for the volume measurement of high-frequency percussive ventilators. Biomedical sciences instrumentation 46:93-98.

Riscica F, Lucangelo U, Accardo A. 2010. Development of an innovative instrument for the online characterization of high-frequency percussive ventilators. Atti del Congresso Nazionale di Bioingegneria 2010, pp.141-142.

Ruch TC, Patton HD. (eds). 1966. Physiology Biophysics. Philadelphia, Saunders.

Salim A, Martin M. 2005. High-frequency percussive ventilation. Crit Care Med 33:241.

Scala R, Naldi M. 2008. Ventilators for noninvasive ventilation to treat acute respiratory failure. Respir Care 53(8):1054–1080.

Shaw A., Gregory NL, Davis PD, Patel K. 1976. Flow-volume integrator for respiratory studies. Med Biol Eng 14:695-696.

Stamenovic D, Glass GM, Barnas GM, Fredberg JJ. 1990. Viscoplasticity of Respiratory Tissues. J Appl Physiol 69(3):973–988.

Toussaint M, De Win H, Steens M et al. 2003. Effect of intrapulmonary percussive ventilation on mucus clearance in Duchenne muscular dystrophy patients: A preliminary report. Respir Care 48:940–947.

Velmahos GC, Chan LS, Tatevossian R et al. 1999. High-frequency percussive ventilation improves oxygenation in patients with ARDS. Chest 116:440–446.

Vignaux L, Vargas F, Roeseler J et al. 2009. Patient–ventilator asynchrony during non-invasive ventilation for acute respiratory failure: a multicenter study. Intensive Care Med 35(5):840–846.

Weibel, ER. 1963. Morphometry of the Human Lung. New York, Academic Press.

West JB (ed). 1977. Bioengineering Aspects of the Lung. New York, Marcel Dekker.